TECHNISCHE UNIVERSITÄT WIEN

# DIPLOMARBEIT

## Einsatz und Genauigkeit von Drehtischen in der modernen Produktionsmesstechnik

## Analyse und Evaluierung der Umkehrspanne mittels eines Inkrementalgebers, Laserinterferometers und Koordinatenmessgerätes

ausgeführt zum Zwecke der Erlangung des akademischen Grades eines

## Diplom-Ingenieurs

unter der Leitung von

**Ao. Univ. Prof. Prof.h.c. Dipl.-Ing. Dr.techn. Dr.h.c.**
**Numan M. Durakbasa**
(E311 Institut für Fertigungstechnik und Hochleistungslasertechnik, Abteilung: Austauschbau und Messtechnik / Produktionsmesstechnik und Qualität)

**Dr.-Ing. Jorge M. Bauer**
(E311 Institut für Fertigungstechnik und Hochleistungslasertechnik, Abteilung: Austauschbau und Messtechnik / Produktionsmesstechnik und Qualität)

eingereicht an der Technischen Universität Wien

**Fakultät für Maschinenwesen und Betriebswissenschaften**

von

**Gurur Demirtas**

1128526 (066 482)

Hörlgasse 4/17 1090 Wien

Wien, im April 2016

Gurur Demirtas

TECHNISCHE UNIVERSITÄT WIEN

# MASTER'S THESIS

## Utilisation and accuracy of rotary tables in modern production metrology

### Analysis and evaluation of the reversal error by means of an incremental encoder, laser interferometer, and coordinate measuring machine

Submitted in partial fulfillment of the requirements for the degree of

## Diplom-Ingenieur (M.Sc.)

under the guidance of

**Ao. Univ. Prof. Prof.h.c. Dipl.-Ing. Dr.techn. Dr.h.c.**
**Numan M. Durakbasa**
(E311 Institute for Production Engineering and Laser Technology, Department: Interchangeable Manufacturing and Industrial Metrology / Production Metrology and Quality)

**Dr.-Ing. Jorge M. Bauer**
(E311 Institute for Production Engineering and Laser Technology, Department: Interchangeable Manufacturing and Industrial Metrology / Production Metrology and Quality)

submitted at TU Wien

**to the Faculty of Mechanical and Industrial Engineering**

by

**Gurur Demirtas**

1128526 (066 482)

Hörlgasse 4/17 1090 Wien

Vienna, in April 2016

Gurur Demirtas

TECHNISCHE UNIVERSITÄT WIEN

Ich habe zur Kenntnis genommen, dass ich zur Drucklegung meiner Arbeit unter der Bezeichnung

# DIPLOMARBEIT

nur mit Bewilligung der Prüfungskommission berechtigt bin.

Ich erkläre weiters Eides statt, dass ich meine Diplomarbeit nach den anerkannten Grundsätzen für wissenschaftliche Abhandlungen selbstständig ausgeführt habe und alle verwendeten Hilfsmittel, insbesondere die zugrunde gelegte Literatur, genannt habe.

Weiters erkläre ich, dass ich dieses Diplomarbeitsthema bisher weder im In- noch Ausland (einer Beurteilerin/einem Beurteiler zur Begutachtung) in irgendeiner Form als Prüfungsarbeit vorgelegt habe und dass diese Arbeit mit der vom Begutachter beurteilten Arbeit übereinstimmt.

Wien, im April 2016

Gurur Demirtas

# DANKSAGUNG

An dieser Stelle möchte ich mich bei all jenen herzlich bedanken, die durch ihre Hilfe und Unterstützung zum Gelingen dieser Masterarbeit beigetragen haben.

Danken möchte ich in erster Linie Herrn Ao. Univ. Prof. Prof. h. c. Dipl.-Ing. Dr. techn. Dr. h. c. Numan M. Durakbasa, Leiter der Abteilung Austauschbau und Messtechnik am Institut für Fertigungstechnik und Hochleistungslasertechnik, der die Betreuung meiner Masterarbeit übernommen und mich durch viele hilfreiche Anregungen und konstruktive Kritik unterstützt hat. Durch kritisches Hinterfragen hat er mir immer wieder wertvolle Hinweise gegeben. Er hat mich dazu gebracht, über meine Grenzen hinaus zu denken.

Besonderer Dank gebührt Herrn Prof. Dr. Jorge M. Bauer für seine Zeit und sein Interesse an meiner Arbeit. Die fruchtbaren Diskussionen während seines Aufenthalts in Wien, seine Anregungen und Ermutigungen haben wesentlich zum Gelingen dieser Arbeit beigetragen.

Danken möchte ich auch Frau Dipl.-Ing. Eva M. Walcher, die mich während der Messungen im Präzisionsmessraum und Nanometrologie-Labor begleitet und unterstützt hat.

Weiters bedanke ich mich herzlich beim Herrn em. o. Univ.-Prof. Dipl.-Ing. Dr. techn. Dr. mult. h. c. Peter Kopacek, Leiter der Abteilung für Handhabungsgeräte und Robotertechnik, dafür, dass er als Zweitprüfer in meiner Diplomprüfungskommission meine Arbeit mitbeurteilt hat.

Ebenso gilt mein Dank Herrn Prof. Dr. Burhard Kittl, der sich bereit erklärt hat, den Prüfungsvorsitz zu übernehmen.

Meiner Freundin, Seyda Kigili, die mich immer mit Geduld motiviert und unterstützt hat, danke ich von Herzen.

Nicht zuletzt gebührt meinen Eltern großer Dank, ohne welche dieses ganze Unternehmen schon im Vorhinein niemals zustande gekommen wäre.

# ACKNOWLEDGEMENTS

First of all, I would like to thank all those who have supported and motivated me during the preparation of this master's thesis.

My sincere thanks go especially to Ao. Univ. Prof. Prof. h. c. Dipl.-Ing. Dr. techn. Dr. h. c. Numan M. Durakbasa, Head of the Department of the Interchangeable Manufacturing and Industrial Metrology at the Institute for the Production Engineering and Laser Technology, who has supervised me during my master's thesis with a great commitment. Through critical questioning he has given me all the time valuable information. He has brought me to think beyond my boundaries.

Special thanks go to Dr. Jorge M. Bauer for his time and interest in my work. The fruitful discussions, as well as his suggestions and encouragement during his stay in Vienna have contributed significantly to the success of this work.

Furthermore, I would like to thank Dipl.-Ing. Eva M. Walcher, who guided me during the measurements in the High Precision Measurement Room - Nanometrology Laboratory and support.

I would also like to thank em. o. Univ.-Prof. Dipl.-Ing. Dr. techn. Dr. mult. h. c. Peter Kopacek, Head of the Department of Intelligent Handling Devices and Robotics, who has accepted to be the second examiner in my master's thesis exam committee.

Likewise, my thanks go to Prof. Dr. Burhard Kittl, who has accepted to take the chair of my master's thesis exam committee.

I would like to thank my girlfriend, Seyda Kigili, from the bottom of my heart for her endless support.

Last but not least, my parents deserve a huge thank, without whose presence this whole success would not have been possible.

# KURZFASSUNG

Die ständig zunehmende Komplexität und Vielfalt der industriellen Teilen und Baugruppen haben im Gefolge eine große Nachfrage nach Austauschbarkeit sowie nach präziseren, genaueren, zuverlässigeren und schnelleren Messtechniken und -systemen. In diesem Zusammenhang kommt der Koordinatenmesstechnik immer mehr Bedeutung zu, da sie im Vergleich zur herkömmlichen Messtechnik mehrere Vorteile bietet. Als das Herzstück der Koordinatenmesstechnik ermöglichen sogenannte Koordinatenmessgeräte (KMG) dank ihrer Universalität und Flexibilität herausfordernde Messaufgaben einfacher und schneller durchzuführen. Drehtische stellen dabei eine wichtige Erweiterung für die KMG dar, insbesondere für Messungen rotationssymmetrischer Teile, wie z. B. Zahnräder, Kurbel- und Nockenwellen und Schraubenverdichter. Sie fungieren als vierte Achse der KMG und erweitern nicht nur die Zugänglichkeit der Teilen, sondern erhöhen auch das wirksame effektive Messvolumen. Es muss trotzdem berücksichtigt werden, dass sie auch die Anzahl von möglichen Fehlerquellen erhöhen. Ein typisches Beispiel hier ist die Umkehrspanne, welche die bidirektionale Wiederholbarkeit und Genauigkeit negativ beeinflusst, wenn die Anfahrrichtung umgekehrt wird. Dieser Faktor wird noch entscheidender und wichtiger in den industriellen Anwendungen, wo die Positionierwiederholbarkeit und -genauigkeit von großer Bedeutung sind, wie z. B. bei Schweißrobotern und tragbarer Exoskeletten in der Robotertechnik sowie bei Drehtischen in der Fertigungs- und Präzisionsmesstechnik. Daher ist der Einsatz der hochauflösenden Messgeräte bei der Evaluierung der Positioniergenauigkeitskenngrößen von entscheidender Bedeutung, wenn es um die Sicherstellung und Verbesserung der Produkt- und Prozessqualität geht.

Im praktischen Teil dieser Arbeit wurde eine experimentelle Studie im Präzisionsmessraum und Nanometrologie-Labor der Technischen Universität Wien (TU Wien) durchgeführt, in erster Linie, um die Praxistauglichkeit und Eignung eines linearen magnetischen Inkrementalgebers für die Messung der Positioniergenauigkeitskenngrößen (insbesondere der Umkehrspanne) eines manuellen Drehtisches zu bestimmen. Dies wurde verwirklicht durch die Implementierung geeigneter Messanordnungen, durch die Durchführung der entsprechenden Messungen sowie durch den Vergleich der Messergebnisse mit denen, die gleichzeitig durch ein noch genaueres Messgerät, durch das Laserwinkelinterferometer erhalten wurden. Zusätzlich zu dem Hauptziel, wurden die Positioniergenauigkeitskenngrößen eines hochpräzisen Drehtisches einer KMG evaluiert, zuerst durch das KMG selbst und dann durch das Laserwinkelinterferometer zum Vergleich und zur Überprüfung. Darüber hinaus vermittelt diese Masterarbeit LeserInnen den Stand der Technik in der modernen Produktionsmesstechnik, sowie macht sie mit dem konventionellen und weiterentwickelten Arten der KMG vertraut, z.B. optische/optoelektronische KMG, Multisensor-KMG, Gelenkarm-KMG und industrielle Computertomographie (iCT).

***Schlagworte*** Produktionsmesstechnik, Koordinatenmesstechnik, Koordinatenmessgeräte (KMG), Drehtische, Umkehrspanne, Umkehrspiel, Winkelmesstechnik, Magnetische Inkrementalgeber, Laser-Winkelinterferometer

# ABSTRACT

The ever-increasing degree of complexity and diversity of industrial parts and assemblies brings in its wake a great demand for interchangeability, as well as more precise, accurate, reliable, and faster measurement technologies and systems. In this context, coordinate metrology has become more important than ever, since it offers several advantages compared to conventional metrology. As the core of coordinate metrology, the so-called Coordinate Measuring Machines (CMMs) enable conducting challenging measurements in a straightforward and faster manner due to their universality and versatility.

Here rotary tables represent an important accessory for the CMMs, particularly for the measurement of rotationally symmetric parts, e.g. gear wheels, crankshafts and camshafts, and screw compressors. Acting as the fourth axis of CMMs, not only do they extend part accessibility but also increase the effective measurement volume. However, it must be kept in mind that they also increase the number of possible error sources. A typical example is the reversal error that influences the bi-directional repeatability and accuracy negatively when the approach direction is reversed. This factor becomes all the more decisive and significant in industrial applications where (positioning) precision and accuracy are of great significance, e.g. in welding robots and wearable exoskeletons in the context of robotic technology, and in rotary tables in the context of production technology and precision metrology. Therefore, the utilisation of the high-resolution measurement instruments in evaluating positioning accuracy characteristics is of critical importance when it comes to assuring and improving product and process quality.

In the practical part of this thesis, an experimental study was carried out in the High Precision Measurement Room - Nanometrology Laboratory of the TU Wien mainly in order to determine the practical capability and adequacy of a Hall-effect linear magnetic encoder in measuring positioning accuracy characteristics (in particular, the reversal error) of a manual rotary table. This was realised by implementing appropriate measurement set-ups, by conducting related measurements, and by comparing the measurement results with those obtained simultaneously by a more accurate measurement instrument, i.e. by a laser angle interferometer. In addition to that main goal, the positioning accuracy characteristics of a high-precision rotary table of a CMM was evaluated first by CMM itself, and then by laser angular interferometer for comparison and verification.

Furthermore, this thesis provides readers with the state of the art in the modern production metrology, as well as makes them familiar with both conventional (tactile) and advanced types of CMMs, such as optical/optoelectronic CMMs, Multi-Sensor CMMs, Portable-CMMs, and the industrial Computed Tomography (iCT).

***Keywords*** Production Metrology, Coordinate Metrology, Coordinate Measuring Machines (CMMs), Rotary Tables, Reversal Error, Backlash, Angular Metrology, Magnetic Linear Encoders, Laser Angle Interferometer

# CONTENTS

# LIST OF FIGURES

# LIST OF TABLES

# ACRONYMS

| | |
|---|---|
| 1D | One-dimensional |
| 2.5D | Two-and-a-half-dimensional |
| 2D | Two-dimensional |
| 3D | Three-dimensional |
| 3D-X-ray-CT | Three-dimensional X-ray Computed Tomography |
| a.k.a | also known as |
| A/D | analog-to-digital |
| ABI | application binary interface |
| AFM | Atomic Force Microscopy |
| approx. | approximately |
| ASME | American Society of Mechanical Engineers |
| AuM | Department of Interchangeable Manufacturing and Industrial Metrology |
| AuM | Austauschbau und Messtechnik |
| BIPM | International Bureau of Weights and Measures (Fr.: Bureau International des Poids et Mesures) |
| CAD | Computer-Aided Design |
| CAM | Computer-Aided Manufacturing |
| CAS | Computer-Aided Simulation |
| ccw | counter-clockwise |
| CMM | Coordinate Measuring Machine |
| CMOS | complementary metal oxide semiconductor |
| CMS | Coordinate Measuring System |
| CNC | Computer Numerical(ly) Control(led) |
| CORDIC | COordinate to Rotation DIgital Computer |
| CT | Computed Tomography |
| cw | clockwise |
| DCC | Direct Computer-Controlled |
| DIN | Deutsches Institut für Normung |
| DKP | direct kinematic problem |
| DSLR | digital single-lens reflex |
| DSP | digital signal processor |
| e.g. | exempli gratia (lat.: for example) |
| etc. | et cetera (lat..: and so forth) |
| EURAMET | European Association of National Metrology Institutes |
| FMS | Flexible Manufacturing System |
| GDT | Geometrical Dimensioning and Tolerancing |
| GMA | Society for Metrology and Automation Engineering |
| GmbH | Gesellschaft mit beschränkter Haftung (Eng.: Limited Company) |
| GPS | Global Positioning System |
| GUM | Guide to the Expression of Uncertainty in Measurement |

| | |
|---|---|
| i.e. | id est (lat.: that is) |
| I/O | input/output |
| IC | integrated circuit |
| iCT | industrial Computed Tomography |
| iMERA | implementing Metrology in the European Research Area |
| ISO | International Organization for Standardization |
| KMG | Koordinatenmessgerät |
| LCD | liquid-crystal display |
| LED | Light Emitting Diode |
| LPU | law of the propagation of uncertainty |
| LSL | lower specification limit |
| MCS | machine coordinate system |
| mCT | medical Computed Tomography |
| MEMS | Micro-electromechanical systems |
| MPE | maximum permissible error |
| NAVSTAR | Navigational Satellite Timing and Ranging |
| NC | Numerical(ly) Control(led) |
| NDT | Non-Destructive (Material) Testing |
| NEMS | Nano-electromechanical systems |
| NIST | National Institute of Standards and Technology |
| NMI | National Metrology Institute |
| NPL | National Physical Laboratory |
| PB-free | lead-free |
| PC | Personal Computer |
| PCB | Printed Circuit Board |
| PLC | Programmable Logic Controller |
| PLC | Product Life Cycle |
| ppi | pulse per inch |
| ppm | pulse per millimetre |
| ppr | pulse per revolution |
| PTB | Physikalisch-Technische Bundesanstalt |
| PUMA | Procedure for Uncertainty Management |
| PWM | pulse-width modulation |
| QC | Quality Control |
| rpm | round per minute |
| SCM | Scanning Confocal Microscopy |
| SDD | source-detector distance |
| SEM | Scanning Electrone Microscopy |
| SI | International System of units (Fr.: Système International d'unités) |
| SMR | spherically mounted retro-reflector |
| SOD | source-object distance |
| SPM | Scanning Probe Microscopy |
| SSM | Scanning Stylus Microscopy |
| STL | stereolithography |
| STM | Scanning Tunneling Microscopy |
| TQM | Total Quality Management |
| TSSOP | thin-shrink small outline package |
| TTL | transistor–transistor logic |
| TU Wien | Technische Universität Wien |
| USA | United States of America |
| USL | upper specification limit |

| | |
|---|---|
| vCMM | Virtual CMM |
| VDC | volts direct current |
| VDE | Association for Electrical, Electronic and Information Technologies (Ger.:Verband der Elektrotechnik, Elektronik und Informationstechnik) |
| VDI | Association of German Engineers (Ger.: Verein Deutscher Ingenieure) |
| VDI/VDE | Association of German Engineers/Association for Electrical, Electronic and Information Technologies (Ger.: Verein Deutscher Ingenieure/Verband der Elektrotechnik, Elektronik und Informationstechnik) |
| VIM | International Vocabulary of Metrology (Fr.: Vocabulaire International de Métrologie) |
| WCS | workpiece coordinate system |
| X-ray-CT | X-ray Computed Tomography |
| z. B. | zum Beispiel (Ger.: for example) |

# LIST OF SYMBOLS

| | |
|---|---|
| $A\uparrow$ or $A\downarrow$ | Unidirectional positioning accuracy of an axis |
| $E\uparrow$ or $E\downarrow$ | Unidirectional systematic positioning error of an axis |
| $R\uparrow$ or $R\downarrow$ | Unidirectional positioning repeatability of an axis |
| $R_i\uparrow$ or $R_i\downarrow$ | Unidirectional positioning repeatability at a position |
| $\bar{x}_i\uparrow$ or $\bar{x}_i\downarrow$ | Mean unidirectional positioning deviation at a position |
| $(X_{p4}, Y_{p4}, Z_{p4})^T$ | Coordinates of the probe tip in the rotary table coordinate system |
| $-Z_r\alpha_{rx}$ | Error motion in the x direction |
| $-Z_r\alpha_{ry}$ | Error motion in the y direction |
| $-Z_r\varepsilon_r(\theta)$ | Error motion in the tangential direction |
| $-r\varepsilon_t(\theta)$ | Error motion in the z direction |
| $A$ | Constant supplied by the manufacturer |
| $A$ | Bi-directional positioning accuracy of an axis |
| $B_i$ | Reversal error at a position |
| $B$ | Reversal error of an axis |
| $E_{AC}$ | Tilt error motion of C around X-axis |
| $E_{BC}$ | Tilt error motion of C around Y-axis |
| $E_{CC}$ | Angular positioning error motion of C |
| $E_{XC}$ | Radial error motion of C in X-axis direction |
| $E_{YC}$ | Radial error motion of C in Y-axis direction |
| $E_{ZC}$ | Axial error motion of C |
| $E$ | Bi-directional systematic positioning error of an axis |
| $E$ | Error on size |
| $FA_A$ | Axial four-axis error of sphere A |
| $FA_B$ | Axial four-axis error of sphere B |
| $FA$ | Axial four-axis error |
| $FR_A$ | Radial four-axis error of sphere A |
| $FR_B$ | Radial four-axis error of sphere B |
| $FR$ | Radial four-axis error |
| $FT_A$ | Tangential four-axis error of sphere A |
| $FT_B$ | Tangential four-axis error of sphere B |
| $FT$ | Tangential four-axis error |
| $K$ | Constant supplied by the manufacturer |
| $MPE_E$ | Maximum permissible error |
| $MPE_{FA}$ | Maximum permissible error for axial four-axis error |
| $MPE_{FR}$ | Maximum permissible error for radial four-axis error |
| $MPE_{FT}$ | Maximum permissible error for tangential four-axis error |
| $MPE$ | Maximum permissible error |
| $M$ | Mean bi-directional positioning error of an axis |

| | |
|---|---|
| $N$ | Number of fringes passed |
| $N$ | Number of input quantities |
| $P_i$ | Target angular positon |
| $R_i$ | Bi-directional positioning repeatability at a position |
| $R$ | Bi-directional positioning repeatability of an axis |
| $S$ | Centre-to-centre distance between two retro-reflectors |
| $U$ | Expanded measurement uncertainty |
| $X_A$ | Radial component of sphere A |
| $X_B$ | Radial component of sphere B |
| $X_i$ | Expanded measurement uncertainty |
| $X_{p4}\alpha_{rx}$ | Error motion in the z direction |
| $Y_A$ | Tangential component of sphere A |
| $Y_B$ | Tangential component of sphere B |
| $Y_{p4}\alpha_{ry}$ | Error motion in the z direction |
| $Y$ | Measurement result as a complete statement |
| $Z_A$ | Axial component of sphere A |
| $Z_B$ | Axial component of sphere B |
| $Z_r\varepsilon_t(\theta)$ | Error motion in the radial direction |
| $Z_r$ | Height of the point P |
| $\Delta L$ | Linear distance change |
| $\Delta h$ | Height difference between the centres of sphere A and sphere B |
| $\alpha_{rx}$ | Squareness error between $x$ axis and $\mathbf{O_4Z_4}$ |
| $\alpha_{ry}$ | Squareness error between $y$ axis and $\mathbf{O_4Z_4}$ |
| $\bar{B}$ | Mean reversal error of an axis |
| $\bar{x}_i$ | Mean bi-directional positioning |
| $\delta\mathbf{O_4}$ | Vector expressing linear motions of point $O_4$ |
| $\delta_r(\theta)$ | Radial error motion |
| $\delta_t(\theta)$ | Tangential error motion |
| $\delta_x(\theta)$ | Linear error of the origin coordinate system in direction |
| $\delta_y(\theta)$ | Linear error of the origin coordinate system in direction |
| $\delta_z(\theta)$ | Linear error of the origin coordinate system in direction |
| $\epsilon_k$ | Band energy in momentum space. |
| $\lambda$ | Wavelength of laser |
| $\mathbf{O_4X_4Y_4Z_4}$ | A fifth coordinate system on the rotary table |
| $\mathbf{O_4}$ | Origin of the coordinate system |
| $\mathbf{O_4}$ | Vector of origin of the rotary table system in **OXYZ** system |
| $\mathbf{P_4}$ | Probe tip vector in the rotary table system |
| $\mathbf{R}^{-1}(\theta)$ | Inverse rotational matrix of the rotary table |
| $\theta$ | Argument angle in cylindrical coordinates |
| $\theta$ | Rotated angle |
| $\varepsilon_r(\theta)$ | Angular error motion about the radial axis |
| $\varepsilon_t(\theta)$ | Angular error motion about the tangential axis |
| $\varepsilon_x(\theta)$ | Tilt motion of the rotational axis about $x_4$ |
| $\varepsilon_y(\theta)$ | Tilt motion of the rotational axis about $y_4$ |
| $\varepsilon_z(\theta)$ | Error of rotated angle $\theta$ |
| $d$ | Displacement |

| | |
|---|---|
| $i$ | Number of measurement points |
| $j_n$ | Normal backlash in gearboxes |
| $j_t$ | Circular backlash in gearboxes |
| $j$ | Number of measurement cycle |
| $k$ | Specified degree of confidence |
| $r$ | Radial distance from the axis of rotation of the rotary table |
| $r$ | Radius in cylindrical coordinates |
| $s_i$ | Estimator for the unidirectional axis positioning repeatability |
| $u_c(y)$ | Combined measurement uncertainty of $y$ |
| $x_{ij}$ | Positioning deviation |
| $y$ | Best estimation for the measurand $Y$ |
| $z_4$ | Axis of rotation |

# 1

# INTRODUCTION

*"I often say that when you can measure what you are speaking about, and express it in numbers, you know something about it; but when you cannot measure it, when you cannot express it in numbers, your knowledge is of a meagre and unsatisfactory kind."*

Lord Kelvin (Scientist, 1824 - 1907)

This chapter first provides a brief introduction to the motivation and problem statement of this thesis work, and then describes the methodological approach used as well as the scope and limitations. Lastly the structure of the thesis work is given chapter by chapter.

## 1.1 Motivation and Problem Statement

With the ever-increasing degree of complexity and diversity of industrial parts and assemblies, production environments are currently going through a transition period. Conventional factories are shifting from their traditional systems to smart/cyber factories with fully integrated virtual automation networks. This industrial evolution, often referred as *Industry 4.0*[1], has simultaneously impacted and shaped the ongoing challenges and trends in the field of production metrology. Therefore, the demand is increasing at a tremendous rate for more precise, accurate, holistic and faster metrological systems.

Since their first entrance to the market, the conventional stand-alone tactile (contact) CMMs have fulfilled many challenging tasks and established themselves as a versatile and flexible solution. Although meanwhile numerous other systems have been developing in the field of coordinate metrology, the conventional stationary mechanical type CMMs are still considered as most accurate coordinate systems and therefore have not lost their dominant importance and market share yet. On the other hand, that dominance brings in its wake the necessity to improvement of those machines in terms of measurement accuracy, precision and speed.

As an important extension and accessory of CMMs and iCT, rotary tables are one of the key elements which plays an important role to achieve those

1 **Industry 4.0** (Ger.:Industrie 4.0) *"refers to the idea that manufacturing is undergoing a fourth industrial revolution characterized by the individualization of products under the conditions of highly flexible production. Tasks that are currently still performed by a central master computer will be taken over by components. Components will network with one another in an intelligent way, carry out their own configuration with minimal effort, and independently meet the varying requirements of production"*[1].

goals. Similar to their functional utilisation in machine tools, they have established themselves also in conventional and coordinate metrological applications. Not only can rotary tables extend the part accessibility feature of workpieces or specimens but they also increase the overall system accuracy, despite the fact that they actually increase the number of sources contribute to measurement uncertainty. These sources, errors and their evaluation are important issues when it comes to assuring and improving the product and process quality.

In this context, there are several important subjects regarding the positioning accuracy of rotary tables. Aside from uni- and bi-directional repeatability, the reversal error is an important issue which needs to be dealt with and optimised in order to obtain more meaningful and accurate measurement results. Therefore, apart from reducing backlash by special designs and mechanisms, it is also of great importance to utilise or develop measurement set-ups which enable measuring the reversal error of rotary table systems in an accurate, cost-efficient and straightforward way.

## 1.2 Purpose and Significance of the Study

This thesis work has basically two main goals. In the theoretical part, it provides readers with the state of the art in the modern production metrology by making them familiar with both conventional (tactile) and advanced types of CMMs, i.e. optical and optoelectronic CMMs, Multi-Sensor CMMs, Portable-CMMs, and iCT. Furthermore, the utilisation, importance and accuracy characteristics of rotary tables in modern production metrology is explained.

As far as the practical part of this thesis work concerned, the main focus lies in designing, developing and implementing a measurement set-up equipped with a magnetic Hall-effect incremental linear encoder, in order to perform off-axis rotational measurements, and capture angular position information. In particular, a quite typical positoning error in rotary tables, i.e. reversal error, which causes inaccuracies in positioning, and affects bi-directional repeatability negatively, was measured and evaluated. In addition, the capability of the aforementioned measurement instrument and set-up was checked and verified by a more accurate measurement instrument as well, i.e. by a laser angle interferometer.

The practical part of the thesis was thought as a preparatory step for a collaborative project being developed at the Department of Interchangeable Manufacturing and Industrial Metrology (AuM) of TU Wien. In this ongoing project, a special gearbox for the utilisation purposes on wearable exoskeletons was designed and developed. The related patent application was made for that gearbox with a very low backlash value, and the decision is being waited at the time being. It is of great importance gathering angular position information accurately for a proper and effective function of wearable exoskeletons. Therefore the utilisation of encoders and positioning accuracy of rotary tables are issues that deserves special attention.

Analogous to this purpose, it is quite beneficial designing and implementing a measurement set-up equipped with a magnetic Hall-effect incremental linear encoder to measure reversal error in a manual rotary table as accurately as possible, and compare and verify the results by means of a more

accurate measurement instrument, e.g. by a laser angle interferometer, in order to determine practical capabilities of aforementioned magnetic Hall-effect incremental linear encoder in sensing angular position information in off-axis rotary applications.

Furthermore, it is also useful to investigate whether and to what extent the measurement of reversal error of a CNC rotary table is possible by means of a CMM and a standard reference sphere.

The measurements conducted on the set-up with the high-precision CNC rotary table;

- It was investigated whether and to what extent the measurement of reversal error of a CNC rotary table is possible by means of a CMM and a standard reference sphere.
- This was checked by measuring the same characteristics through a laser angle interferometer system (in the sequel of the measurements conducted by CMM), however, this time in a more limited measuring range.

## 1.3 Methodological Approach

To achieve aforementioned goals of the thesis work, after the literature review and defining the research issues, firstly, the optimal arrangement for the first measurement set-up including magnetic linear encoder was designed and necessary components were determined. Secondly, the required components were either purchased or manufactured.

After the measurement set-up was arranged and mounted properly, the measurement strategy was defined and measurement steps were planned. It was followed by a series of experimental measurements conducted by the author in the High Precision Measurement Room - Nanometrology Laboratory of the AuM at TU Wien. The obtained results were checked there by a more accurate measurement instrument, i.e. by a laser angular interferometer, and those results from different sytems were compared to each other and evaluated statistically to perform an analysis for the reversal error of the manual rotary table.

Subsequently, it was investigated whether and to what extent the measurement of reversal error of a CNC rotary table is possible by means of a CMM and a standard reference sphere. The verification was realised by another series of measurements by laser angle interferometer. Similar to previous process, results from different sytems were compared to each other and evaluated statistically to perform an analysis for the reversal error of the CNC rotary table.

## 1.4 Scope and Limitations

Due to the scope of this research there are some limitations that need to be addressed.

First of all, although modern production and coordinate metrology deals with surface geometries and properties as well, the theoretical

part of this thesis work mainly focuses on its applications on inspecting macro-geometrical features of industrial parts and assemblies.

Secondly, it should be noted that the practical part of this thesis work was aimed to build a preparatory basis for a project being developed at the AuM of TU Wien. Thus, the measurement instrument and set-up, which the related developer professors would like to implement for a similar purpose in the main project, was utilised and tested within the framework of this master's thesis, yet in a more straightforward example, i.e. in measuring reversal error of a manual rotary table.

Finally, since all the measurements are conducted in the High Precision Measurement Room - Nanometrology Laboratory of the AuM of TU Wien, the influences of ambient conditions on the measurement results and thus the measurement uncertainty could be kept at very low values.

## 1.5 Thesis Structure

The structure of this thesis can be broken down into five general parts:

Chapter 1 first provides a brief introduction to the motivation and problem statement of this thesis work, and then describes the methodological approach used as well as the scope and limitations. Lastly the structure of the thesis work is given chapter by chapter.

Chapter 2 consists of six sections and the first section (Section 2.1) represents an overview of the production metrology by explaining the historical evolution of its understanding, particularly within the framework of quality management. Furthermore, its importance and role in the Product Life Cycle (PLC) were given. The second and last subsection of this section is mainly based on the article [2] and summarises the main findings and ideas, which were discussed in the Association of German Engineers/Association for Electrical, Electronic and Information Technologies (Ger.: Verein Deutscher Ingenieure/Verband der Elektrotechnik, Elektronik und Informationstechnik) (VDI/VDE) Assembly. It represents the major challenges and trends waiting the manufacturing metrology to face with prospect to 2020. Then, in the second section (Section 2.2), first, a brief introduction of coordinate metrology was given by explaining its main characteristics and the measurement approach used. The third section (Section 2.3) gives first an overview of conventional (tactile) CMMs and CMSs by explaining the several different construction types, types of probing systems, related standards and guidelines, advantages and drawbacks as well as application areas. Then the main principles and structures of optical, optoelectronic and multisensor CMMs and CMSs were explained, followed by a subsection which describes a for medical purposes well-known, however for the industrial field recently and rapidly developing technology, Three-dimensional X-ray Computed Tomography (3D-X-ray-CT). It was described by explaining and discussing the principle of X-Ray tomography, advantages of this technology over conventional metrology instruments and systems, its application fields as well as by pointing out the main differences between iCT and mCT. The last subsection is dedicated to coordinate metrology applications

for micro- and nano-scale. In the fourth section (Section 2.4), rotary tables, their role in production metrology, and their integration with CMMs were represented, followed by a discussion on available international standards and guidelines for them. The fifth section (Section 2.5) explains some metrological terms and make clear distinctions between some widely misunderstood definitions. In the sixth section (Section 2.6) a quite important metrological concept, measurement uncertainty, was described in detail. The seventh section (Section 2.7) explains the positoning accuracy characteristics of rotary tables and axes. In the eighth section (Section 2.8) the concept of reversal error was introduced. The ninth section (Section 2.9) explains the definition of backlash, its measurement methods, and anti-backlash designs. The tenth section (Section 2.10) represents a solid theoretical background on a quite important subject for this thesis work, i.e. for encoders. Their classification according to various aspects was given and the most important points on their applications were pointed out. Lastly in the eleventh section (Section 2.11) the most important aspects of the laser interferometry technology were described by giving an overview of their working principle.

Chapter 3 explains the structure and design of the experimental measurements that conducted by the author in the High Precision Measurement Room - Nanometrology Laboratory of the AuM at TU Wien. Applied methodology, existing parameters and various key points were also described.

Chapter 4 represents the measurement results obtained in the present investigation, followed by the evaluation and statistical analysis of the related data.

As last chapter, Chapter 5 summarises the whole thesis, discusses its main findings, as well as provides readers with a discussion on open issues related to this subject which should be dealt within the framework of future research.

# 2

# THEORETICAL BACKGROUND AND STATE OF THE ART

*"It would be possible to describe everything scientifically, but it would make no sense; it would be without meaning, as if you described a Beethoven symphony as a variation of wave pressure."*

Albert Einstein (Theoretical physicist, 1879-1955)

This chapter consists of six sections and the first section (Section 2.1) represents an overview of the production metrology by explaining the historical evolution of its understanding, particularly within the framework of quality management. Furthermore, its importance and role in the PLC were given. The second and last subsection of this section is mainly based on the article [2] and summarises the main findings and ideas, which were discussed in the VDI/VDE Assembly. It represents the major challenges and trends waiting the manufacturing metrology to face with prospect to 2020.

Then, in the second section (Section 2.2), first, a brief introduction of coordinate metrology was given by explaining its main characteristics and the measurement approach used. The third section (Section 2.3) gives first an overview of conventional (tactile) CMMs and CMSs by explaining the several different construction types, types of probing systems, related standards and guidelines, advantages and drawbacks as well as application areas. Then the main principles and structures of optical, optoelectronic and multisensor CMMs and CMSs were explained, followed by a subsection which describes a for medical purposes well-known, however for the industrial field recently and rapidly developing technology, 3D-X-ray-CT. It was described by explaining and discussing the principle of X-Ray tomography, advantages of this technology over conventional metrology instruments and systems, its application fields as well as by pointing out the main differences between iCT and mCT. The last subsection is dedicated to coordinate metrology applications for micro- and nano-scale.

In the fourth section (Section 2.4), rotary tables, their role in production metrology, and their integration with CMMs were represented, followed by a discussion on available international guidelines and standards for them.

The fifth section (Section 2.5) explains some metrological terms and make clear distinctions between some widely misunderstood definitions.

In the sixth section (Section 2.6) a quite important metrological concept, measurement uncertainty, was described in detail.

The seventh section (Section 2.7) explains the positoning accuracy characteristics of rotary tables and axes.

In the eighth section (Section 2.8) the concept of reversal error was introduced.

The ninth section (Section 2.9) explains the definition of backlash, its measurement methods, and anti-backlash designs.

The tenth section (Section 2.10) represents a solid theoretical background on a quite important subject for this thesis work, i.e. for encoders. Their classification according to various aspects was given and the most important points on their applications were pointed out.

Lastly in the eleventh section (Section 2.11) the most important aspects of the laser interferometry technology were described by giving an overview of their working principle.

## 2.1 Production Metrology

*Production metrology*[2] is defined as "*the generic term for all activities connected with measurement and testing functions to be provided in the industrial development process of a product*"[4]. Measurement and the inspection of the geometrical features of workpieces is an essential field which constitutes the basis for task spectrum of production metrology together with two other main areas; functional inspection and material testing. In order to assure, manage and improve the quality of products, measurement and test data are required in almost every stage of the product development process. Providing such information constitutes the most significant objective of the production metrology, and it begins from the first life stages of a product, i.e. the development and design, and expands to the providing the customer with information related to the product and process quality. Technical tasks and aspects are, however, not the only part, which the production metrology is limited to. Its scope involves also the related organisational aspects within the context of production and metrology. [4]

In addition to the quality control of production processes and products, control of profitability needs to be taken into consideration as well, and they all together form the basis of total production metrology. It includes following points [5, 6]:

- Continuous monitoring of the production instruments and processes as well as products
- Occasional verification and review of economic efficiency
- Continuous application of Non-Destructive (Material) Testing (NDT)
- Application of destructive material inspection on a sample basis

2 While the term '**manufacturing metrology**' is most commonly used in the German language, the term '**production metrology**' is also typically found outside of Europe to refer to metrology within the context of production. [3, 4] The term production metrology was preferred in this thesis work.

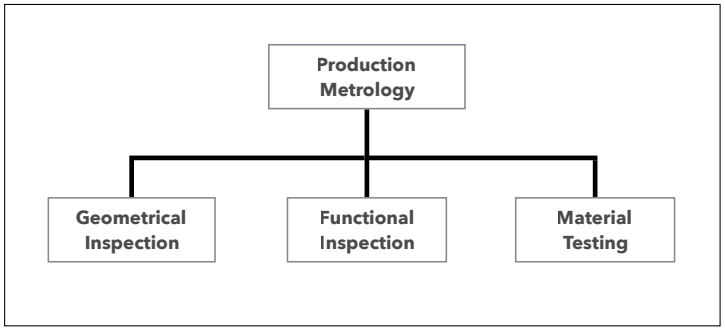


**Figure 2.1**: Three main task fields of production metrology

### 2.1.1 Historical Evolution of Production Metrology

In ancient and medieval times, dimensional measurement was to the fore. With the beginning of the industrialisation, *Taylorism*[3] and the division of labour had been the most dominant wave in the production, which enabled significant improvements and facilitations. Lastly this revolutionary philosophy has been taken one step further by *globalisation*. [8]

Inevitably, these changes have affected and formed the modern understanding of the production metrology. In the course of time, the definition and the understanding of the term *quality* has conceptually changed. First, it has been related merely to product or production, then, to the whole company or organisation. For the time being, it has become a general management task in the top management responsibilities, i.e. Total Quality Management (TQM), which does not only require the integration of organisation-internal elements such as all employees and workers but also the external relationships with the suppliers and customers. Thus, it takes into account several important subjects such as internal and external customer satisfaction, long-run organisational success, society and environment. [8]

In the light of this comprehensive concept of the TQM, the production metrology has been evolved from *checking, measuring, determining and eliminating of (defective) parts after their production* into a concept, which has centralised around the *preventive* measures against the production of those possible defective parts. Thus, it aims a production which is *in control*. [8]

So, all in all, production metrology has changed in several different aspects:

- *Scope*: Modern production metrology must support not only the production processes but also the whole PLC.
- *Time*: Inspection planning begins before or, at latest, simultaneously with the design phase, not after it has been completed.
- *Content and Aim*: From *checking and eliminating* to *preventing* the defective parts with the aid of production and processes which

3 The term **Taylorism** "*refers to Frederick Winslow Taylor, who insisted on the use of an outside observer (also known as (a.k.a) manager/supervisor) to ensure the most efficient use of labors' bodies down to the very last minutia of movement. He minimized any unnecessary activity, reducing each gesture to a single repetitive, mechanical task, as if the human body were just another machine operating in the factory*" [7].

**Table 2.1:** Historical evolution of production metrology within the framework of quality management (*adapted from* [8])

| Period | Issues, Milestones, Examples | Goals |
|---|---|---|
| Ancient times | Egypt, pyramids, length measurements | |
| Dark age | Guilds masters, norms | |
| Beginning of the 20th century | Taylorism, division of labour, quality inspection | |
| World War II | Stewart, control charts, sampling systems, ... | Compliance with technical standards |
| 1960 | Quality assurance, error prevention | |
| 1970 | Integrated quality assurance, design, sales | Fitness for use (Juran) |
| 1980 | System standards, TQM, general management | Fulfilment of customer needs and expectations |
| 1990 | Awards, integrated-QM, inclusion of Top-Management | Fulfillment of several stakeholders' needs |
| 2000 | Integrated-QM industry orientation under a single roof, inclusion of all employees from all levels, worldwide | Refinement of stakeholders, more focus on the environment, safety |
| 2010 | Processes, controlled processes | |
| 2020 | ... | ... |

are *in control*.

If the improvement measures are limited to changes in the production, this is described by the small quality control loop (Figure 2.2). If otherwise, i.e. if the target of the *controlled* production can only be achieved by means of the measures beyond the manufacturing, e.g. by design modifications or changes in suppliers, one speaks of the large quality control loop (Figure 2.2). [8]

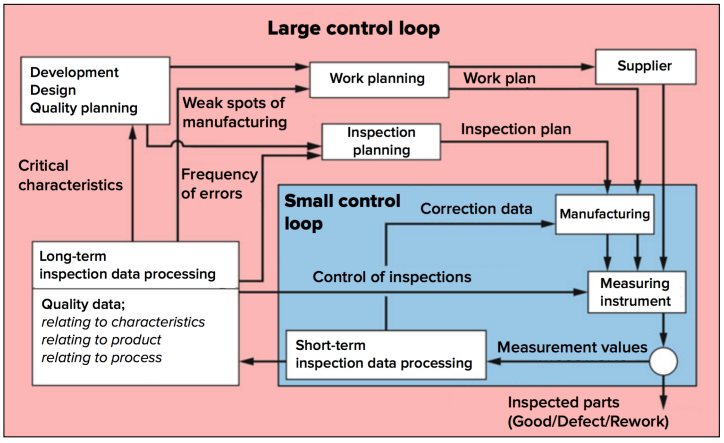


**Figure 2.2:** Production metrology in the small and large quality control loops (*adapted from* [8])

### 2.1.2 Challenges and Trends in Production Metrology

The worldwide existing major tendencies affect almost every industry around globe, and as an indispensable consequence they also shape the future of production technology. Using the available resources more efficiently, controlling the novel process technologies, manufacturing more flexibly and raising the transparency are the subjects, which are of the greatest importance for the production technology and related industries. In their roadmap for manufacturing metro-

logy*[2] Association of German Engineers (Ger.: Verein Deutscher Ingenieure) (VDI) outlines the major challenges and movements in production metrology with four key terms: *more flexibly*, *more accurate*, *more reliable*, and *faster*, which will be addressed in depth in the following sections. [2]

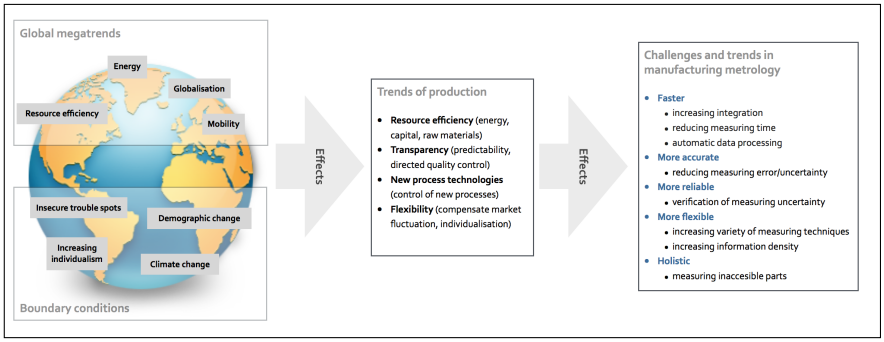


**Figure 2.3:** Global megatrends and their effects on the upcoming challenges and trends of manufacturing metrology (*adapted from* [2])

FASTER Time is perhaps the most important value of humankind. As in every other part of human life, time or in other words *doing the things faster* is always one of the first issues that needs to be thought when it comes to conducting science, technology, and in this particular case, to designing, producing and measuring industrial parts and assemblies. Be it for the reasons of competitiveness or building more efficient production and measurement processes, it is always aimed to reduce the work times and cycles as much as possible.

In a (production) metrological point of view, *faster* or *faster processes* can be interpreted in two ways. Firstly, gathering the required (dimensional) information regarding the product quality in a briefer time by improving, optimising, and perhaps combining the already existing measurement techniques and processes [2]. In this context, optical techniques are of great importance. Secondly, conducting measurements and gathering measurement results more rapidly by integrating metrological approaches and applications to production steps more compactly and tightly, which can be realised particularly with the help of automation [9].

Not only does this help to reduce or even eliminate the times required for the transportation to the measuring unit or instrument but it also makes the information and results related to measurements directly available in production, thereby allowing the incorporation of control loops, for instance.

MORE ACCURATE As the competitiveness in the industrial market rises rapidly, so does the internal and external customers' demands regarding to quality of the parts and assemblies. Although *accuracy*[4] is the keyword here for the better quality specifications, its correct interpretation and usage is realised by using the term *measurement uncertainty*[5] according to the International Vocabulary of Metrology

4 See Section 2.5 for the proper definition of the term **Accuracy** or more precisely **Measurement Accuracy**.

5 See Section 2.5 for the proper definition of the term **Measurement Uncertainty**.

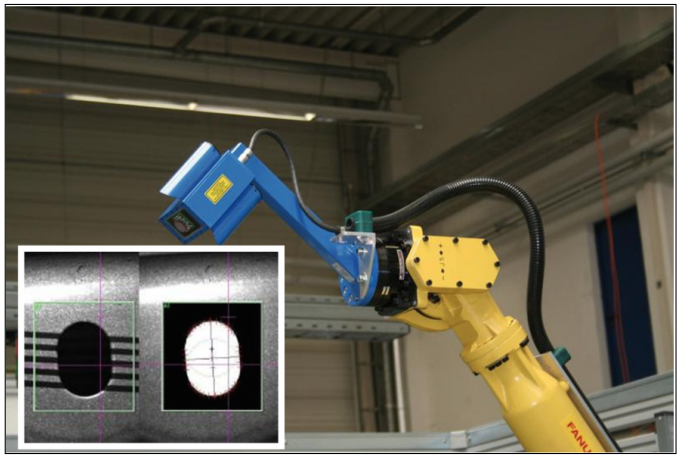

**Figure 2.4:** Faster metrology for the inspection of automotive body components by the utilisation of multi-line triangulation sensor on robots to optically detect position tolerances for stamping holes [10]

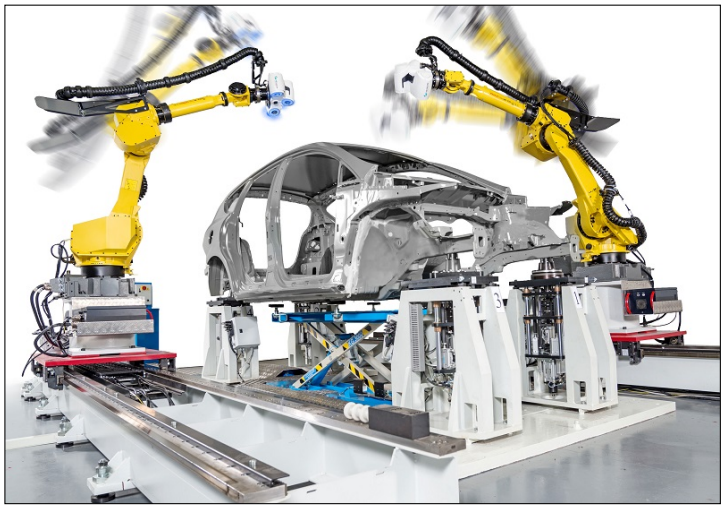

**Figure 2.5:** Faster metrology with the aid of automated non-contact in-line measurement solutions [11]

(Fr.: Vocabulaire International de Métrologie) (VIM) [12]. Reducing the measurement uncertainty, and gathering more accurate results are therefore one of the most challenging aims in every area of modern production metrology.

This affects the coordinate metrology both in macro-, micro- and nano-scale. In this context, a better accuracy is an indispensable demand for the measurement systems, given the fact that the tolerances are getting more and more tighter[6].

Increasing demands on measurement accuracy bring in its wake that the techniques from other some relevant disciplines, e.g. from geodesy, are being used and adapted more and more often in manufacturing metrology. Besides that, the developments in technology of optical and opto-electronic systems as well as the decrease of the computation cost

6 See also Section 2.6.1 for a comprehensive understanding of the relationship between the measurement uncertainty and the decision rules according to the ISO 14253-1

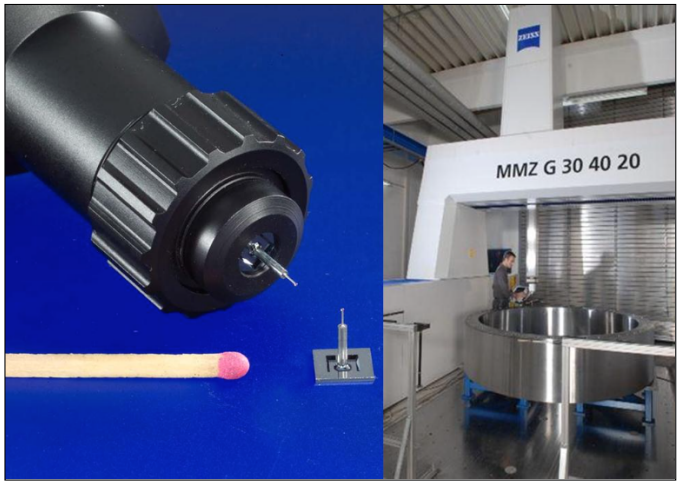


**Figure 2.6:** More accurate measurements both on macro- and microscale [2, 13]

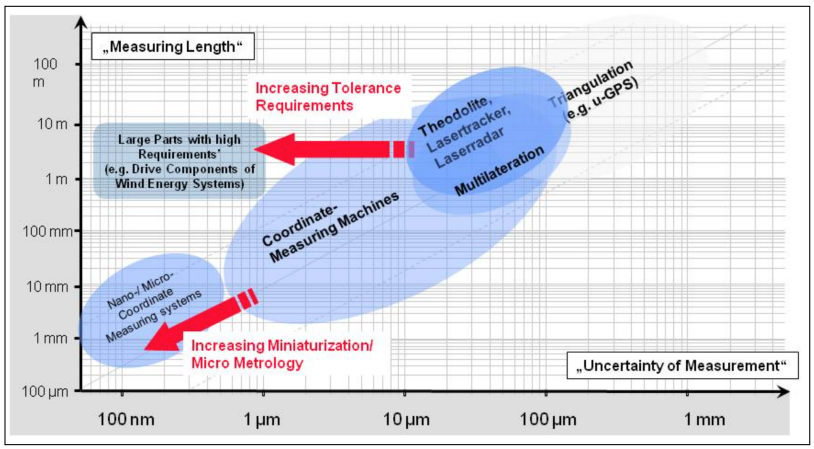


**Figure 2.7:** Ongoing trends and challenges of accuracy (measuring uncertainty) depending on the measurement instrument used [14, 15]

and time broaden the application spectrum of digital photogrammetry and laser-trackers [16].

Furthermore, increasing miniaturisation triggers a demand for greater levels of accuracy [17]. Figure 2.7 shows the order of magnitude of these trends from an industrial perspective. There is an obvious correlation between measurement uncertainty and dimension. Additionally, the need to check tighter tolerance for large dimensions is visible.

Last but not least, measurement of electrical characteristics [18] and material properties [19] causes a demand for more accurate measurement results as well, and therefore monitoring and correction of environmental influences gain more and more importance.

MORE RELIABLE Every measurement result requires the statement of measurement uncertainty, otherwise it could not be considered as complete and meaningful. Therefore the importance of determination, evaluation, and especially the reduction of measurement uncertainties increases rapidly.

In addition to the standardised procedures for abovementioned goals, custom-tailored solutions according to different measurement tasks will establish themselves, which are obviously facilitated in comparison to the standardised procedures. Besides, documentation on measurement uncertainty will probably be necessary for product impacting the whole safety of produced goods in industries such as aviation and the medical devices. This will consequently trigger improvements in safety and reliability [20].

Moreover, the importance of Computer-Aided Simulation (CAS) of measurement processes mainly based on the *Monte-Carlo method* [21] for determining measurement uncertainty will probably continue to grow.

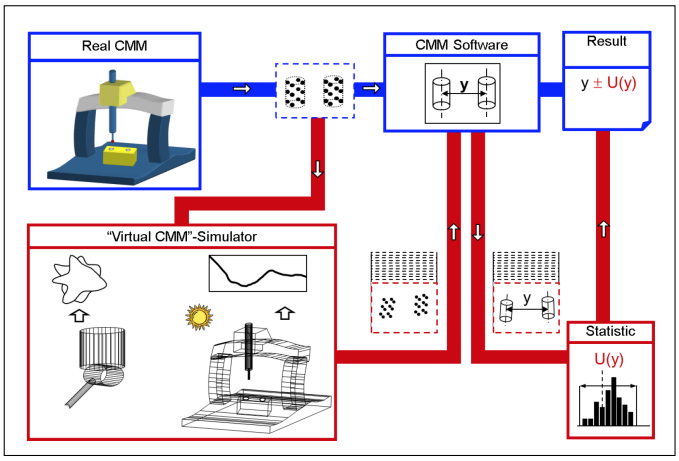


**Figure 2.8:** Utilisation of Monte-Carlo simulation to estimate measurement uncertainty in CMMs: Interaction between *Virtual CMM* and CMM software [22, 15]

MORE FLEXIBLE As in the combination of different production technologies, several measurement methods are also getting combined into compact systems that increase the flexibility and adaptability of whole measurement process. Those systems are called *Multisensor Measuring Machines*[7] (Figure 2.9). Since they consist of several different sensors and measuring principles, the level of system complexity as well as the required training time and effort for the measurement personnel increase significantly.

HOLISTIC Nowadays, the technologies which holistically register the shape of a product are used in production metrology all the more frequently. Apart from the photogrammetry and fringe projection [23], by means of Computed Tomography (CT), it is even possible to register structures, which are not accessible from the outside [24]. CT is used to determine defects in castings or for running dimensional plausibility checks, and for many other challenging measurement tasks. CT systems have already reached measurement times which makes it possible to integrate them into the precisely monitored production systems and processes, i.e. for in-line utilisation [25].

7 See Section 2.3.6 for a more detailed overview of Multisensor Measuring Machines.

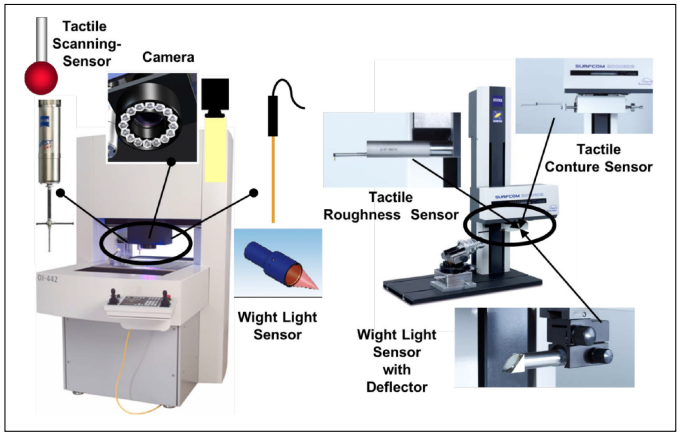


**Figure 2.9:** Types of Multisensor implementation: Parallel sensor implementation on a CMM (left), changeable sensor implementation on surface texture measuring device [2]

Computerised control and evaluation systems represent here a vital part, and accordingly, the need for a faster and more efficient integration of computer systems with production itself and production metrology, i.e. Industry 4.0, is indispensable. [2]

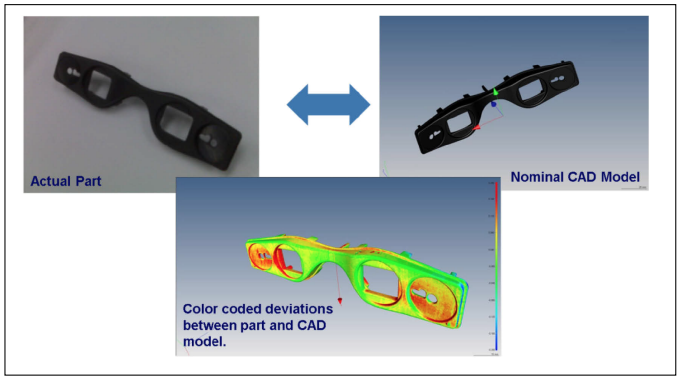


**Figure 2.10:** Easy-to-understand colour-coded presentation of measurement results obtained by a *holistic* measuring system [2]

Moreover, due to the holistic techniques, the presentation of measurement data has become easier and more straightforward to understand, especially for the first-glance reviews. This is ensured, e.g. by coloured visualisation of the deviations between actual data and the nominal model (Figure 2.10). Nevertheless, because of the necessity to the visual interpretation for the representation, and due to the low usability for automatic evolution, it is not probable that they will replace the tolerance characteristics defined according to ISO within the framework of a function-oriented evaluation.

## 2.2 Coordinate Metrology

Coordinate metrology is a universal measurement method, in which the surface of the workpiece in a coordinate system is scanned point by point. The characteristics to be determined are defined from those

obtained surface points in several intermediate steps. As a very versatile and flexible method it can be applied for a wide range of tasks, and therefore stands out due to its universality. [8]

The principle of coordinate metrology consists of touching the *real* area element of a workpiece point by point, and combining the probing points together mathematically (Figure 2.11). This creates a *numeric image* of the surface as associated geometrical feature (e.g. a plane, a circle or a cylinder). The assignment is done either manually or automatically via algorithms. [8]

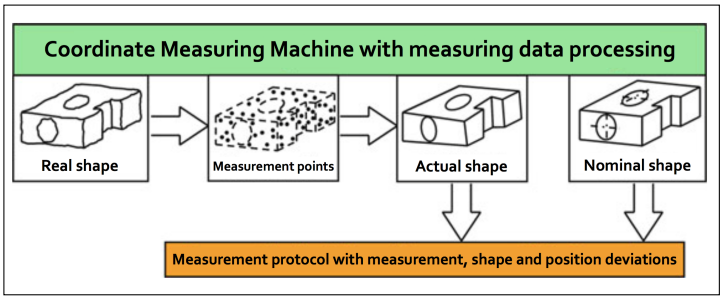


**Figure 2.11:** Main principle of the coordinate metrology (*adapted from* [8])

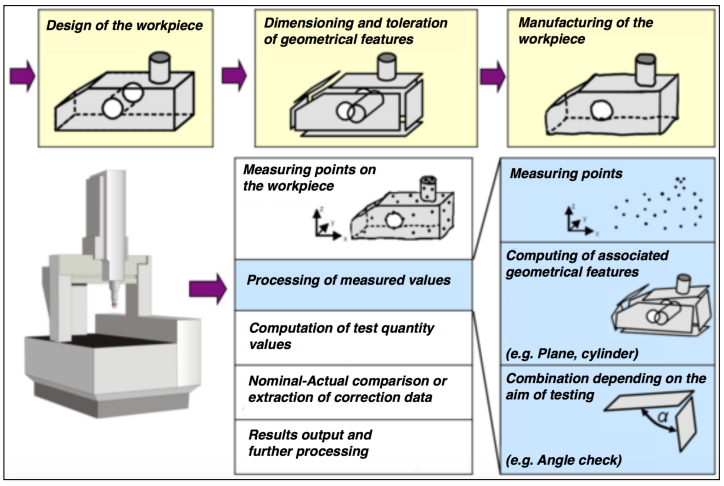


**Figure 2.12:** Main principle and workflow of the coordinate metrology in detail (*adapted from* [26])

The associated geometrical feature is geometrically ideal, and serves as a reference for the determination of dimensions, as well as for the calculation of geometrical deviations. The function of a workpiece is determined by size, shape, position and surface geometry of its elements. The coordinate metrology can be used to identify characteristics of the following feature groups: [8]

- Dimensions, distances and angles
- Form deviations
- Positional relations

In contrast, conventional measuring equipments with only one measurement axis normally allow to measure only individual points, distances or diameter of geometrical features. Interaction of characterist-

ics of all geometrical features, which are often crucial for the function of a workpiece, can be assessed only in a common reference system. The CMM represents such a reference system. It captures the shape of the workpiece, however, also with restrictions. Dimensions, form and position of geometrical features can be grasped point by point, and while scanning a lot of points, they can be captured also along a line or curve. [8]

There are characteristics that can be determined directly on the associated geometrical feature (e.g. diameter, length, roundness, axis, perpendicularity, straightness, flatness). Other characteristics arise from the linking of two or more associated geometrical features: Distance, angle, intersection point, symmetry point, axis, plane or perpendicularity. The measured points, which gathered by CMM at the true shape of the workpiece, are compared to the geometrical data of the nominal shape and the deviations from the nominal dimensions, as well as shape and position characteristics are determined from this comparison (Figure 2.11). [8]

### 2.2.1 Measurement Approach

CMMs can be used versatilely for individual measurements, small and medium series. They are used to test complex workpieces such as engine and transmission housings, pump bodies, turbine blades, steering knuckles, steering struts, gears, worm gears and threaded spindles. In this regard, contacting and/or non-contacting sensors are utilised to capture and collect required measurement points. [8]

CMMs with three measuring axes arranged perpendicular to each other in the x-, y-, and z-direction (Cartesian coordinate system) are most commonly used. In addition, there are CMMs with angular measurement systems [27].

If the real surface were geometrically perfect, it would be enough to touch them with the mathematical (theoretical) minimum number of points. Nevertheless, the true figure has more or less great form deviations, so it is not ideal geometrically. Therefore the mathematical minimum number of probing points is not sufficient to approximate to the actual area. The probing points represent only a sample of the infinitely many points on the surface. Number and location of the measurement points should be so selected, that they are representative of the considered surface, and allow a measurement with demanded measurement uncertainty. [8]

**Table 2.2:** Minimum required number of probing points

| Geometric Element | Mathematical (Theoretical) Minimum Number | Metrological (Practical) Minimum Number |
|---|---|---|
| **Point** | 1 | 1 |
| **Line** | 2 | 3 |
| **Circle** | 3 | 4 |
| **Plane** | 3 | 4 |
| **Sphere** | 4 | 6 |
| **Cylinder** | 5 | 8 |
| **Cone** | 6 | 12 |

The measured points in the coordinate system of the CMM do not give the *true* picture of the workpiece shape. The probe (stylus-tip), usually a ball, is not a point but a body with a finite expansion. Consequently, equidistant bounding volume arises from the touched geometrical features. The coordinates of the measured points lie in front of the workpiece surface (Figure 2.13). To calculate a point of the touched workpiece surface, the stylus-tip centre must be shifted in the workpiece surface equidistantly. The measuring point evaluation for free-form surfaces (e.g. body parts) is particularly difficult. [8]

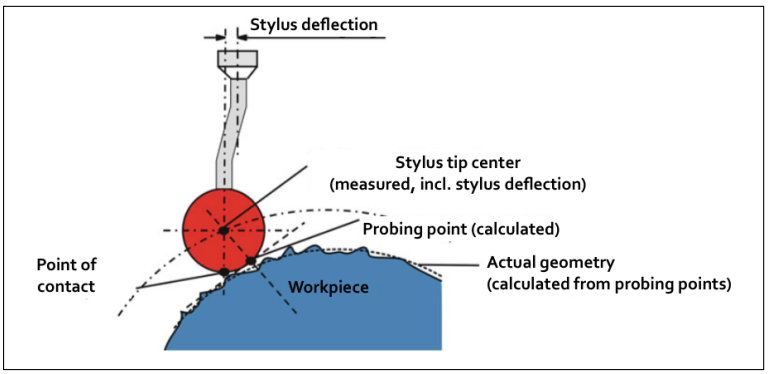


**Figure 2.13:** Measuring point evaluation (*adapted from* [8])

With such surfaces, whose mathematical function is not known, the surface-normal must be calculated on the basis of several touches around a probing point. The measuring point evaluation is an important task to calculate the actual geometry. Furthermore, there are two other issues; the probe radius correction to compensate for the flattening of the probe body, and the stylus deflection under the influence of measuring force. The measuring systems of the CMM grasp the stylus-tip centre as a substitute for the probing point which does not have to coincide with the point of contact (Figure 2.13). The actual geometry of the workpiece is calculated from the probing points. [8]

## 2.3 Coordinate Measuring Machines and Systems

### 2.3.1 Introductory Overview

For single inspection tasks of non-complex products, commonly used (One-dimensional (1D)) inspection instruments, e.g. vernier callipers, screw micrometers and height measuring devices, are often sufficient and suited. However, for more complex inspection tasks, e.g. positional tolerances or repetitive measurements, conventional CMMs are very useful. During the last decades CMMs have become an indispensable instrument in the production metrology. Besides conventional CMMs, there exist many other CMSs which are more and more used in coordinate metrology.

Although CMM can be defined in several ways, according to the related part of the ISO 10360 standard [27], CMM defined as "*a measuring system with the means to move a probing system and capability to determine spatial coordinates on a workpiece surface*" [27].

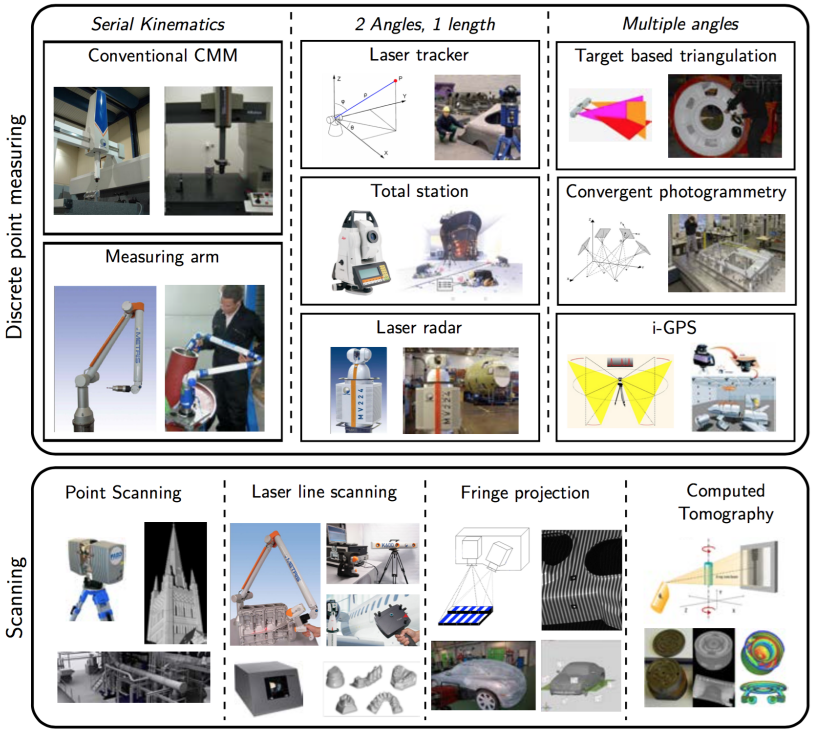


**Figure 2.14:** A classification of common CMSs [28]

Each CMM is composed of following main components (Figure 2.15) [29]:

- A mechanical body which consists of three axes and linear and/or angular displacement transducers,
- A probe head, which carries the sensor that captures and collects the measurement points on the part and therefore conducts the actual measurement,
- A unit to assure the control, and
- A computer with accessory equipment for printing and software to calculate, analyse and display the measurement results. There is often a network, to which the computer connected in order to receive CAD data and programs and to send reports and information related to measurements conducted.

A Cartesian reference coordinate system is formed by the three frames of a CMM, and the probe head is mounted. Displacement along a coordinate path is evaluated by means of scales or transducers. Typical steps of a measurement by a CMM can be summarised as follows: [29]:

- Calibration of the stylus or probe tip with respect to the probe head reference point normally using a calibrated sphere (provided an electromechanical 3D probe is used)
- Determination of the workpiece position and orientation (workpiece coordinate system (WCS) in relation to the machine coordinate system (MCS))
- Measurement of the surface points on the workpiece

- Evaluation of the geometric parameters of the workpiece
- Representation or reporting of the measurement results

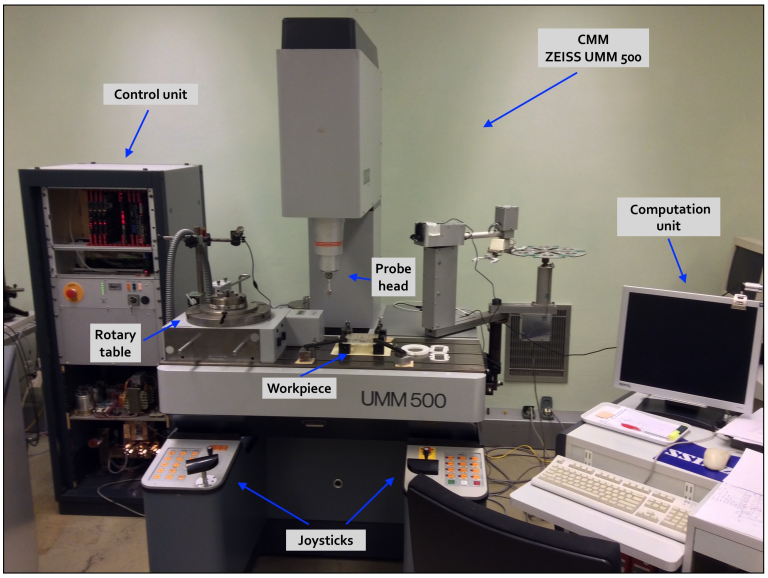


**Figure 2.15:** A typical conventional CMM and its main components

CMMs can be identified as systems which enable to conduct the above-mentioned steps and therefore as *main players* in the coordinate metrology.

There exist important advantages when the coordinate metrology is compared to the conventional metrology. A summary of these significant advantages is given in Table 2.3.

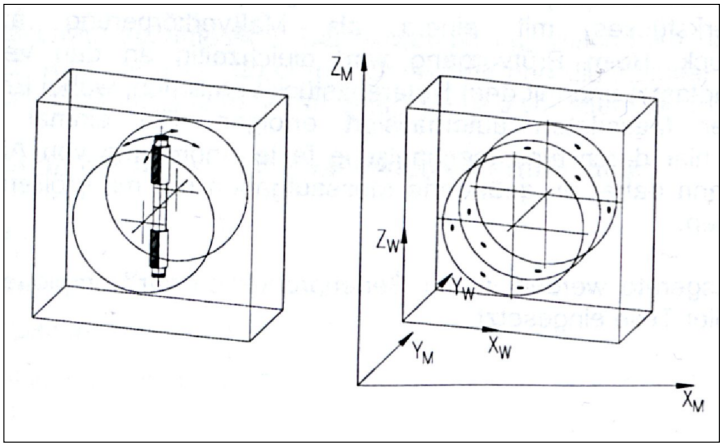


**Figure 2.16:** Conventional metrology vs. coordinate metrology [30]

## 2.3.2 Probing Systems for CMMs

Probing systems builds the core of the coordinate metrology. Although there are various types of sensors and probing systems available, they can be classified into two broad categories, i.e. contact probing systems, and non-contact probing systems. While the contact probing systems register the structures by touching the workpieces, non-contact

**Table 2.3:** Comparison between characteristics of conventional surface plate metrology and coordinate metrology [29]

| **Surface Plate Metrology** | **Coordinate Metrology** |
|---|---|
| Manual and time-consuming alignment of workpiece | Manual alignment not necessary |
| Single-purpose measuring instruments are difficult to adapt to changing measuring tasks | Simple adaptation to changing measuring tasks by software |
| Comparison of individual measurements with artifact dimensions, that is, gage blocks, ring gages, or others | Comparison of measurements with mathematical or numerical models |
| Separate determination of size, form, location, and orientation with different setups | Determination of size, form, location, and orientation in one setup using one reference system |
| Individual performing measurements must be highly skilled | Individual performing measurements need not be skilled if a program is prepared for the task |
| Manual nature of methods hinders throughput — cannot be made automatic | Throughput less dependent on operator — can be made fully automatic |

probing sytems do not have to touch the workpieces mechanically, they use other technologies and methods than mechanical contact. Due to this fact they enable conducting faster measurements with considerably higher measurement point densities. On the other hand, contact (tactile) probing systems provide better features in terms of reliability and accuracy. A further classification of these two categories of probing systems is illustrated in Figure 2.17.

Touch-trigger probes can be assumed as the most popular and common contact probing systems. Their principle can be explained with following steps [28];

- Probe approaches the workpiece surface,
- Probe tip touches the surface,
- Stylus is deflected,
- Detection of the stylus deflection is realised by the probe sensor, i.e. by strain gauges or electrical switch,
- CMM is triggered to read out the positional information of the axes, and
- Diameter of the stylus-tip is taken into consideration, and the required positional information of the point on the workpiece surface is obtained.

On the other hand, some probing systems are more capable than merely detecting the stylus deflection. They can also measure the amount of this deflection. These systems are referred to as *measuring* probes and provides usually better accuracy values compared to the touch-

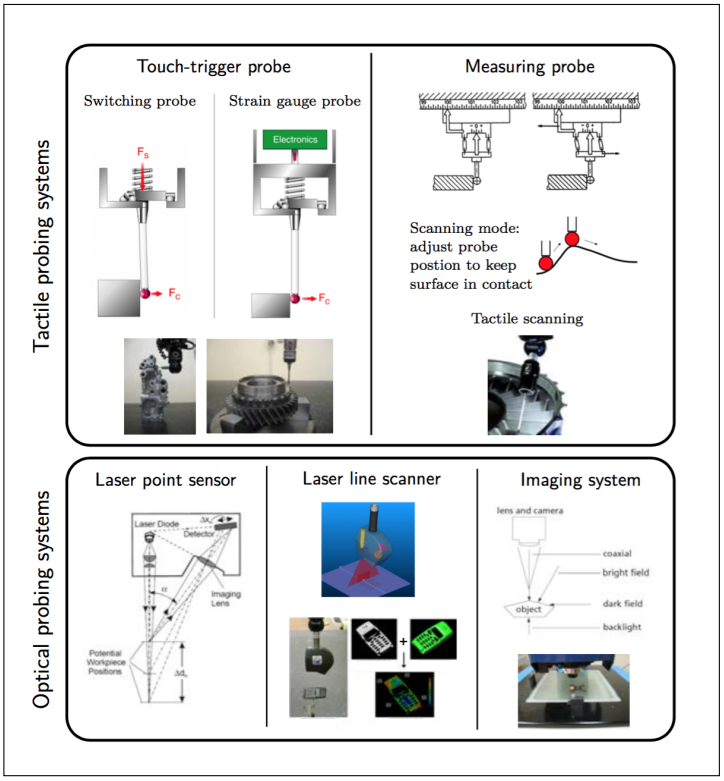


**Figure 2.17:** A classification of various probing systems for CMMs [28]

trigger probes. Furthermore, as the amount of deflection is determined, this data can be evaluated as a feedback for CMM. Thus, it becomes possible to *scan* a certain path while the stylus tip is regularly in contact with the workpiece surface. Figure 2.17.

In context of non-contact probing systems, Two-dimensional (2D) probing systems come into prominence. In addition to the vision probes which are mostly used on special dedicated CMMs, laser line scanners have also established themselves recently as a very useful measurement solutions. The biggest advantage they offer is the relatively high measurement speed. Due to this fact they are very often utilised in measuring free-form surfaces with partly complex structures, e.g. mould products and car bodies. However in terms of accuracy, the contact probing systems are not overcome yet by laser line scanners. [28].

### 2.3.3 Related standards and guidelines for CMMs

Although there exist several but basically similar national standards and guidelines such as VDI/VDE 2617 and American Society of Mechanical Engineers (ASME) B89 4.1, the worldwide most recognised and widespread applied standard for CMMs is the international standard ISO 10360 issued by ISO, and due the scope of this thesis, only its most significant and related parts for this thesis work will be covered in the following sections, i.e. Part 2 and Part 3.

#### 2.3.3.1 ISO 10360: Acceptance and reverification tests for CMMs

The ISO 10360 standard is actually a series of standards and explains the required procedures and steps to conduct performance evaluation tests for conventional CMMs. Among the several parts of the standard, the most important and therefore the most often utilised part is the second part; i.e. the ISO 10360-2:2009. It explains the required steps of a performance test in order to evaluate size measuring performance.

Table 2.4 gives an overview of all current standards in the ISO 10360 series.

**Table 2.4:** Overview of ISO 10360 standard series (April 2016)

| Part | Content |
|---|---|
| ISO 10360-1:2000 + Corr 1:2002 | Vocabulary |
| ISO 10360-2:2009 | CMMs used for measuring linear dimensions |
| ISO 10360-3:2000 | CMMs with the axis of a rotary table as the fourth axis |
| ISO 10360-4:2000 + Cor. 1:2002 | CMMs used in scanning measuring mode |
| ISO 10360-5:2010 | CMMs using single and multiple stylus contacting probing systems |
| ISO 10360-6:2001 + Cor. 1:2007 | Estimation of errors in computing Gaussian associated features |
| ISO 10360-7:2011 | CMMs equipped with imaging probing systems |
| ISO 10360-8:2013 | CMMs with optical distance sensors |
| ISO 10360-9:2013 | CMMs with multiple probing systems |
| ISO 10360-10 | Laser trackers for measuring point-to-point distances |
| ISO/WD 10360-11 | Computed tomography |
| ISO/FDIS 10360-12 | Articulated arm CMMs |

*Size test* A set of five material standards of size (step gauge or gauge blocks) is measured under seven different orientations on the CMM. Each measurement is repeated three times. The shortest material of size should be smaller than 30 mm, the longest should be longer than 66 % of the largest spatial diagonal of the measuring volume of the CMM. For each of the 105 measurements, the error on size $E$ is calculated. All errors are plotted on a graph as a function of the measured length.

The error on size, $E$, should not exceed a given maximum permissible error (MPE), and $MPE_E$ is usually expressed in the following way:

$$MPE_E = \pm[A + \frac{L}{K}] \tag{2.1}$$

where $MPE$ is the maximum permissible error[8]. In other words, $MPE$ is the tolerance. The $A$ and $K$ terms are constants supplied by the manufacturer, and $L$ is the measured length in millimetres. For a typical machine, the specification might look like

$$MPE_E = 2.5 + \frac{3L}{1000}[\mu m] \tag{2.2}$$

In case of acceptance tests, these values are stated by the manufacturer of the CMM. In case of reverification tests, they are defined by the

8 It should be noted that just $E$, not $MPE$, is also used.

user. The latter could be useful when the CMM is installed in a non-conditioned environment and a lower accuracy is allowed. The result of a ISO 10360-2 test is fail or pass, it should never be the purpose of this test to define the MPE values.

### 2.3.4 Contact Type (Tactile) CMMs and CMSs

A conventional CMM has, just like many manufacturing machines, a Cartesian X-Y-Z–configuration. At the end of the Z-axis a probing system is mounted. The probing system, which can be moved in 3D-space, detects points on the surface of the workpiece. These points are used to reconstruct features (e.g. circles, lines, planes, cylinders). The feature parameters and the relationships between the features allow to evaluate the tolerances. Figure 2.15 illustrates the different CMM components, the CMM structure and the probing system are discussed in the next sections.

#### *2.3.4.1 Conventional Stationary Types of Tactile CMMs*

The basic CMM consists of three axes, each provided with a guide way that enables precise movement along a straight line. Each guide way has a carrier that moves along. The carrier enables the second carrier to move along a straight line based on the first guide way. Each axis is fitted with a precision scale that records the position of the carrier measured from a reference point. The measuring probe is fitted to the carrier on the third axis. When the measuring probe touches the object being measured, the measurement system records the position of all three axes.

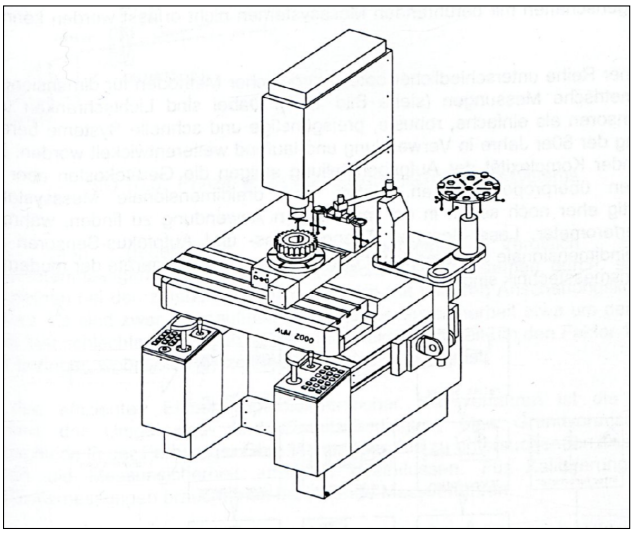

**Figure 2.18:** 3D CAD drawing of a typical conventional CMM; UMM 500 of Zeiss company [30]

There exist several physical configurations for CMMs, and most of those are demonstrated in *ISO 10360-1:2000 + Cor.1:2002 - Geometrical Product Specifications (GPS) – Acceptance and reverification tests for co-ordinate measuring machines (CMM) – Part 1: Vocabulary* (Figure 2.19). All the configurations have a method of moving the probe along three

axes relative to the object. Although there are many designs of CMMs they can be grouped into five basic types as follows:

- Cantilever type
- Bridge type
- Horizontal arm type
- Column type
- Gantry type

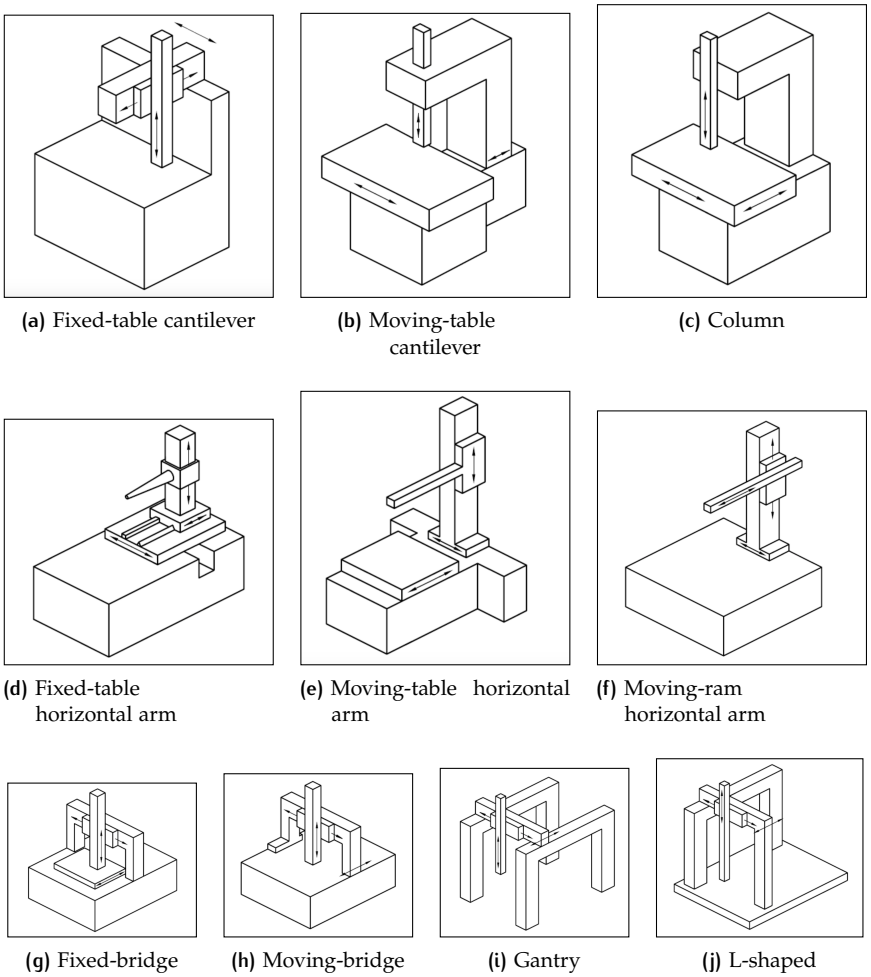


**Figure 2.19:** Different construction types of CMMs [31]

CANTILEVER TYPE CMM In the cantilever configuration a vertical machine ram in Z-axis, to which the measuring probe is attached, makes a movement on a cantilever beam in Y-axis and the cantilever beam itself moves perpendicularly to Y- and Z-axes, e.g. along the X-axis.

This type of CMMs offer good accessibility features and allow high speeds and accelerations, due to the fact that the column is not heavy and has a large supporting base. Moreover, the *Abbé's principle*[9] has

9 According to **Abbé's principle**, the scale of a linear measuring system should be collinear with the spatial dimension or displacement to be measured. If this is not the case, the measurement must be corrected for the associated Abbé Error.

been complied so far as possible in the arrangement of measuring systems, and therefore they have small measuring uncertainties. That is the main reason of their widely utilisation for precision measurements on gages and master parts. As the projecting part of the column structure is rigid and therefore must be short, this configuration is only suitable for small measuring ranges.

BRIDGE TYPE CMM Bridge type CMM configuration is the most widely used one among several different CMM configurations. They can be classified into two sub-categories depending on whether the table or the bridge structure is the moving element. What the both sub-category have in common is that a vertical ram in Z-axis, to which the measuring probe is attached, makes a movement along the Y-axis on a horizontal beam which is called bridge. In the first sub-category of the bridge type configuration, i.e. in moving-bridge configuration, the movement of the bridge takes place along the X-axis on guideways on the fixed table and so the probe is carried. In the second sub-category, i.e. in fixed-bridge configuration, this time the bridge stays fixed to the CMM bed and the table moves with workpiece on it along the X-axis.

The common advantages of both sub-configurations are the high rigidity, and as a consequence high measuring accuracy and small deviations. While on the one hand the compact bridge structure enables this high rigidity, on the other hand existence of a bridge limits the accessibility, which is their common drawback.

Specific advantage of the moving-bridge configuration is the fact that they allow and facilitate the measurement of very heavy workpieces (The workpiece does not move) due to their rigid structure. Their drawbacks are that two columns move at different places. This may result in twisting of the portal. The drives of the columns can be designed as combination drives with position rules to reduce of this effect. This type of CMM represents a good compromise between the demands for good accessibility, large measuring volume, low cost and low measurement uncertainty.

Specific advantage of the fixed-bridge configuration is the very low measurement uncertainty due to the rigid structure. The disadvantages are can be summarised as follows. Firstly, smaller operating speeds because of the fact that the heavy table together with the workpiece must be moved. Secondly, the weight of the workpiece is limited, and finally this configuration is suitable only for a small measuring volume.

COLUMN TYPE CMM The column configuration of CMMs are akin to vertical milling or drilling machines, and are also referred to as universal measuring machines. The table is moved in X- and Y- directions in this design. The advantages of column type CMMs are their high accuracy and rigidity values.

HORIZONTAL ARM TYPE CMM In the horizontal arm type CMM there exists a horizontal arm that moves in X-axis. Different from the other CMM configurations, where the probe is mounted to the Z-axis arm, it is mounted to the Y-axis arm in horizontal arm type CMMs. The most important advantage this configuration bring itself is the large

measuring volumes, and being free from obstruction. They are used for the inspection of large objects, e.g. an automotive body.

GANTRY TYPE CMM Gantry-type configuration represented by a structure, in which the vertical ram (Z-axis) moves vertically relative to the horizontal beam (X-axis), which itselfs moves along two rails mounted on the floor. Advantages of this configuration are the easy accessibility and possibility of the measurement of large workpieces.

SUMMARY AND COMPARISON OF DIFFERENT TYPES CMMs can be categorised according to their structural configuration. These different designs of CMMs have all their advantages and drawbacks against each other and the decision for their choice should be given in the light of information about the measurement tasks that will be conducted with CMM. Thereby, area of application, precision, accuracy and measuring range are typical decisive points. Moreover, the achievable measurement deviation is often an important criterion. [8] Table 2.5 demonstrates the main characteristics and application areas of the most common CMM configurations and their general application.

**Table 2.5:** Characteristics and application areas of the most common CMM configurations and their general application [29]

**The Most Common CMM Configurations and Their General Application**

| Applications/ Configuration | Moving Bridge | Fixed Bridge | Cantilever | Horizontal Arm | Gantry |
|---|---|---|---|---|---|
| | 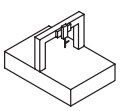 | 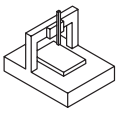 | 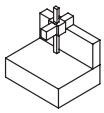 | 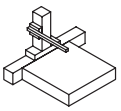 | 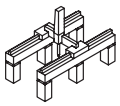 |
| General-purpose applications | X | X | X | X | |
| Accuracy | X | X (gage calibration) | | | |
| Large parts | | | | X (car bodies, large castings) | X (aerospace structures, large vehicles) |

### 2.3.4.2 Articulated Measuring Arms

As a next generation of conventional stationary type tactile CMMs, articulated measuring arms have established themselves as inexpensive and versatile measuring devices. Due to their characteristics, they enable to conduct dimensional measurements faster and more efficiently. The most significant advantage they bring with is the high flexibility. Unlike with conventional CMMs, using measuring arms there is no need to bring parts to be measured back-and-forth from workshop to measurement labs or rooms. Instead of bringing parts to be measured to the measuring instruments, measuring instruments are brought to the parts to take measurements. Due to that flexibility they are able to provide a better feedback exactly there and under those conditions, where also manufacturing takes place. Besides that, portable measuring arms are considered as a more economical solution in comparison to conventional CMMs, which makes them used widespread in several different industries.

However, conventional articulated measuring arms utilise the same probing technology as the conventional CMMs, i.e. tactile, and that fact makes them sensitive to ambient conditions, especially to vibrations and temperature. Therefore, nowadays, a majority of measuring arms (with tactile probes) are either combined with optical scanners or outdated by armless portable measurement devices.

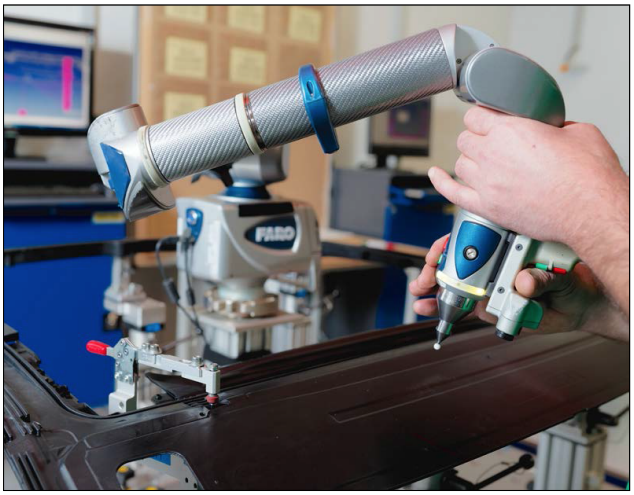


**Figure 2.20:** An articulated measuring arm [32]

Furthermore, if the whole working or measuring volume is considered, their volumetric accuracy is not consistent everywhere. Actually, this specification relies on the resolution of the encoders at each articulation of the arm (an arm is usually provided with 6 joints). Thus, the more the measurements are taken away from the basis of the arm, the less the articulations of the arm will have to rotate (for the same displacement of the effector), which results in an overall lower resolution. Regarding the working volume of measuring arms, it is quite small compared with other portable CMMs; it is therefore often required to reposition the device (performing *leapfrogs*) at several locations to complete the inspection. [33]

### 2.3.5 Non-Contact Type (Optical) 3D-CMMs

Methods of optical 3D coordinate metrology pursue three essential objectives. First of all, mobile optical methods and measuring devices enable the measurements of very large components from aviation and ship-building industries, which normally can not be carried into the the measuring volume of a conventional CMM. In the optical 3D coordinate metrology, the measuring device is brought close to the workpiece or built around the workpiece. Secondly, optical 3D measurement methods are often very fast, so that dynamic measurements are possible. In that way, e.g., movements of the component during assembly can be pursued, the assembly process can be accelerated or deformation of the workpiece as oscillations of a wing can be measured. Thirdly, methods of optical 3D coordinate metrology are utilised in order to register a great deal of touch points laid densely side by side on free-form surfaces, with a reasonable expenditure of time. [8]

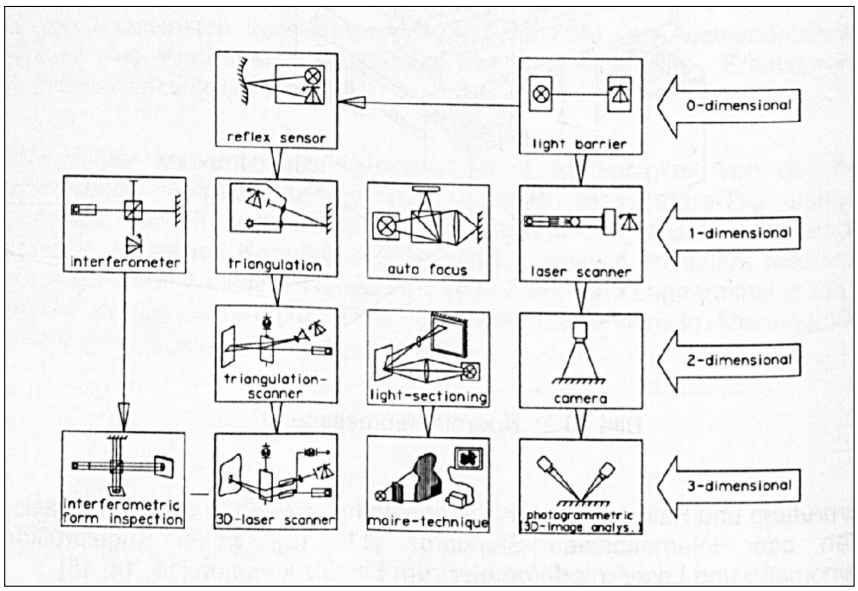


**Figure 2.21:** Overview of optoelectronic CMSs [30]

These methods are used both for quality assurance as well as for reverse engineering applications. By the current possibilities of manufacturing technology (multi-axis milling centres, rapid-prototyping methods, etc.), complex geometries and free-form surfaces are becoming more frequently construction and design elements. Many of these components are not reducible to simple geometrical features any more. Therefore, when measuring these components, often the touch points themselves stay in the focus, and not the resulting geometrical features. An appropriately large density of touch points are necessary, so that the surface can be represented by touch points at any curvature. The density varies according to the quality requirements and change of curvature. The necessary point clouds typically include some ten thousand, hundred thousand, and in special cases even a few million touch points. This fact puts high demands on the measurement technology:

- High velocity of the measuring point collection,
- Methods for calculating touch points from the measuring points,
- Methods for processing and representation of the touch points (point clouds),
- High computing power and storage capacity for data processing.

Optical measuring methods, which record a large number of measuring points practically at the same time, are particularly suitable to achieve reasonable measurement times. A large number of factors influence the interaction between the surface of the workpiece and the light used by the measuring method. It brings in its wake that a single measuring point may have a large measurement uncertainty in relation to the required measuring uncertainty at the surface representation. This measurement uncertainty could be heavily reduced due to the large number of measuring points and special methods for calculating the touch points from measuring points. Graphical methods are

ideal for the assessment of the measurement results. The representation of the individual touch points in a spatial coordinate system is only in special cases expedient. Measured surfaces can be illustrated very demonstratively as form of surface meshes. In order to do this, adjacent touch points are pooled to polygons.

Depending on the size of the displayed surface segment and existing local surface curvature, another maximum polygon area is permitted for a good quality of display. In that way it is, e.g. possible to illustrate the level surfaces with very big polygons accurately enough. Radii and edges, however, require many times smaller polygon faces. The task of appropriate processing methods for polygonisation is therefore to determine the optimal polygon area for each local situation. During this process, the amount of data may be reduced significantly, which has a positive effect on further processing steps. To strengthen the spatial appearance of the displayed surfaces, the grid is completed with a texture. Monochrome textures are widespread. Only through the targeted use of light sources during the presentation of this surface textures on the screen creates shadow and thus the impression of depth for the measurement result. Further possibilities to generate spatial impression are pseudo colour height displays.

#### 2.3.5.1 Fringe-Projection Method

Fringe projection methods have seen an enormous boost by the rapid development of the camera technology and the performance of Personal Computers (PCs). They provide nowadays fast and complete 3D information, in particular, on free-form surfaces. [8]

*Measuring principle* The measuring principle of fringe projection relies on the fact that multiple light sections are placed on the workpiece by using projected fringes, either simultaneously or in quick succession. These light sections are recorded down by a camera from a different direction (Figure 2.22a). The fringes can be created by using a projector. The narrower the fringes are, the greater is the vertical resolution. Workpiece shape affects the distortion of the line pattern. Workpiece geometry, i.e. a point cloud with very large point density, can be calculated from distorted line pattern recorded by the camera. The assignment between the dislocations of fringe and the heights of the workpiece can be determined by calibration with a known standard. [8]

At the time being, fringe projection systems are frequently offered with two cameras as well, both for technical and economic reasons (Figure 2.22b). In such an arrangement, the projector is used merely as a light source, which creates the marks on the workpiece surface. The actual triangulation is carried out by two cameras, which arranged lateral to it. The advantage of the arrangement with two cameras lies especially in the problem of the projector. In order to create sufficient contrast fringes, powerful lamps in the projector are required, which generate significant waste heat. The resulting deformations of the optical components in the projector can lead to the loss of accuracy. Added to this is the fact that most advanced optics for projectors are significantly more expensive and come in a smaller variety than those for cameras. In the two camera set-up, the projector is used mainly as

a *marking system*, which enables the identification of the surface points in both cameras. Inaccuracies in the projection do not have any impact here, since the actual measurement conducted by two cameras. Alternatively, the measurement can be performed between the camera and the projector, and a plausibility check or increase in accuracy can be achieved by comparison of the results. [8]

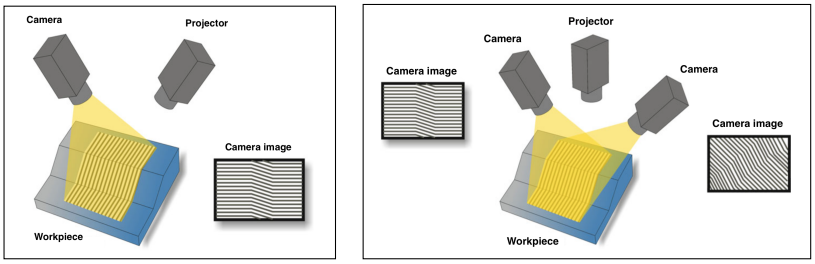


**(a)** Principle and set-up of fringe-projection

**(b)** Principle and set-up of fringe-projection (with 2 cameras)

**Figure 2.22:** Fringe-projection (*adapted from* [8])

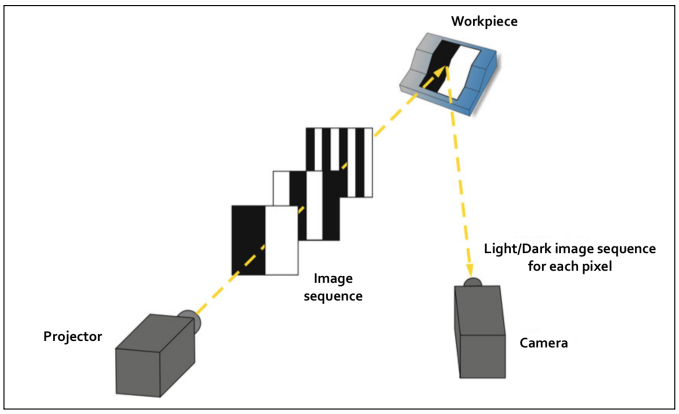


**Figure 2.23:** Gray-code method for estimation of absolute position (*adapted from* [8])

Furthermore, the utilisation of two cameras offers, as a matter of course, the opportunity to avoid shiny and shadowed areas, since there is a higher probability of that at least one camera can capture this area properly. These benefits comes, however, with the costs of an additional camera. A particular difficulty of the fringe projection method is the determination of the absolute position. Since the projected fringe is not *numbered*, they can not clearly assigned to the projector position just from the camera image. The most common method to determine the absolute position is the so-called *Gray-code* method, at which only one after the other very wide and increasingly finer fringes are projected (Figure 2.23). From this image sequence, it is possible to perform the assignment of the fine fringes clearly. Then, on the finest fringe level, often sinusoidal fringes are projected, from which sub-pixel accuracy can be achieved over the determination of the phase position. These methods require the recording of image sequences with typically 8 to around 16 images. In that way the recording speed is reduced. [8]

*Characteristics and Discussion* The fringe-projection method using image processing is an automated method for measuring flat or curved areas with diffusely reflective surface. Problems can occur when measuring surfaces with very high reflectivity (mirror) or very low reflection (matte black surface). In these cases, the surface may be sprayed with a diffusely and highly reflective material to enhance the measurement results. [8]

For this purpose, the developer powder is often used for the dye penetration. This is a lime powder, which can be easily wiped off the surface again after the measurement. In the group of fringe-projection methods, there is a wide range of possibilities to create, record and to evaluate the fringes. They differ in achievable measuring ranges, accuracies, speed and the ability to enable dynamic measurements etc.. Measurement uncertainties of up to the range of 0.1 mm can be achieved. There is a linear correlation between measurement range and measurement uncertainty. There exist several ways to enlarge the measuring range [8]:

- The fringe-projector with camera is attached to a motion platform (CMM, robots, etc.) and moved over the workpiece. Similar to the measurements *in the image* and *at the image* in the Two-and-a-half-dimensional (2.5D)-coordinate metrology, the measurement data of both measurement systems are linked together.
- Markers are used to link several images in association with photogrammetrical methods.
- Fringe-projector and camera are led as moving system around the component. A camera, which is attached to a fixed position relative to the workpiece, serves for determining the measuring positions and linking of data. It only has to be ensured that this camera (co-)captures each time at least a part of measuring points, which are measured by the moving system [34].
- If the images overlap in some areas, the image information itself can be used to link the 3D information. E.g. correlation methods are used or marks are applied onto the workpiece, which are visible in several images. These are then detected computationally, and made to coincide. However, this method only works with highly structured components, which allows an unambiguous assignment of the measuring fields. Compared to other linking methods, it is easier to use, however less accurate, since the measurement deviations add up in the individual point clouds.

The fringe-projection with multiple images is not only carried out for the extension of the measuring range. Often, measurements from different directions are carried out to grasp, e.g., areas with reflections or areas shaded by steps and landings. In these cases, either the workpiece remains fixed in place (at big workpieces) and the mobile fringe projector records sub-areas from different perspectives, or the fringe-projector remains stationary and the workpiece is moved. [8]

*Applications* Complex free-form surfaces have sometimes the property that the fringes impinge on the surface with an adverse angle. This leads e.g. to so-called *highlights*. These are areas on the workpiece, which shine very brightly, since direct reflection occurs. If the qual-

ity of each measured data recorded together when measuring, (e.g. by evaluation of the local contrast), the best data can be selected and therefore the quality of the measuring results can be improved by multiple measurements from different directions. Nowadays, fringe projection methods are already well-established in many areas. [8]

They are used, e.g., in the tool construction, for the digitisation of free-form surfaces, within the framework of the rapid-prototyping, for quality assurance, for fault detection, in the search for cracks and folds, and in the optimisation of thermo-forming processes of sheet metal parts. Fringe-projection methods produce measurement point clouds in predetermined grids, which is provided by the camera and projector positions. These orient themselves by camera pixels, and not by the workpiece structure. In comparison to tactile coordinate metrology, in which a feature (e.g. an edge or a corner) can be probed directly, usually only a point cloud around the feature can be obtained by fringe projection. The actual feature is obtained by numerical post-processing of the point cloud (e.g. production of cutting elements in compensation areas by the point cloud). [8]

#### 2.3.5.2 Measuring Instruments with Photogrammetry Principle

By the development of the digital photography, photogrammetry has become a useful and versatile measurement tool, in particular, for large workpieces. [8]

*Measuring principle* Photogrammetry means traditionally "*measuring from photos*"[35]. It was invented in 1858 by the architect Albert Meydenbauer. Instead of measuring directly on scaffoldings, he suggested to produce construction drawings from photos. Since the advent of the first aircraft at the beginning of the last century, so-called air images used to produce maps. At the end of the last century the digital photography and industrial image processing enabled the new applications of photogrammetry in industrial metrology. [8]

Basis of the photogrammetry is ability to infer the 3D coordinates or the shape of a workpiece by stereo measurement from two images taken from different directions. Applications in production metrology usually work with coded markers, which are fixed onto the workpiece. Then, using a commercially available digital camera, several images are taken from different directions (Figure 2.24a). Alternatively the workpiece lies in a measuring volume, where it can simultaneously be recorded practically. It must be ensured that always as many markers as possible are visible in several images. This increases the redundancy, and reduces the measurement uncertainty. The digitised images are searched in an image processing program according to the markers, which are known by the program. If these markers are found, the 2D coordinates of these markers are evaluated with the known methods of photogrammetry, and the 3D coordinates of the markers are calculated. In terms of computation, photogrammetric evaluations can be very intensive. [8]

*Characteristics and Discussion* Photogrammetry provides the 3D coordinates of points in space, which are determined by the corresponding markers (Figure 2.24b). Before starting the measurement, it must be therefore ensured that such appropriate markings are placed at

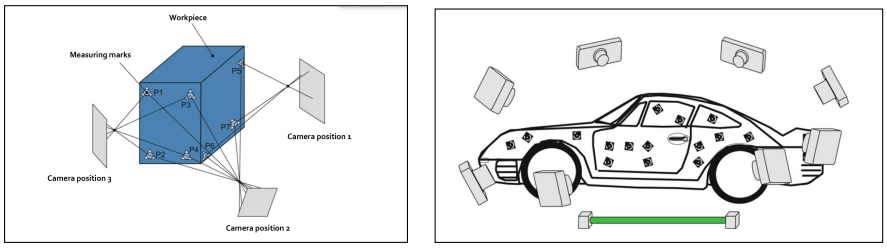


**(a)** Measuring principle **(b)** Application of photogrammetry

**Figure 2.24:** Photogrammetry (*adapted from* [8])

all relevant positions. Modern photogrammetric systems work with high-resolution digital single-lens reflex (DSLR) cameras. Very good, low-distortion lenses must be used. Thus, size-dependent reproducibility is achieved, such as $3\,\mu m + 7\,\frac{\mu m}{m}$ $(3\,\sigma)$. Photogrammetry systems can be combined very well with other scanners (see e.g. fringe projection). They provide then the reference coordinate system to the marked points, in which the data obtained by the scanners are latched. [8]

*Applications* Utilisation of photogrammetry in the manufacturing metrology is strongly gaining importance due to the advances in the camera and computer technology. If one uses several stationary cameras and flash illumination, dynamic processes can be observed, e.g. the deformation of containers under load. Also, the straightening by bending, the elastic-plastic deformation of metal sheets and tubes can be optimized by the utilisation of photogrammetry. The photogrammetry is used at the fringe projection method as well, e.g. for a first and mostly rough assignment of several images from different directions. If only one camera is used, the procedure is very easy to handle. If the markers are once applied, one moves around the workpiece and takes pictures with only a few 100 g heavy camera. [8]

A few minutes after the reading of the digital images, the 3D coordinates of points can be compared in a 3D CAD system with models of the desired geometry. The application of the markers limits the possible point density. Instead of markers, which can be seen on the measuring object shown in Figure 2.24b, high-contrast geometrical elements/features can be used as well. The photogrammetry provides data only on selected workpiece points (structures or markers). This distinguishes it significantly from fringe-projection, which provides camera-bound point clouds. [8]

#### 2.3.5.3 Theodolite

At the time being, only the basic principle of modern theodolites is same with their venerable predecessors. They have evolved to such measuring instruments that can also be found in industrial metrology applications. [8]

*Measuring principle* Theodolite is an angle measuring device and was originally used in geodesy (land surveying) and astronomy (observation of celestial bodies). The first beginnings of this measuring technology are known from the 16th century. A theodolite consists essentially

of a measuring telescope, a vertical and a horizontal pitch and several levels for the alignment of the device (Figure 2.25). [8]

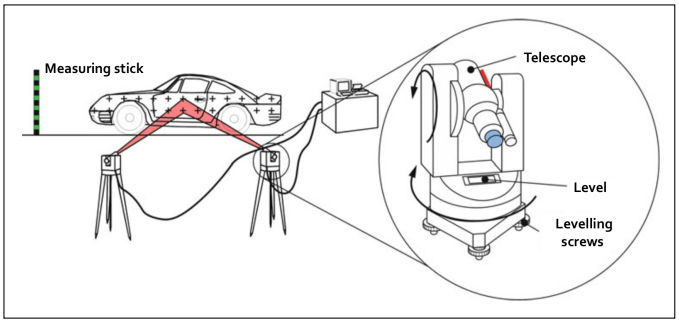


**Figure 2.25:** Principle and set-up of theodolite (*adapted from* [8])

*Characteristics and Applications* The measuring method is based on triangulation principle. The markers are targeted from different directions by telescope and coordinates in space are determined through angle calculations. The method is particularly suitable for the monitoring of individually selected measurement points, e.g. connection or assembly points. Hence, in the manufacturing metrology, theodolites are used to measure big workpieces e.g. in the ship construction, in the road technology, in the airplane construction, or in the development of robots and transfer lines. Advantages are the mobility of the devices and the very large measuring range. Their measuring uncertainty lies typically in the range of 0.1 mm to 1 mm with measuring ranges of some 100 m. [8]

### 2.3.5.4 Laser-trackers

Nowadays, laser-trackers are used frequently and widespread in the industrial manufacturing of larger components. They allow the position regulation in some meters of distance and are often used in combination with locally measuring tactile or optical sensors. [8]

*Measuring principle* The laser-tracker combines a theodolite with a laser interferometer [36]. The laser-tracker consists of a tripod, on which the laser interferometer is placed. The laser beam of the laser interferometer can move freely in the space through two motor-driven rotational axes (Figure 2.26) with highly-accurate angle measurement systems. The reflector is positioned on the workpiece, and can change its position by hand, by other axes of motion, or by the motion of the workpiece itself. This position change is detected by a sensor in the tripod of the laser tracker, and the both axes of rotation are tracked. The current position of the reflector in the space is calculated from the distance information of laser interferometer and from the both angular information. [8]

*Characteristics and Discussion* The measuring range of laser-trackers lies in the range of 50 m. Their typical measurement uncertainty value is about $40\,\mu m\,m^{-1}$. Measuring frequencies are achieved in the kHz range. The advantage of this measuring process lies in the possibility to scan location coordinates in space as well as to capture and evaluate many measurement points in small time intervals. The laser

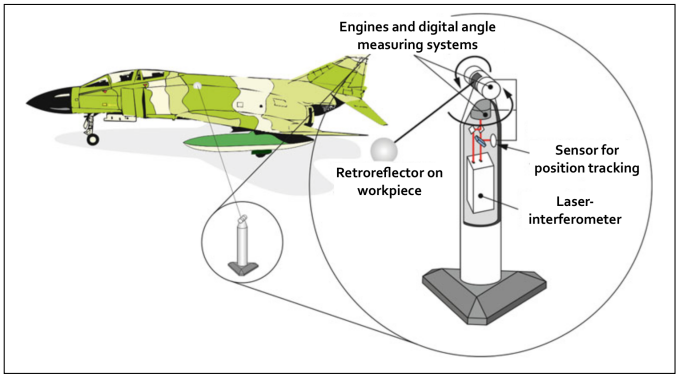


**Figure 2.26:** Principle of laser-trackers (*adapted from* [8])

beam must not be interrupted during the measurement. All measuring points must be visible from a point of view. [8]

*Applications* Laser-trackers are used together with other measurement and handling devices to monitor the assembly of very large workpieces (e.g. in aircraft construction, shipbuilding, railway and wagon construction). Other applications include scanning of large free-form surfaces, motion and vibration analysis e.g. of aircraft wings. [8]

LASER-TRACKERS WITH CONTACT PROBING SYSTEM In this measuring principle, the laser-tracker is also equipped with a camera (Figure 2.27). Further, the mobile measuring system has a *smart probing system* (Figure 2.27). The wireless probing system consists of a standard stylus with ball tip for contacting probing, reflectors, as well as Light Emitting Diodes (LEDs). With the help of these reflectors and LEDs, the laser-tracker recognises the position and orientation of the hand-operated probing system, and can calculate the probing coordinates of the ball tip in the space with this information. [8]

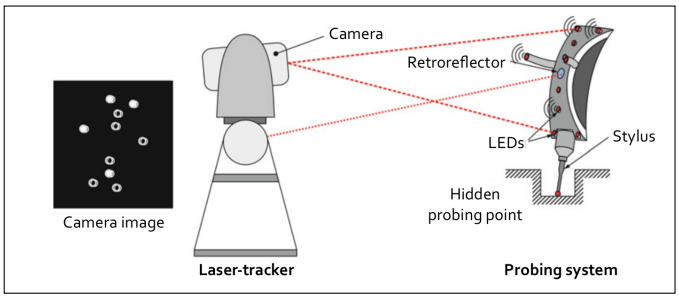


**Figure 2.27:** Laser-trackers with contact probing system (*adapted from* [8])

As a portable CMM, the laser-tracker with contacting probing system is particularly suitable for measurement of large workpieces and hidden touch points, which can not be viewed and recognised directly from the laser-tracker. Measurement uncertainties in the range of $0.1\,\mathrm{mm}$ U ($k = 2$) at a measuring range of $15\,\mathrm{m}$, and motions of the probe system up to $1\,\mathrm{m\,s^{-1}}$ can be obtained. [8]

LASER-TRACKERS WITH NON-CONTACT PROBING SYSTEM In this measuring principle, the laser-tracker is equipped with a camera (Figure 2.28). This smart probing system consists principally of a non-contact oper-

ating probe according to laser triangulation principle. Using a lens or a rotating polygon mirror, laser line on the surface of the workpiece is generated, and the deformation of this line is recorded by a camera. The coordinates (x/y/z) of the workpiece surface relative to the probing system can be calculated from this data. The position and orientation of the probing system in the space is re-calculated with reflectors and LEDs of laser-tracker with integrated camera. [8]

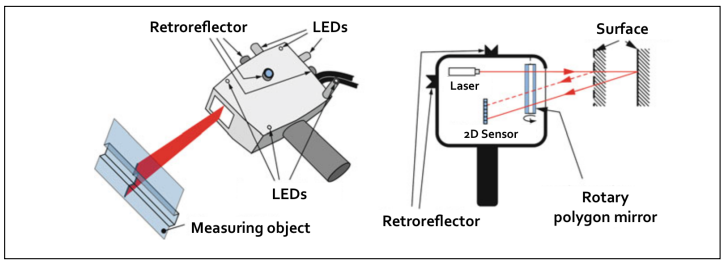


**Figure 2.28:** Laser-trackers with non-contact probing system (*adapted from* [8])

*Applications* The laser-tracker with non-contact probe system is particularly suitable for digitisation and measurement of free-form surfaces e.g. in the context of reverse engineering. The laser-tracker calculates the position and orientation of the probe system within a measuring range of up to 30 m. The probe system usually operates with laser line lengths of 50 mm to 100 mm, with average working distances and measuring ranges of 50 mm, and with measurement uncertainties of U = 0.05 mmto0.1 mm (k = 2). [8]

### 2.3.5.5 Laser-tracers

Laser-tracers are the most accurate distance measurement systems for large dimensions, and are therefore used mainly for calibration of machine tools, etc.. In contrast to laser-trackers, laser-tracers are based only on highly accurate distance measurements using interferometry. As with the laser-tracker, an interferometer, which tracks a target in space, serves as transducer (Figure 2.29a). For this, the interferometer is also automatically updated in two spatial axes. To compensate for inaccuracies of the axes of rotation and guides, a high-precision ball with a form deviation of few nanometres in the centre of rotation of the interferometer serves as a reference. By using three tracers in space (Figure 2.29b), the measurement of angles can be waived, and a significantly higher resolution is obtained in the space in comparison to that with a laser-tracker. [8]

*Characteristics and Discussion* Laser-tracers achieve very high accuracy values. Their typical measurement uncertainty value is 0.2 µm + 0.3 µm $m^{-1}$, and a resolution of 0.001 µm is achieved. This fact is more remarkable, as these values are achieved within measuring ranges of up to 15 m. Laser-tracer should, of course, be used in strictly-controlled climatic conditions, so as they show their actual performance. [8]

The measuring paths from tracer stations to the target must be free at any time, since only relative measurements are possible with the interferometric measuring principle, and the measuring signal gets lost in case of an interruption. [8]

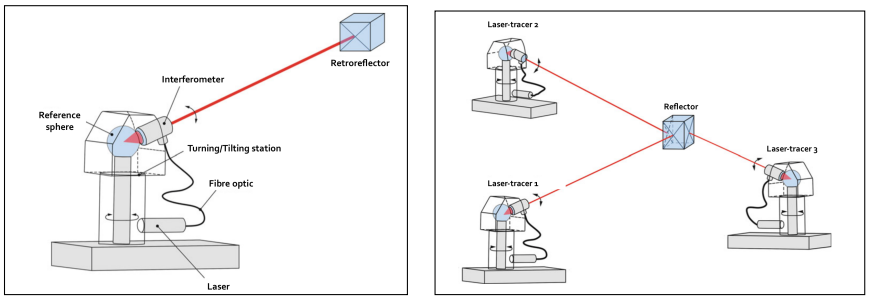


**(a)** Principle of laser tracers **(b)** Application of laser-tracers

**Figure 2.29:** Laser-tracers (*adapted from* [8])

*Applications* Laser-tracers are utilised for highly accurate calibration of machine tools or CMMs, or as a reference measurement system for the calibration of other measuring devices. [8]

#### 2.3.5.6 Absolute-Measuring Interferometer

The high-end measuring devices of great accuracy at large distances are the absolute-measuring interferometers. They enable position measurements with an accuracy of up to $0.5\,\mu m\,m^{-1}$ on measuring paths of up to $20\,m$, and at the same time with up to 100 channels. [8]

*Measuring principle* A classic interferometer has a narrowly defined uniqueness range in the order of magnitude of a half wavelength of light. Greater distances can be determined by counting the interference fringes. In contrast, at the absolute-measuring interferometer, the absolute position of the measuring reflector is determined directly. This can be achieved by measuring with multiple wavelengths simultaneously. The resulting beats produce synthetic wavelengths, which can be much larger than the originally used light wavelengths. [8]

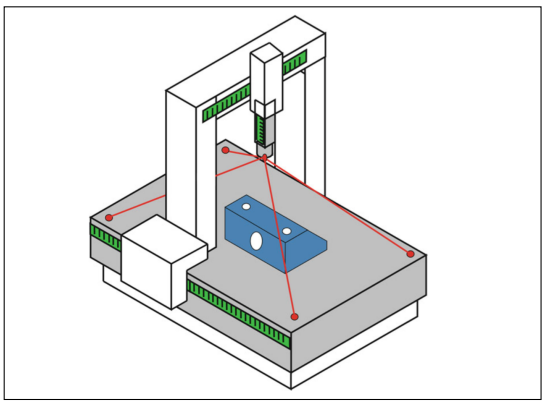

**Figure 2.30:** Principle of absolute-measuring interferometer (*adapted from* [8])

At the absolute-measuring interferometer the wavelength of a laser with defined frequency is tuned very quickly [37], so that there exist many different wavelengths, which are suitable for the production of synthetic wavelengths. For the exact knowledge of the each used laser wavelength, a gas absorption cell with many well-defined and stable absorption lines serves as a measuring scale. The tunable (diode-)laser

with control, as well as the reference cell can be integrated together with the evaluation computer in a separate housing, so that only the measuring beam can be placed into the desired position by means of a simple fibre. [8]

*Characteristics and discussion* At normal interferometers the measuring beam may never be interrupted during the measurement, since thereby the absolute measurement position would have been lost. It is not so with the absolute-measuring interferometer. Absolute measurement of the distance of the measuring beam can be interrupted at this type of interferometer. Once the beam is free again, the current position is determined automatically. The synthetic wavelength allow hereby the rough definition of distances, which, combined with the individual wavelengths, guarantees very high measuring accuracy of the system. Currently, these interferometers can be built with up to 100 channels, so that the simultaneous 3D position determination of multiple points is possible. [8]

*Applications* This technology allows to determine of the absolute position with an uncertainty of $0.5\,\mu m\,m^{-1}$ in a measurement volume of up to $20\,m \times 20\,m \times 20\,m$. As a consequence, a variety of applications arises; from the calibration of large machine tools to the metrological monitoring of the production machines or devices in the operation, from metrological monitoring of robot movements to the measurement of deformations and vibrations in buildings and systems (Figure 2.30). It should be noted that for the measurement, in any case, the reflectors need to be mounted to the measuring positions. [8]

#### 2.3.5.7 Indoor GPS

Global Positioning System (GPS) is known from the military technology. Nowadays, the term GPS is used in common parlance for the satellite-based GPS Navigational Satellite Timing and Ranging (NAVSTAR), which was developed in the United States of America (USA). It was officially put into operation in 1995 and has always been further developed. [8]

*Measuring principle* GPS is based on satellites that constantly orbit the earth and send out signals. These signals can be received from GPS sensors, and be transformed to position information of the sensor on the earth. Theoretically, each sensor requires signals from 3 transmitters to calculate its position. In practice, signals from as many transmitter as possible are utilised to simplify the technology, or to achieve higher accuracies of position information. [8]

Nowadays, position information is worldwide available with a positional uncertainty of a few metres. However, even in the case of utilisation of particularly sensitive receivers without direct *visual contact* to many satellites indoors as e.g. in large assembly halls, the GPS technology operates only severely limited. The basic principle of localisation in indoors is also interesting in production technology. Instead of satellites in space, a wealth of laser transmitters are used, which emit infrared pulses, and are mounted, e.g., at the ceiling of assembly halls stationarily (Figure 2.31). Sensors can be fixed to the parts of ships and airplanes, to robots, or to mobile measuring head systems, and receive these signals and then calculate their position from these signals. [8]

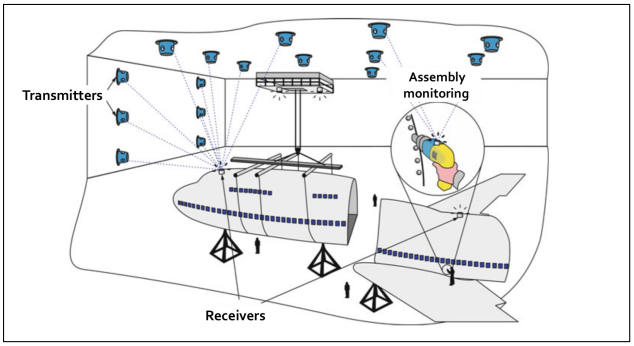


**Figure 2.31:** Principle of Indoor-GPS (*adapted from* [8])

If the transmitters are mounted once in sufficient density, measurements are possible practically in the whole hall volume without big changeover effort. It must only be ensured that there is direct visual contact between as many transmitters and receivers as possible. Beside the introduced technology, a variety of other methods is available in the meantime, which based on optical or radio principles in measuring ranges of few meters to 100 m, and position or measuring uncertainties in the range of 0.1 mm to 10 mm. A comprehensive overview can be found in [38]. [8]

*Applications* The systems are utilised in ship and aircraft construction, as well as for adjustment and programming of robotic assembly lines in automotive industry. Safety aspects can be taken into account as well. Collisions between humans and robots can be prevented by motion analysis, without the need to use more inflexible mesh fences or light barriers. [8]

Moreover, assembly movements can be tracked and counted to ensure, e.g., that all rivets, screws etc. are tightened during manual activities (Figure 2.31). [8]

#### 2.3.5.8 3D Scanners

A 3D scanner is a device that analyses a real-world object to capture its shape. The collected data is then used to construct a digital 3D model. Although 3D scanners are mostly used for industrial design, reverse engineering, and prototyping, several QC applications require the use of such devices to perform inspections. 3D scanners allow the inspection of a part without having to make any physical contact on it. Also, applications requiring a high density of measurement data, such as when a surface profile Geometrical Dimensioning and Tolerancing (GDT) needs to be computed, should make use of 3D scanners as they allow the measuring of a very high amount of data in a very effective way. [33]

OPERATING PRINCIPLES OF SCANNING DEVICES There are several types of 3D scanning technologies that use completely different principles. They are grouped into two main categories: active scanners and passive scanners. Each category includes several technologies to achieve the 3D digitisation; however, only the relevant ones, for QC or inspection applications, are described here. Each technology has dis-

tinctive features, but the global workflow is the same for 3D scanning devices [33]

### 2.3.6 Multisensor CMMs and CMSs

Multisensor CMMs use a combination of several of the sensors described in the previous sections. The properties of these sensors usually depend on their various applications (Figure 2.32). In this context, their distinguishing characteristics include the size of the object features they can probe, the type of object features they can probe (edge, surface), and their suitability for rapidly acquiring large numbers of measured points (scanning). In order to perform complex measurement tasks, it is usually necessary to use several different sensors for a single measuring run. [39]

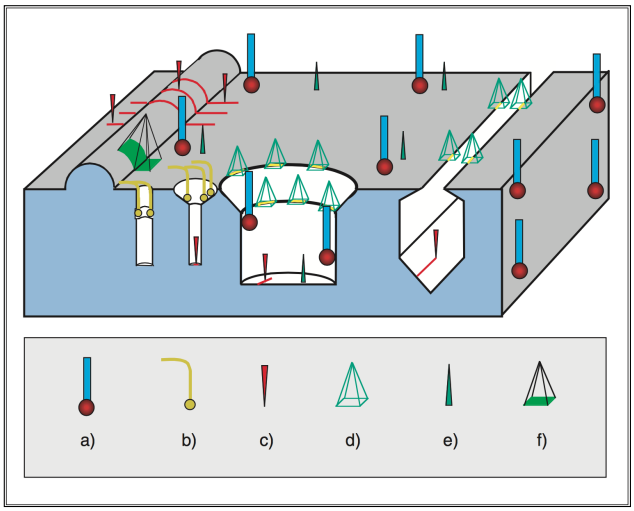


**Figure 2.32:** Typical applications of different sensors within the framework of multisensor technology; a) Mechanical stylus b) Werth Fiber Probe[a] c) Laser d) Image processing e) Autofocus f) 3D-Patch [40]

*a* Werth Fiber Probe is a patented tactile sensor of Werth company for high-precision measurement of micro-component structures.

At the time being, there are several different types of sensors available. Each of those tactile, optical, optoelectronic or other several types of sensors work differently, thus they enable conducting measurements based on different physical principles. It is not unusual that two measurement results are different, delivered for two identical measurements conducted by using different sensors for the same geometric feature of the same workpiece. This is also possible even by the utilisation of same type of sensors (e.g. due to different stylus tip diameters or different probing forces). The challenging demand to the future Multisensor-CMMs or in general to the measurement instruments is the fact that they should ideally deliver same measurement results regardless of utilised sensor types, measurement place and time.

There exist two possibilities when using multiple sensors. Beside the utilisation of several sensors of same type, one can also use or combine different types of sensors according to application demands. Furthermore, the measurement data obtained by the same kind of sensors is

referred to *homogeneous* measurement data, whether in case of different types of sensors (e.g. tactile and optical), or sensors with different features (e.g. optical sensors with different resolutions) they are called as *inhomogeneous* measurement data.

Within the context of Multisensor-CMMs, the surfaces or surface features to be inspected and measured by different types of sensors can also differ according to abovementioned characteristic differences between them. Subsequently, the measurement results delivered by each sensor have to be *fused/merged* considering their different characteristics. As far as the *fusion* of measurement results gathered by different sensors concerned, there are two main steps[10]. First of all a process called *rough-registration* is realised, followed by a more specific step called *fine-registration*. According to the required degree of detail, the latter step can become less significant and therefore shorter. [26]

The success of the combination of different sensors within Multisensor-CMMs mainly depends on three criteria;

- Interoperation of sensors,
- Appropriate processing of signals for the measurement task, and
- Linkage of measurement data delivered by sensors.

Sensors can be mounted both to the same and different axes, and a special attention should be paid to prevent any collision. There exist mainly four different machine configurations. Complex workpieces can also be measured by utilisation of a rotary table. It should also be noted that the measurement volume of CMMs with multiple sensors are less than those with single sensor by the distance between sensors. Furthermore, the integration of CT systems into Multisensor-CMMs is an interesting issue, since it is a vital step when it comes to obtaining holistic models of workpieces in the light of measurement data.

Table 2.6 gives an overview of advantages and drawbacks of different sensors according to several measurement characteristics.

Summarising, the convenient advantages Multisensor-CMMs bring with themselves can be listed as follows;

- Different geometric features on a workpiece are inspected and measured by *most suitable* sensors for those specific sub[26]tasks, and a holistic model of the workpiece is obtained in only a measurement run.
- The interior of a workpiece can be inspected by iCT, whereas its external features are inspected and measured by a tactile sensor. This is especially advantageous when measuring metal workpieces with plastic external surfaces, which is otherwise highly problematic due to the overexposure.

### 2.3.7 Industrial Computed Tomography (iCT)

As a versatile technique, CT has established itself and has been utilised frequently in related medical applications since 1970's. In 1990's, a possible extension of its application areas in the context of industrial

10 More detailed information about those steps are presented in [26].

**Table 2.6:** Advantages and drawbacks of various sensors[a] within the context of multisensor technology (adapted from [41])

| Characteristics | TD | TS | WFP | IP | AF | MF | WLP | CFP | LLP | WCP | CT |
|---|---|---|---|---|---|---|---|---|---|---|---|
| Non-contact | 0 | 0 | 0 | 2 | 2 | 2 | 2 | 2 | 2 | 0 | 2 |
| None/Negligible probing forces | 0 | 0 | 2 | 2 | 2 | 2 | 2 | 2 | 2 | 0 | 2 |
| Small features are measurable | 1 | 1 | 2 | 2 | 2 | 2 | 2 | 2 | 0 | 1 | 2 |
| Many measuring points | 0 | 1 | 1 | 2 | 0 | 2 | 1 | 1 | 2 | 1 | 2 |
| Very small probing error | 1 | 1 | 2 | 2 | 1 | 1 | 1 | 2 | 0 | 1 | 1 |
| Rotatable/Pivoted | 2 | 2 | 2 | 2 | 2 | 2 | 0 | 0 | 2 | 0 | 2 |
| Scanning is possible | 0 | 2 | 2 | 2 | 0 | 0 | 2 | 2 | 2 | 2 | 2 |
| Dirty dimensions are graspable | 0 | 0 | 0 | 0 | 0 | 0 | 0 | 0 | 0 | 0 | 2 |
| Suitable for roughness measurements | 0 | 0 | 2 | 0 | 0 | 1 | 1 | 1 | 0 | 2 | 0 |
| Strongly dependent on surface | 0 | 0 | 0 | 1 | 1 | 1 | 2 | 2 | 2 | 0 | 0 |
| Travel paths are normally required | 2 | 2 | 2 | 0 | 0 | 0 | 0 | 0 | 0 | 2 | 0 |
| Edges are measurable | 0 | 0 | 1 | 2 | 0 | 1 | 1 | 1 | 0 | 0 | 0 |
| Surfaces are measurable | 2 | 2 | 2 | 0 | 2 | 2 | 2 | 2 | 2 | 2 | 2 |
| Material structure is measurable | 0 | 0 | 0 | 0 | 0 | 0 | 0 | 0 | 0 | 0 | 2 |
| *0: not relevant; 1: partially relevant; 2: relevant* | | | | | | | | | | | |

a *TD: tactile discrete; TS: tactile scanning; WFP: Werth Fiber Probe; IP: Image processing; AF: Autofocus; MF: Multi-focus; WLP: Laserpoint-sensor, CFP: Chromatic sensor; LLP: Laserline-sensor; WCP: Werth Contour Probe; CT: CT sensor*

production, e.g. in NDT, had been a promising issue for industrial manufacturers and research institutes, especially due to its high capability to capture volumetric data of workpieces. This has enabled an easier analysis, control and detection of internal structural defects or blowholes of workpieces. iCT systems which were developed for those purposes, were also used to conduct dimensional measurements, and gather geometrical information about technical objects. However, the attainable measurement accuracies were in the range of a few millimetres, and therefore a widespread application for technical measurements was not realistic. Since there was an obvious demand for development of iCT systems, which can be used specifically for metrological purposes, the first CMM with and integrated iCT system was represented in 2005. Unlike any other metrological system, iCT has made it possible to analyse internal structures of parts and assemblies without cutting them into sections and destroying them. In addition to this unique benefit, as a rather new technology, iCT has enabled conducting quite faster measurements with a tremendously increased density of measuring points in comparison to other dimensional metrology solutions.

#### 2.3.7.1 Principle of X-Ray Tomography

Main components of a typical iCT system can be classified as follows:


**Figure 2.33:** Overview of an iCT system [42]

- An X-ray source (either fan beam or cone beam source)
- An X-ray detector (either line or flat detector)
- A rotary table between X-ray source and detector
- A computation unit

The fundamental working principle of iCT systems relies on the fact that an X-ray beam consisted of photons sended out of an X-ray source penetrates through the workpiece, and according to its absorption, scattering and transmission characteristics, as well as interactions with the workpiece, projection images of workpiece are gathered on an X-ray detector. In order to obtain those projected images from several different perspectives, workpiece is placed on a rotary table, hich ensures its precise and accurate rotation at pre-specified angular positions, as well as its precise relative movement between X-ray source and detector.

The X-rays trying to penetrate the workpiece can be either transmitted (and reach to detector), scattered or absorbed. The term *attenuation* is used to explain the phenomena of intensity reduction of absorbed or scattered X-rays. Attenuated X-rays cannot reach the detector, and the amount of attenuation depends on many factors, e.g. material density and composition, as well as penetration length. Besides, X-ray power is the main decisive factor for the energy of X-rays. An X-ray detector consisting of photo diodes and scintillating crystals grasps those X-rays which are transmitted through the workpiece and thus 2D gray images of workpiece are obtained at several pre-determined angular positions of rotary table. As the next step, those obtained related data and 2D section images are processed by a computation unit in order to visualise and acquire a 3D model of the scanned workpiece. This model consists of so-called *voxels*[11], each of which represents a local attenuation of the workpiece.

Similar to 2D image processing, the actual measured points are calculated from the voxel data by using a suitable threshold process. In the first four steps in Figure 2.35b, this process is illustrated.

The sensors currently used on some systems are able to capture up to 4 million image points. Typically, several hundred to a few million measurement points are derived in the measured volume. These points are

11 The term **voxel** stands for *volumetric pixel*, and can be thought as an analogue 3D correspondence to pixel (2D) in optical technology.

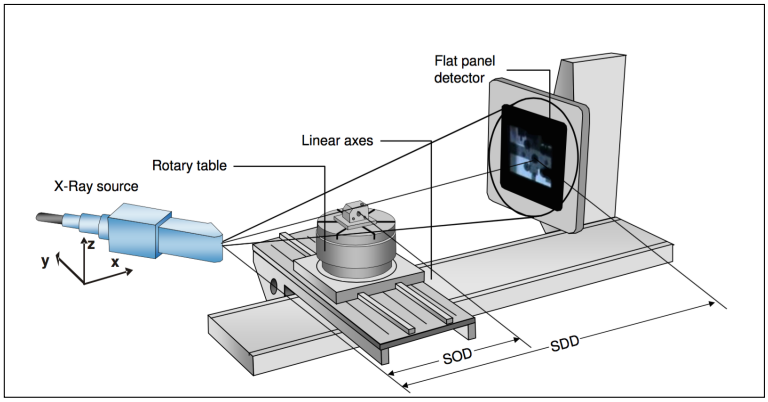


**Figure 2.34:** Main structure and components of an iCT system [43]

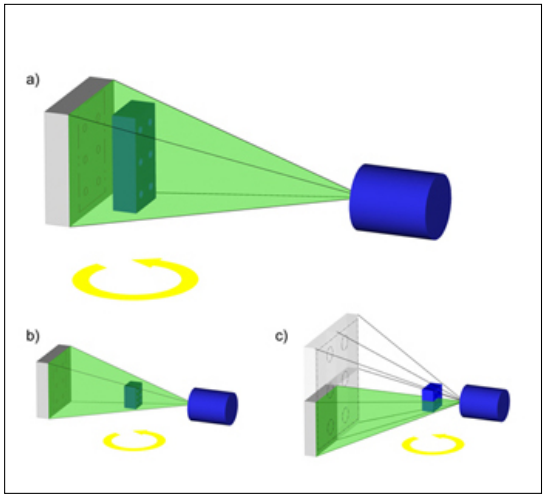


**(a)** X-ray tomography; a) Basic principle b) Magnification adjustment c) Stitching of images

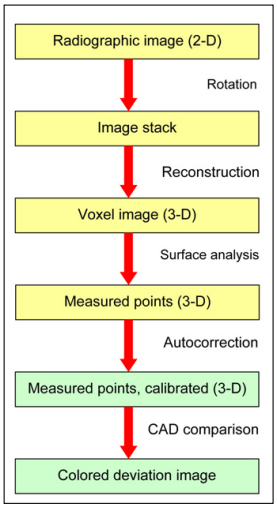


**(b)** Processing steps for X-ray tomography measurement

**Figure 2.35:** Fundamental stages of iCT [44]

distributed evenly across the surface of the part being measured. Structures in the interior of the measured object, e.g. hollow cavities or under-cuts, are also captured. The measurement points can be evaluated using familiar methods of coordinate metrology. Similar to measurement using image processing, it is possible to change the magnification using tomography (Figure 2.35ab) in order to capture small parts with higher magnification or larger parts completely with lower magnification. To do this, either the measured object is positioned in the radiation path, or the X-ray components (X-ray source and detector) are moved in an axial direction relative to the object being measured. In some cases, the size of the sensor or the number of pixels available is still not enough to meet the requirements of the measuring task. In such cases, several images are stitched together (Figure 2.35ac) by moving the rotary table with the measured object relative to the X-ray components. Reconstruction of the voxel volume image is then accomplished on the basis of these stitched 2D images.

#### 2.3.7.2 Advantages over Other Metrology Systems

There are several reasons for the utilisation of iCT systems in metrology applications instead of other metrology instruments and sytems. Possibility of inspecting internal areas of workpieces, no need for fixturing, and enormous gain in measuring time represent only some of them. However, it should be noted that this beneficial technology has also some drawbacks, e.g. in terms of measurement uncertainty and traceability. Table 2.7 demonstrates those main advantages and drawbacks of iCT systems.

**Table 2.7:** Advantages and drawbacks of iCT (partly *adapted from* [45])

| Advantages | Drawbacks |
|---|---|
| Non-destructive inspection of interior geometry and structures | Lack of standardisation |
| Tremendously reduced measuring time and effort | Numerous and complex influence quantities |
| High amount of collected measuring points and data cloud | Artifacts reduce measurement capability |
| Enables the scanning and inspection of workpieces of almost any colour, form, surface and material (i.e. multi-material) up to certain values of physical characteristics of X-rays and workpiece (i.e. penetrable thickness and material density) | Measurement of multi-material workpieces can be problematic |
| The potential of future application areas is very promising, particularly in the context of in-line metrology | Lack of traceability due to the often unknown measurement uncertainty |

#### 2.3.7.3 Industrial CT vs Medical CT

Although iCT and mCT do not differ in the basic operational principle, their specific functional characteristics are not same, since they are utilised to achieve different objectives. One of the most distinguishing factors here is the object or thing to be investigated. In case of medical applications, it is nothing but the human body, and therefore the X-ray intensity must be limited to certain values, since it can be dangerous otherwise. This relatively lower X-ray intensity limits the image quality, clarity and accuracy. Although the achievable accuracies lie in the range of millimetres, this is mostly sufficient for medical applications, e.g. for tumor diagnosis. However, for industrial and particularly for metrological purposes, measurement accuracies in the range of micrometres are required nowadays. Since there is no risk of being harmed for industrial workpieces, unlike humans, higher X-ray intensities are applied in order to obtain more clear and accurate measurement results. [46]

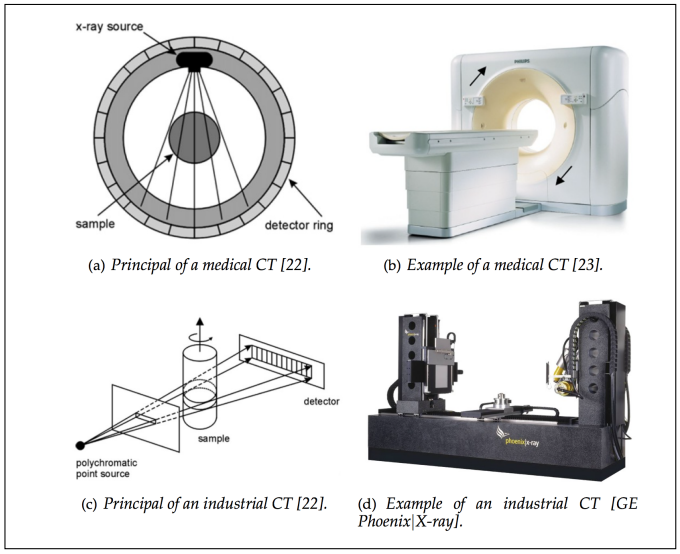


(a) *Principal of a medical CT [22].*

(b) *Example of a medical CT [23].*

(c) *Principal of an industrial CT [22].*

(d) *Example of an industrial CT [GE Phoenix|X-ray].*

**Figure 2.36:** iCT vs. mCT (*adapted from* [45])

Characteristics of iCT and mCT scanners differ in following important issues: [45]

- Amount of applied energy ($< 200\,keV$ for mCT and up to $15\,MeV$ for iCT scanners)
- Type of the investigated matter (i.e. blood, tissue and bone for mCT; wood, metals, concrete, ceramics and composites for iCT scanners)
- In mCT the patient stays still, and the scanner rotates around the patient, whereas in iCT the object is the moving part, which is rotated by means of a rotary table
- Attainable system resolution ($1\,mm$ to $2\,mm$ for human subjects in mCT and $< 0.5\,mm$ (macro CT systems) and $10\,\mu m$ to $20\,\mu m$ (micro CT systems) for iCT systems)

There are several modifications and adjustments of mCT scanners' characteristics in order to have suitable, capable and custom-tailored iCT scanners for industrial metrology purposes. First of all, applying higher energy and more intense X-rays ensures a more effective penetration, particularly in case of dense materials. Second, utilisation of finer X-ray detectors and/or smaller focal spot sizes contributes for a better resolution. Third, integration times are prolonged, which enhance the signal-to-noise ratio, and compensate for the loss in signal from the diminished output, as well as in source and detector efficiency. [45]

#### 2.3.7.4 Applications for iCT

Utilisation of iCT in industrial field facilitates and accelerates several kind of challenging processes in various application areas. The most important ones of them are explained briefly in following. In Figure 2.37 a more structured overview is given.

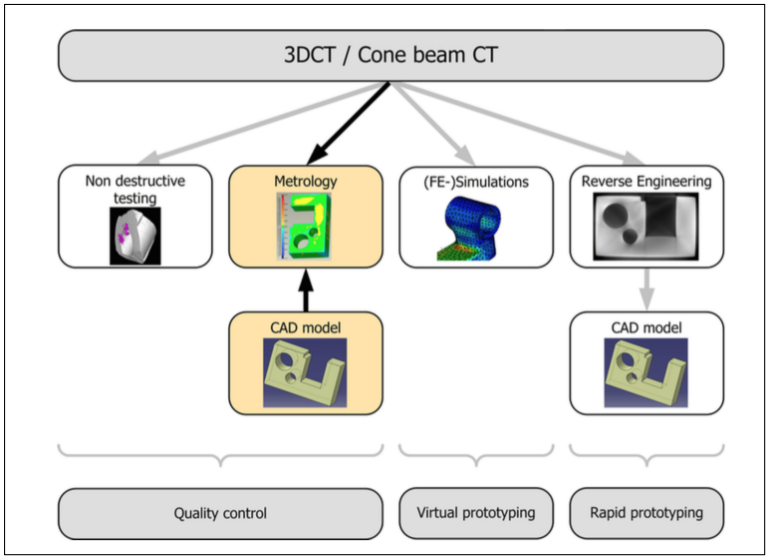


**Figure 2.37:** Classification of application areas of iCT in QC, virtual and rapid prototyping [47]

*Part-to-CAD comparisons* iCT allows conducting a comparison between the workpiece and its CAD model. The result of a iCT measurement is typically a 3D point cloud and within the framework of Part-to-CAD comparison it gets matched with the points of CAD model in order to determine dimensional differences, deviations and gather informations related to accuracy. In this regard, often the different colours are used in representation of models to improve readability and interpretation of results, deviations and analysis. This also includes the detection of insufficient and surplus material, contortions and distortions. Due to the beneficial characteristics of iCT, this complicated process is relatively fast and straightforward. [48]

*Part-to-Part comparisons* In this case, the colour-coded visual results of iCT are used e.g. to compare same kind of but different parts from the identical mold or workpieces manufactured from different lots or by different tools. Thus, iCT enables users to identify dimensional and other deviations between those parts (often in comparison to a *gold standard* part), and facilitates to conduct quality analyses for them. [48]

*Dimensional inspections* Workpiece drawing and a CAD model are used to program dimensions, and due to this capability iCT dimensional inspections delivers two times faster results than the conventional metrology solutions. A completed dimensional inspection protocol can be created merely in a few minutes after the programming and scanning of the part. [48]

*Assembly analysis* As it is very hard and troublesome to observe assembly details, and detect possible faults, they are often dropped beneath the radar. As a solution to this problem, iCT enables the fast detection and straightforward analysis of features e.g. inclusions, fit, seals, voids, interface and interference. The particularity of iCT lies in its ability to conduct those tasks without disassembling or sectioning the part. To detect poor fit and function, previously hidden components in assemblies can be now checked with ease by iCT. [48]

*Reverse engineering* As mentioned before, the typical end result of a 3D iCT scan is a 3D point cloud. In the sequel of a 3D iCT scan, this point cloud can be transformed to a data file in stereolithography (STL) format in order to create a CAD model. By means of this CAD model, molding or 3D printing of very accurate prototypes can be realised in an efficient and smooth manner. [48]

#### 2.3.7.5 International Standards and Guidelines for CT

In the context of tactile and optical coordinate metrology, there exist international standards and guidelines that are recognised and utilised widely around the world. They explain related procedures for these metrology instruments, and build a common basis for their understanding. In the context of iCT, however, such standards and guidelines regarding the application of iCT systems for metrological purposes, and evaluation of measurement error and uncertainty sources are still under development. The main reasons behind that are the high number and complexity of influence factors, and the lack of know-how about its characteristics, as the application of this technology for in the area of metrology is a relatively new approach. Therefore, it is not yet possible either to state correct measurement uncertainty values or ensure the traceability of measurements conducted by means of iCT systems. A more comprehensive overview of standards and guidelines for iCT is given in [49].

Table 2.8 lists the currently available international standards regarding the utilisation of CT systems. They mainly describe the general principle and terminology CT. Besides, there exist another guideline issued by the VDI/VDE Society for Metrology and Automation Engineering (GMA). This guideline, i.e. VDI/VDE 2630, aims to explain the characteristics of CT systems regarding their applications in metrology, and to build a common understanding basis for comparison and traceability purposes. It consists of the following parts:

- Part 1.1: Basics and definitions
- Part 1.2: Influencing variables on measurement results and recommendations for computed tomography dimensional measurements
- Part 1.3: Guideline for the application of Deutsches Institut für Normung (DIN) EN ISO 10360 for coordinate measuring machines with CT-sensors
- Part 1.4: Measurement procedure and comparability
- Part 2.1: Determination of measurement uncertainties in measurements using CT systems (in preparation)

### 2.3.8 Micro- and Nano-Coordinate Metrology

The challenges in production metrology have been greatly influenced and shaped by advances in manufacturing engineering. Unlike a couple of decades ago, at the time being, technological advances in production environments have been tried to be predicted in a systematic way in the light of the ongoing and future challenges as well as trends. Those all dynamics are summarised in roadmaps (e.g. implementing

**Table 2.8:** International standards for CT [49]

| International Standard | Title |
|---|---|
| ISO 15708-1 | Non-destructive testing – Radiation methods – Computed tomography – Part 1: Principles (2002) |
| ISO 15708-2 | Non-destructive testing – Radiation methods – Computed tomography – Part 2: Examination practices (2002) |
| EN 16016-1 | Non-destructive testing – Radiation methods – Computed tomography – Part 1: Terminology (2011) |
| EN 16016-2 | Non destructive testing - Radiation method - Computed tomography - Part 2: Principle, equipment and samples (2011) |
| EN 16016-3 | Non destructive testing - Radiation method - Computed tomography - Part 3: Operation and interpretation (2011) |
| EN 16016-4 | Non destructive testing - Radiation method - Computed tomography - Part 4: Qualification (2011) |
| ISO/WD 10360-11 | Geometrical product specifications (GPS) - Acceptance and reverification tests for coordinate measuring machines (CMM) - Computed tomography (2011) |
| ASTM E 1695-95 | Standard test method for measurement of computed tomography (CT) system performance (2006) |
| ASTM E 1441-11 | Standard guide for computed tomography (CT) imaging (2011) |
| ASTM E 1570-11 | Standard practice for computed tomographic (CT) examination (2011) |
| ASTM E 1672-12 | Standard guide for computed tomographic (CT) system selection (2012) |

Metrology in the European Research Area (iMERA) roadmaps) which give a systematic overview of various development aspects over time.

As far as the micro- and nano-technology concerned, abovementioned advances affect the dimensional metrology to a great extent. There are many challenges to overcome both in the field of optical lithography and multi-scale, truly 3D traceable nano-measuring technology. Those are mentioned in the iMERA Roadmap *Dimensional metrology for micro- and nano-technologies* [50] with prospect up to 2025 (Figure 2.38).

In a general point of view, miniaturisation of products (e.g. implantable insulin pumps, mobile phone cameras), and integration of micro- and nanotechnology into the parts and products whose size can be classified as traditional (e.g. easy-to-clean surface modifications, embedded systems) can be considered as two of the most important advances. In this context, there exist two main approaches; *top-down* and *bottom-up*. The former is used mostly in microtechnology, whereas the latter is founded in nanotechnology applications. [51]

In bottom-up approach the analytical tools from solid matter physics or materials science, e.g. Scanning Probe Microscopy (SPM), is modified and adapted for metrological applications. On the other hand the top-down approach contains the miniaturisation of traditionally sized metrology instruments and systems, e.g. conventional CMMs, in order to measure micro features and characteristics. In this regard, smaller probing forces and elements, a better resolution for axes, as well as improved repeatability for miniaturised probing systems are required [52]. While the bottom-up approach is particularly beneficial for nanotechnology, the top-down approach is used mainly in microtechnology. A mixture of those both approaches as a hybrid solution is also possible. [51]

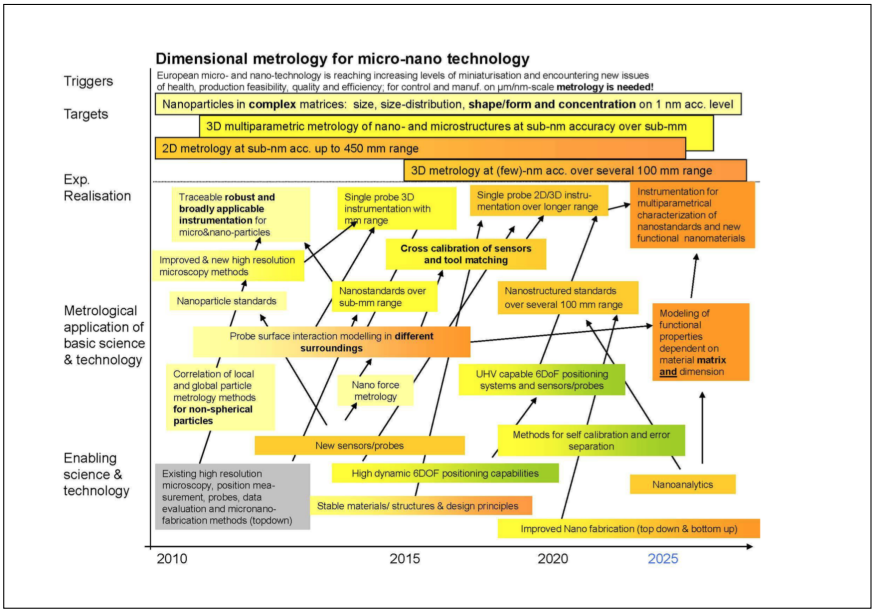


**Figure 2.38:** Roadmap - Dimensional metrology for micro- and nano-technologies [50]

Measurements conducted on micro- and nanometre range are more sensitive against the ambient conditions and effects, in comparison to those conducted on macroscopic level. The main reasons behind that are the finer resolution valeus, and very large ratio between measuring range and resolution. Figure 2.39 demonstrates the measuring range and resolutions for different methods. [51]

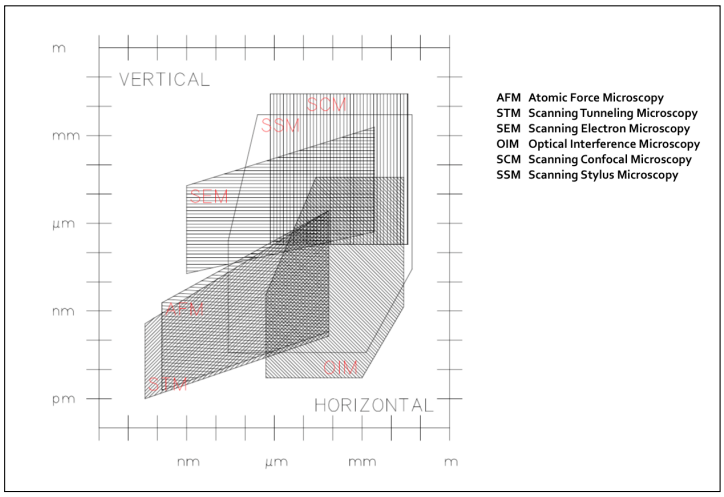


**Figure 2.39:** Measuring resolution and measuring range for different methods [53]

### 2.3.8.1 Related machines and systems in universities and institutions

In the following the characteristics of some related micro- and nanomeasuring machines and systems available in universities and institutions are summarised. [54] Table 2.9 gives also a compact overview.

VERMEULEN'S MACHINE Vermeulen's machine was developed at the Eindhoven University of Technology by the group of Prof. Schellekens.

Table 2.9: Overview of available micro- and nano-CMMs

| Name | Institute/Company | Measuring range [$mm^3$] | 3D Measurement uncertainty [$nm$] |
|---|---|---|---|
| **Ruijl - ISARA** | Philips centre for manufacturing research | 100 x 100 x 40 | 30 |
| **ISARA 400** | IBS Precision Engineering | 400 x 400 x 100 | 109 |
| **Vermeulen - F25** | Eindhoven University of Technology | 100 x 100 x 50 | 100 |
| **van Seggelen** | Eindhoven University of Technology | 50 x 50 x 4 | 25 |
| **Ilmenau** | Ilmenau University of Technology | 25 x 25 x 5 | 30 |
| **PTB** | ptb} | 25 x 40 x 25 | 100 |
| **Peggs** | npl} | 50 x 50 x 50 | 50 |

In this design, the Abbe principle could be fulfilled in two axes; an intermediate was applied to enable the utilisation of linear scales. Besides, air bearings were used in this design. The measuring volume of Vermeulen's machine is $100\,mm \times 100\,mm \times 100\,mm$.

RUIJL'S MACHINE A 3D CMM by Ruijl in the Philips centre for manufacturing research. It has a special design that enables conducting measurements according to the Abbe principle in all 3 axes. A solid zerodur block, which is the measurement reference, moves with the workpiece in 3 directions, and meanwhile it is measured by 3 flat mirror laser interferometer systems..

VAN SEGGELEN'S MACHINE In this design, the Vermeulen's machine was improved and miniaturised further. The most significant modification is the utilisation of a double flexible hinge system. It ensures the straightness of movement in the z-direction.

ILMENAU MACHINE Ilmenau machine is a nanomeasuring machine which was developed at the Ilmenau University of Technology. It is equipped with 3 laser interferometers, and therefore is similar to the Ruijl's machine in this aspect.

PTB A 3D micro measuring system, i.e. (3D-MME), which is based on a commercial CMM, was developed by Physikalisch-Technische Bundesanstalt (PTB). It enables conducting coordinate measurements on microstructures with a measurement uncertainty of $< 100\,nm$. Its measurement range is $25\,mm \times 40\,mm \times 25\,mm$.

## 2.4 Rotary Tables and Their Applications in Modern Production Metrology

### 2.4.1 Introductory Overview

Rotary tables are disc-shaped units which are utilised both in machining (in machine tools), in non-cutting automation and in production metrology applications, mainly to position workpieces accurately and precisely. Due to their structure, they allow related workers and operators to conduct drilling or cutting operations of a workpiece at quite precise positional intervals around their rotation axis. According to application area and purpose, rotary tables differ both in construction form, rigidity, and stiffness. The demands on the accuracy and stiff-

ness in the machining are higher than those in the non-cutting area. Shortest switching times are required in the automation. [55, 56]

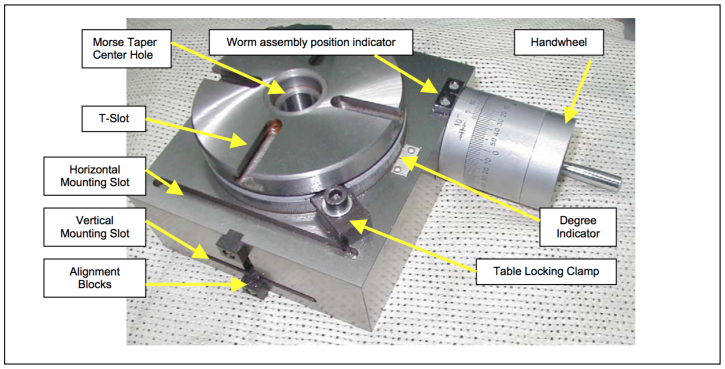


**Figure 2.40:** A typical rotary table and its components [57]

As far as the control of rotary tables concerned, there are manually controlled or CNC types. For specific application purposes, some types are designed and constructed to be utilised with a positioning plate (e.g. dividing or indexing plates). Depending on these design and application aspects, they are also called (rotary) indexing tables/heads or dividing tables/heads. [55, 56, 58]

A stable and solid base is considered as a common element of rotary table units, and by means of clamps, it is possible to mountit to a separate table or fixture. In a very simple and straightforward point of view, rotary tables are nothing but rotating discs that ensure accurate and precise positioning of workpieces during various different machining or measuring processes. It is possible to rotate their disc portion freely for indexing purposes or to turn them by means of a mountedcontrol arm, i.e. by worm wheel. In applications, where precision is extremely important, duplex-type worm wheels are utilised to rotate rotary tables. The main reason behind that is the compensation of backlash. In automated machining, the CNC is frequently utilised to rotate rotary tables. [55, 58]

As a flexible and versatile element, rotary tables are nowadays utilised widely in many specific industrial applications, e.g. drilling holes in flanges and machining spanner flats on bolts. Cutting complex arcs, curves, as well as round pieces with protruding tangs are some of the specific applications that are realised (easier) by means of a rotary table. Moreover, in case of they are run by a stepper motor, and used together with a CNC milling machine and tailstock, rotary tables can also be utilised instead of a lathe. [55, 58]

APPLICATIONS IN MACHINING A rotary table is a part of a machine tool, on which workpieces are clamped for machining. It has a vertical and/or often also horizontal rotation axis, around which the rotary or indexing table with the clamped workpiece can be rotated in order to conduct related machining process at different positions or on the rotating workpiece. [56]

There are machine tools with continuously rotating rotary tables, e.g. vertical turning mills, gear shaping machines and gear hobbing machines. In other machines, a Numerical(ly) Control(led) (NC) rotary

table is controlled and further clocked freely-programmable (e.g. in keyway slotters, milling machines, grinding machines or machining centres). Depending on the application, servo motors with backlash-adjustable gearbox or direct drives with torque motors are utilised as drive units. Rotary indexing tables with fixed pitch (e.g. $8 \times 45°$) are used in rotary transfer machines. Within rotary transfer machines, rotary indexing table transports workpieces from a machining station to another. Manual indexing heads can also be attached on a machine afterwards. [56]

APPLICATIONS IN AUTOMATION Rotary indexing tables with cam drive often form the core of the related systems in assembly machines, welding units, screen printing units and pad printing units. On an additional indexing plate, rotary indexing table transports workpieces from station to station. [56]

FURTHER APPLICATIONS Beside the application cases in machines for machining and production processes, rotary tables are also used for transportation or for the all-round presentation of objects. (e.g. Imperia-Statue in Konstanz). In shop-windows, goods are presented all-round on rotary tables, in particular, heavy and bulky computer monitors and televisions can be aligned for different viewing directions. Revolving stages, devil's wheels (amusement ride), roulettes, rotary tables for food presentation are also some of the further application examples. Moreover, image presentations with 360°-view simulate the views which are made possible by a rotary table. A round, however, rotary table called equipment was developed by Franz Wurz and has been in operation since about 1990 in Teesdorf driving safety training centre, and replaced by a skidding plate meanwhile. They used to be utilised for generation of skidding with motor vehicles. [56]

### 2.4.2 Rotary tables in coordinate metrology

Application areas of rotary tables are not limited those in machining and automation. Also in modern coordinate metrology, rotary tables are considered as one of the most crucial and purposive accessories. There exist various types of them for modern production metrolgoy applications. In addition to the rotary tables which can be acquired as an external unit, there are also built-in versions which are designed as an integrated element of a CMM. These versatile and flexible elements bring many advantages when they are utilised on CMMs as fourth axis[12].

Rotary tables are mainly used for measuring tasks at rotary bodies with recurring geometries such as gears, hob cutters, rotors and impellers. Despite the fact that their use is thought mainly for the rotary bodies, they also show advantages at measuring of prismatic workpieces. Due to their structure, not only do they ensure a better and easier accessibility to all sides of a part being measured but they also increase measuring speed, and consequently reduce measuring times significantly. They extend the effective usable measuring volume, and make the measurement of quite large workpieces by relatively small

12 It should be noted that the rotary tables on CMMs as *fourth axis* do not increase measuring dimensions, i.e. it stays as 3D, however, they improve the flexibility to a great extent and expedite the measurements.

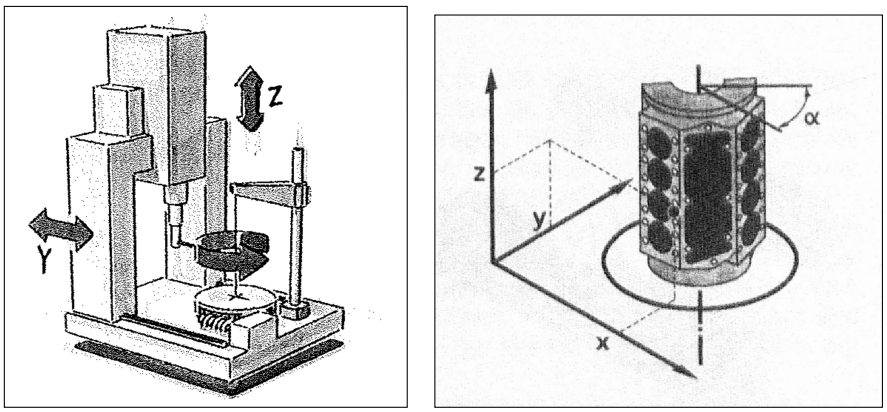


**(a)** Utilisation of a rotary table on a CMM [59]

**(b)** 4-axis-structure on a CMM [60]

**Figure 2.41:** Rotary tables and CMMs

CMMs possible. Moreover, they enhance the measuring accuracy, since it is not necessary anymore to move the CMM with its all three axes (e.g. in case of a gear measurement). These and several further advantages they bring with them can be summarised as follows [26, 61];

- The required transverse area of translational movements can be reduced significantly by rotating the workpiece into a convenient position, which leads to smaller machine sizes for the same range of measurement tasks. Due to this fact, measurements are less affected by temperature influences, and more accurate measurement results are gathered.
- Form inspections can be conducted also on workpieces with tight tolerances by utilising a sufficiently precise working rotary table and a high-precision measuring touch probe, where only the rotary table is rotated during the measurement.
- The rotation of the form element to be measured into a convenient position often enables the utilisation of simple probes, and saves complicated probe changes.
- Complex workpieces (e.g. bores with under-cuts) can be rotated into a convenient position with respect to the machine axes, whereby the accessibility of the targeted touch points are improved (even without a articulating probe), and CNC programming becomes simpler and clearer.

As already mentioned, those advantages become more and more obvious and purposive when measuring rotationally-symmetrical parts (e.g. gears and hob cutters). Nevertheless, it should be noted that additional error sources are caused as well by rotary tables when they are utilised within CMSs. [62]

In this regard, the workpiece to be measured is placed on a rotary table that has a precision driving motor and an angle measuring system. By turning the rotary table in accurately set angular steps, the workpiece is brought to appropriate positions for related measurement tasks. The probe head does not have to be rotated precisely, due to the fact that the rotary table fulfil this requirement. Thus, it brings the advantage

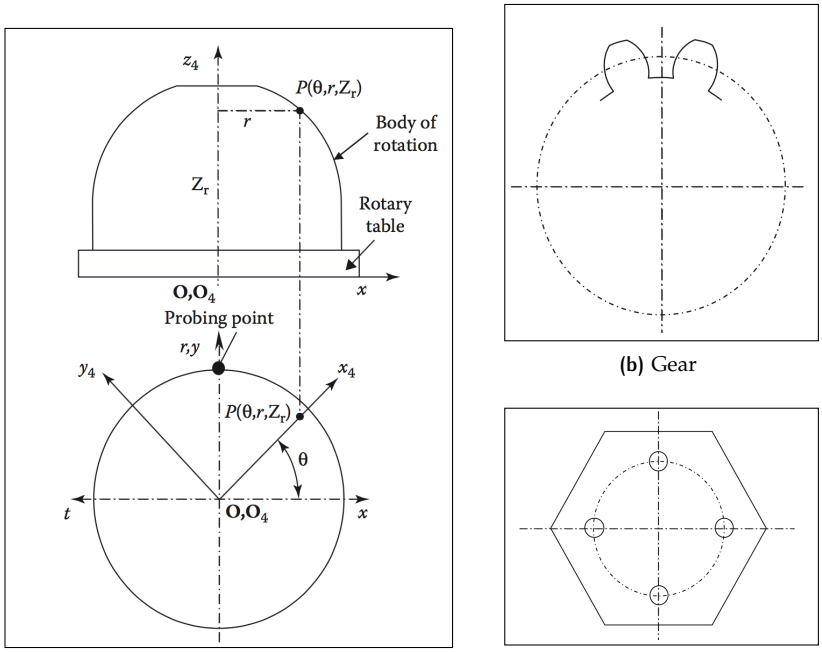


(a) Body of rotation

(b) Gear

(c) Polyhedron with equally spaced holes

**Figure 2.42:** Features measured with a rotary table [29]

of utilising only a basic probe head control to access and gather measuring points which otherwise would be very hard or even impossible to reach. Beside the MCS and WCS, a polar coordinate system (aligned on the rotational axis) is utilised by rotary tables used on CMMs. Due to the relatively high complexity, computation units are of great importance, when it comes to conducting the conversion between those coordinate systems. [59]

After a calibration process, the position and the direction of the rotational axis of rotary table are known, and taken into account by means of computer software. The workpiece which is mounted on rotary table can be measured in different but precisely-defined angular positions. Software calculates and settles the angular position of rotary table together with its position and direction, so that the results are (after the evaluation) represented in such a way that as if no rotary table were utilised. [26]

As far as their utilisation purposes concerned, two aspects push themselves to the fore, i.e. solely for supplying of repositioning capability, or as a vital element of a whole coordinate metrology chain. If they are utilised as in the latter situation, rotary table errors ought to be taken into account when generating an error map for computational error correction algorithms. Usually, a horizontal surface face plate is utilised by rotary tables to support the measuring object. However, there exist also vertical types. A capstan type friction wheel drive system can be utilised for servo drive in order to eliminate or compensate for the backlash. Thus, the lost motion between rotary table and servo motor is compensated, and it enhances the ability of servo system to position accurately in a more stable way. [62]

Besides, an air switch is utilised frequently, when using air bearings in rotary tables. The reason behind that is the need to engage and disengage the drive by a cylinder which is actuated by abovementioned air switch. It facilitates free rotation for manual operation, and expedites positioning procedures. Rotary table is exactly situated on kinematic mounts, and the air pressure is switched off when conducting measurements. Moreover, air jet pads can be utilised for a smoother operation. When they are actuated, the table is enabled floating on a level flat surface. It becomes especially significant and purposive if the rotary table is moved frequently to different positions on the CMM for diverse applications. [62]

### 2.4.3 Geometric Model of a CMM with a Rotary Table

In [29], a detailed geometric model for CMMs with a rotary table is given within the context of error compensation and this subsection summarises its relevant and significant parts for this thesis work.

*Coordinate systems* As the rotary table is rotated, the workpiece mounted on the rotary table rotates with it as well. A fifth coordinate system, $\mathbf{O_4X_4Y_4Z_4}$, is defined on the rotary table in order to determine its mathematical model (Figure 2.43). Commonly, the axis $z_4$ is specified as the axis of rotation. Its intersection point with **OXY** plane, $\mathbf{O_4}$, represents the origin of the coordinate system, and the coordinate system $\mathbf{O_4X_4Y_4Z_4}$ rotates together with the rotary table. $\mathbf{X_{4o}}$ and $\mathbf{Y_{4o}}$ stand for the initial positions of $x_4$ and $y_4$, respectively, and $\mathbf{O_4X_{4o}}$ lies parallel to the plane **OXZ**. [29]

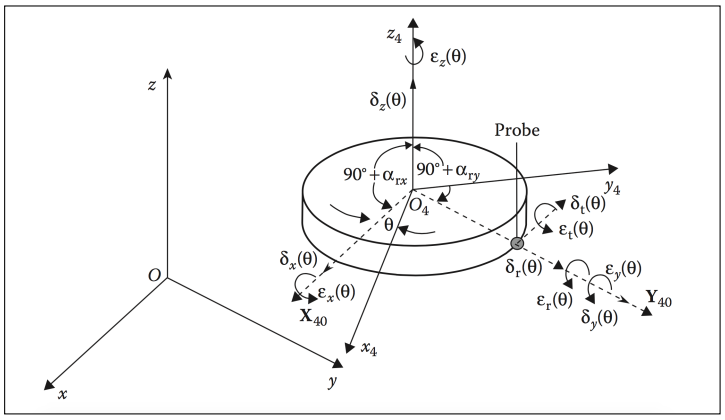


**Figure 2.43:** Geometric model of a rotary table [29]

*Individual errors* Due to the fact that the rotary table is rotated by an angle $\theta$, all the individual error motions of rotary table are specified dependent on $\theta$. Those six error motions can be broken down into two groups: [29]

- The linear errors of the origin of coordinate system $\mathbf{O_4}$; $\delta_x(\theta)$, $\delta_y(\theta)$ and $\delta_z(\theta)$; and
- The angular errors of axis $z_4$ about three mutually perpendicular axes; $\varepsilon_x(\theta)$, $\varepsilon_y(\theta)$., and $\varepsilon_z(\theta)$.

$\varepsilon_z(\theta)$ is the error of rotated angle $\theta$, while $\varepsilon_x(\theta)$ and $\varepsilon_y(\theta)$ are tilt motions of the rotational axis about two other axes $x_4$ and $y_4$.

Nevertheless, sometimes it is more straightforward and useful to measure and represent those error motions in a different way, i.e. in a cylindrical coordinate system. This becomes particularly advantageous when the bodies of rotation are measured, given the fact that all cross sections of a body of rotation, which are perpendicular to the axis of rotation, consist of circles. That cylindrical coordinate system, $(\theta, r, Z_r)$, is defined by the argument angle, $\theta$, by the radius,$r$, and by the height of point $\mathbf{P}$, $Z_r$, respectively (Figure 2.42a). In case of the measurement of bodies of rotation, solely error motions in the radial direction generates errors in measurement, and it is plausible to break down them into two subcategories, i.e. tangential error motion $\delta_t(\theta)$ and radial error motion $\delta_r(\theta)$. When measuring bodies of rotation, the former has a negligible impact. The tangential and radial directions do not vary with rotation. [29]

Both $x$ and $y$ direction are suitable for the definition of radial direction. The workpiece is touched by the probe in that selected radial direction. As far as a moving bridge type CMM concerned, consideration of the following two facts makes the selection of the $y$ direction as the radial direction reasonable. First, the component for $y$ motion is lighter than that for $x$ motion. Second, while there exist Abbe offsets in both $y$ and $z$ directions for $x$ motion, there is merely Abbe offset in $z$ direction for $y$ motion. [29]

The calibration of $\delta_r(\theta)$ can be realised simply by utilising an indicator to determine the $y$ deviation of a well-centred reference mandrel. Reference mandrel rotates together with the rotary table and has a quite small roundness error. Elimination of its mounting eccentricity is realised simply by simply by data processing. As far as its roundness error concerned, either multistep or reversal techniques are required. The tangential direction, on the other hand, is $90°$ counterclockwise turned about the axis $z_4$ against radial direction (Figure 2.43). So as to determine the $X$ deviation of the reference mandrel, calibration of $\delta_t(\theta)$ can be realised by means of an indicator. [29]

Moreover, breaking down the tilt error motions into two subcategories, i.e. into angular error motion about the radial axis $\varepsilon_r(\theta)$, and angular error motion about the tangential axis $\varepsilon_t(\theta)$, is also plausible. If the point $\mathbf{P}(\theta, r, Z_r)$ is considered, angular error motion about the tangential axis generates an error motion in the radial direction, $Z_r\varepsilon_t(\theta)$, and error motion in the $z$ direction, $-r\varepsilon_t(\theta)$. Similarly, angular error motion about the radial axis generates an error motion in the tangential direction, $-Z_r\varepsilon_r(\theta)$. [29]

In addition to linear and angular error motions, there exist also squareness errors between the $x$ and $y$ axes of the CMM, and the axis of rotation. That between $y$ axis and $\mathbf{O_4Z_4}$, $\alpha_{ry}$ generates an error motion $-Z_r\alpha_{ry}$ in the $y$ direction, and an error motion $Y_{p4}\alpha_{ry}$ in the $z$ direction, whereas the one between $x$ axis and $\mathbf{O_4Z_4}$, $\alpha_{rx}$ generates an error motion $-Z_r\alpha_{rx}$ in $x$ direction, and an error motion $X_{p4}\alpha_{rx}$ in $z$ direction. $X_{p4}$ and $Y_{p4}$ represent here the coordinates of probing point in $\mathbf{O_4X_4Y_4Z_4}$. [29]

*Geometric model for measuring bodies of rotation* In case of the measurement of a body of rotation, and if the radial and tangential directions are defined by the $+y$ and $-x$ directions of the CMM, respectively,

the equivalent total error motion of the probe at point $(\theta, r, Z_r)$ can be written as; [29]

$$\theta = -\varepsilon_z(\theta) - [X + \delta_t(\theta) + Z_r\alpha_{rx} - Z_r\varepsilon_r(\theta)]/r \tag{2.3}$$

$$r = Y - \delta_r(\theta) + Z_r[\alpha_{ry} - \varepsilon_t(\theta)] \tag{2.4}$$

$$Z_r = Z - \delta_z(\theta) - r[\alpha_{ry} - \varepsilon_t(\theta)] \tag{2.5}$$

where $X$, $Y$, and $Z$ represent the $x$, $y$, and $z$ components of CMM error motion, which can be calculated from related geometric model equations depending on the machine type. [29]

The error motions generated due to the rotary table are those of the workpiece. When they are transformed to the error motions of the probe, their signs are changed. In case of the $+y$ direction is selected as the tangential direction, and probing is along the $+x$ axis, Equation 2.3 through Equation 2.5 should be transformed to; [29]

$$\theta = -\varepsilon_z(\theta) - [Y + \delta_t(\theta) + Z_r\alpha_{ry} - Z_r\varepsilon_r(\theta)]/r \tag{2.6}$$

$$r = X - \delta_r(\theta) + Z_r[\alpha_{rx} - \varepsilon_t(\theta)] \tag{2.7}$$

$$Z_r = Z - \delta_z(\theta) - r[\alpha_{rx} - \varepsilon_t(\theta)] \tag{2.8}$$

*Geometric model for measuring equally spaced features* In this regard, there exist three characteristics to be measured [29]:

1. The form and dimension errors of individual features;
2. The pitch errors of equally spaced features;
3. The position errors of features with regard to other elements of the part.

As far as the first case concerned, e.g. measurement of the profile error of a tooth, the form, and the dimension error of a hole, the rotary table is held at a certain position; i.e. it is not rotated. Therefore, its errors do not have to be taken into account, and the geometric model of the measurement consists merely of that of the CMM. [29]

In the second case, e.g. when measuring the spacing errors of the holes, and adjacent and cumulative pitch errors of teeth, the probe repeats all but the identical motion to measure each individual feature. Due to the utilisation and rotational movement of the rotary table the probe can measure all the features successively. In contrast to the first case, in this case, solely the errors of the rotary table are taken into consideration. Considering the y-direction as the radial direction, the mathematical model of the measurement becomes as follows; [29]

$$\theta = -\varepsilon_z(\theta) - [\delta_t(\theta) + Z_r\alpha_{rx} - Z_r\varepsilon_r(\theta)]/r \tag{2.9}$$

Considering the $x$ direction as the radial direction, angular spacing error can be formulated as; [29]

$$\theta = -\varepsilon_z(\theta) - [\delta_t(\theta) + Z_r\alpha_{ry} - Z_r\varepsilon_r(\theta)]/r \tag{2.10}$$

Multiplying $\theta$ by $r$ of the characteristic point of the feature is sufficient in order to transform angular spacing errors to linear ones. When the spacing errors of a set of holes are inspected, the centre of the hole is defined according to a certain criterion serves as its characteristic point. [29]

Finally, in the third case, both the CMM and rotary table errors are taken into consideration. Although some parameters, e.g. the tooth direction and thickness, seem like the parameters of the individual feature, they are, in fact, associated to the whole part. The former is estimated with regard to the axis of the gear, and the latter is estimated at the dividing circle, which is associated with other gear parts. [29]

Derivation of the general geometric model of a CMM with a rotary table is realised by means of the following coordinate transformation; [29]

$$\mathbf{P} = \mathbf{R}^{-1}(\theta)\mathbf{P_4} + \mathbf{O_4} + \delta\mathbf{O_4} \tag{2.11}$$

where $\mathbf{P_4} = (X_{p4}, Y_{p4}, Z_{p4})^T$ represents the probe tip vector in the rotary table system, $\mathbf{R}^{-1}(\theta)$ is the inverse rotational matrix of the rotary table, $\mathbf{O_4} = (X_{O4}, Y_{O4}, Z_{O4})^T$ stands for the vector of origin of the rotary table system in **OXYZ**, and $\delta\mathbf{O_4}$ is the vector expressing linear error motions of point $\mathbf{O}_4$. [29]

$$\mathbf{R}^{-1}(\theta) = \begin{matrix} \cos(\theta + \varepsilon_z(\theta)) & -\sin(\theta + \varepsilon_z(\theta)) & \varepsilon_y(\theta) \\ \sin(\theta + \varepsilon_z(\theta)) & \cos(\theta + \varepsilon_z(\theta)) & -\varepsilon_x(\theta) \\ -\varepsilon_y(\theta)\cos(\theta) + \varepsilon_x(\theta)\sin(\theta) & \varepsilon_y(\theta)\sin(\theta) + \varepsilon_x(\theta)\cos(\theta) & 1 \end{matrix} \tag{2.12}$$

A crucial distinctive characteristic of $\mathbf{R}^{-1}(\theta)$ is that because $\theta$ is not an infinitesimal angle, $\cos\theta$ cannot be simplified as 1, and $\sin\theta$ cannot be substituted by $\theta$. The homogenous form of Equation 2.11 can be expressed as; [29].

$$\begin{matrix} X_p \\ Y_p \\ Z_p \\ 1 \end{matrix} = \begin{matrix} \cos(\theta + \varepsilon_z(\theta)) & -\sin(\theta + \varepsilon_z(\theta)) & \varepsilon_y(\theta) & X_{O4} + \delta_x(\theta) - Z_{p4}\alpha_{rx} & X_{p4} \\ \sin(\theta + \varepsilon_z(\theta)) & \cos(\theta + \varepsilon_z(\theta)) & -\varepsilon_x(\theta) & Y_{O4} + \delta_y(\theta) - Z_{p4}\alpha_{rx} & Y_{p4} \\ -\varepsilon_y(\theta)\cos(\theta) + \varepsilon_x(\theta)\sin(\theta) & \varepsilon_y(\theta)\sin(\theta) + \varepsilon_x(\theta)\cos(\theta) & 1 & Z_{O4} + \delta_z(\theta) & Z_{p4} \\ 0 & 0 & 0 & 1 & 1 \end{matrix} \tag{2.13}$$

In case of a perfect CMM with a perfect rotary table;

$$\begin{matrix} X_p - X \\ Y_p - Y \\ Z_p - Z \\ 1 \end{matrix} = \begin{matrix} \cos(\theta) & -\sin(\theta) & 0 & X_{O4} & X_{p4} \\ \sin(\theta) & \cos(\theta) & 0 & Y_{O4} & Y_{p4} \\ 0 & 0 & 1 & Z_{O4} & Z_{p4} \\ 0 & 0 & 0 & 1 & 1 \end{matrix} \tag{2.14}$$

where $(X_{p4}, Y_{p4}, Z_{p4})^T$ are the coordinates of the probe tip in the rotary table coordinate system. The error motions generated by both error motions of the CMM and rotary table can be expressed as; [29]

$$\begin{matrix} X_4 \\ Y_4 \\ Z_4 \end{matrix} = \begin{matrix} X_{p4} \\ Y_{p4} \\ Z_{p4} \end{matrix} - \begin{matrix} X_{p4} \\ Y_{p4} \\ Z_{p4} \end{matrix} \tag{2.15}$$

$Z_{O4}$ and all error motions are usually slight. When all the second-order errors are neglected, and Equation 2.13 and Equation 2.14 are replaced into Equation 2.15, the below equations are attained: [29]

$$\begin{aligned} \Delta X_4 = {} & [\Delta X - \delta_x(\theta) + Z_{p4}\alpha_{rx}]\cos\theta + [\Delta Y - \delta y(\theta) + Z_{p4}\alpha_{ry}]\sin\theta \\ & - (X_p - X_{O4})\sin\theta\varepsilon_z(\theta) + (Y_p - Y_{O4})\cos\theta\varepsilon_z(\theta)) \\ & + Z_p[-\cos\theta\varepsilon_y(\theta) + \sin\theta\varepsilon_x(\theta)] \end{aligned} \tag{2.16}$$

$$\begin{aligned} Y_4 = {} & [-X + \delta_x(\theta) - Z_{p4}\alpha_{rx}]\sin\theta + [Y - \delta y(\theta) + Z_{p4}\alpha_{ry}]\cos\theta \\ & - (X_p - X_{O4})\cos\theta\varepsilon_z(\theta) - (Y_p - Y_{O4})\sin\theta\varepsilon_z(\theta)) \\ & + Z_p[\cos\theta\varepsilon_x(\theta) + \sin\theta\varepsilon_y(\theta)] \end{aligned} \tag{2.17}$$

$$\begin{aligned} Z_4 = {} & [\cos\theta\varepsilon_y(\theta) + \sin\theta\varepsilon_x(\theta) - \alpha_{rx}](X_p - X_{O4}) \\ & + [-\cos\theta\varepsilon_x(\theta) + \sin\theta\varepsilon_y(\theta) - \alpha_{ry}](Y_p - Y_{O4}) \\ & - \delta_z(\theta) + Z \end{aligned} \tag{2.18}$$

### 2.4.4 Acceptance and reverification tests for CMMs with the axis of a rotary table as the fourth axis

As explained in the previous sections, rotary tables have become more and more important in coordinate metrology. Their applications are various, spanning from the measurement of brake drums or hob cutters to the measurement of gears or turbine components. Therefore, it is of great importance to determine their capabilities within the framework of acceptance and reverification tests, as well as interim checks.

Similar to other disciplines and areas, *standardisation* is a keyword here as well, in order to ensure a clear understanding on related technical subjects, and to build a common basis among manufacturers and users for making healthy comparisons when it comes to assessing performance and errors of CMMs with the axis of a rotary table as the fourth axis.

As the third part of the ISO 10360 series of standards, *ISO 10360-3: 2000 Geometrical Product Specifications (GPS) - Acceptance and reverification tests for coordinate measuring machines (CMM) - Part 3: CMMs with the axis of a rotary table as the fourth axis* explains and specifies the necessary steps and procedures that need to be applied to check whether the performance specifications of a CMM with the axis of a rotary table as the fourth axis are consistent with those stated by manufacturer or user.

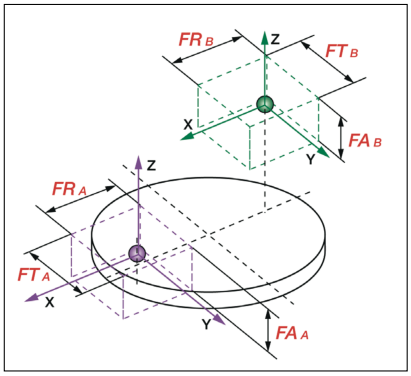


Figure 2.44: Rotary table errors [63]

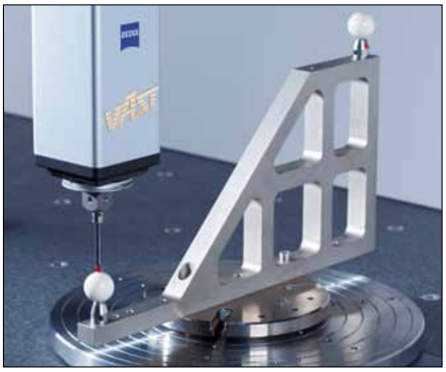

Figure 2.45: A test specimen according to ISO 10360-3 [64]

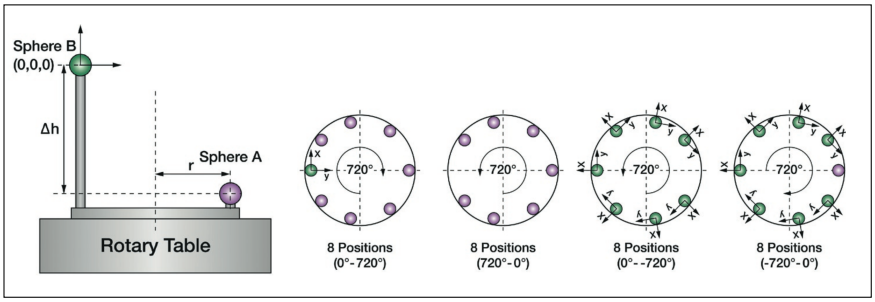


Figure 2.46: Rotary table test [65]

PRINCIPLES The main aim and context of ISO 10360-3:2000 basically consist of determining the measuring capability and errors of CMMs with a rotary table as the fourth axis. It is investigated whether the errors of indication of the rotary table of a CMM remain under predefined error values, i.e. MPEs. [66]

To do that, two spheres, denoted by $A$ and $B$, are mounted on the rotary table to be investigated. Sphere $A$ should be placed as close to the rotary table base as possible, and its centre must be at a radial distance of $r$ from the axis of rotation of the rotary table. Sphere $B$, on the other hand, must be mounted approximately at the same distance, however, its centre must be higher than the centre of sphere $A$ by the amount of $\Delta h$. The default combinations for the values of the $r$ and $\Delta h$ are defined in the standard, and Table 2.10 illustrates them. [66]

As the table rotates, the WCS rotates with it together, thus the measured coordinates of the centre of both spheres are supposed to remain at the same values. In practice, however, there exist more or less some deviations from those theoretical values. In order to determine the errors of the rotary table, a series of measurements are conducted, thus the centres of both spheres are measured at certain angular positions with a predefined measurement pattern. [66]

According to the procedure described in the standard, the related deviations in $x-$, $y-$ and $z-$axis are recorded, followed by the calculation of the largest ranges for each axis and both spheres. Those largest ranges for each axis and of either sphere are then determined as radial, tangential and axial errors, respectively (Table 2.11). [66]

MEASURING EQUIPMENT Two calibrated test spheres, denoted by $A$ and $B$, are used within the framework of acceptance and reverification tests for CMMs with the axis of a rotary table as the fourth axis. There are some limitations and issues related to these test spheres that need to be addressed. First, the diameters of both spheres should be between $10\,mm$ and $30\,mm$, and since only their centres are used to evaluate four-axis errors, their own calibration is not required. It must, however, be ensured that test spheres are mounted rigidly to the rotary table since otherwise errors owing to bending may occur. [66]

SET UP AND PROCEDURE As the first step, both test spheres $A$and $B$ should be mounted on the rotary table according to the $r$ and $\Delta h$ values in Table 2.10[13]. Sphere $A$ should be at a radial distance of $r$ from the axis of rotation of the rotary table, and placed as close to the surface of the rotary table as possible, whereas the centre of sphere $B$ must be higher than the centre of sphere $A$ by the amount of $\Delta h$. Radial distance of sphere $B$ should be approximately the same as that of sphere $A$, i.e. $r$, and both spheres should be approximately diametrical to each other. [66]

**Table 2.10:** Location of the test spheres on the rotary table [66]

| **Combination number** | **Height difference** $\Delta h$ [mm] | **Radius** $r$ [mm] |
|---|---|---|
| 1 | 200 | 200 |
| 2 | 400 | 200 |
| 3 | 400 | 400 |
| 4 | 800 | 400 |
| 5 | 800 | 800 |

Before begining with the measurements, a Cartesian WCS should be defined on the rotary table that fulfils some certain requirements which are listed below [66]:

1. The origin of the WCS is defined as the centre of the test sphere $B$;
2. The axial direction is defined by so-called primary axis, and the primary axis shall be so selected that it is parallel to the axis of the rotary table; and
3. The radial direction is defined by so-called secondary axis, and the secondary axis is defined by means of the centre of test sphere $A$ and the primary axis.

The test begins by measuring the test sphere $B$ in its initial position (Position 0). Then, the rotary table is rotated through seven selected angular positions[14], and the test sphere $A$ is measured in each position. [66]

13 Although the values listed in Table 2.10 are default values defined by the standard for the height difference and radius combination, other values may also be utilised in case of an agreement between the machine manufacturer and the user.

14 It is recommended in ISO 10360-3: 2000 that those seven angular measurement positions should be distributed to at least to 720°, starting from the initial position.

This is followed by the rotation of the rotary table to seven angular positions once again, yet in the opposite direction this time, and the position of the test sphere A is measured at each of those seven angular position. [66]

At the seventh position of this second cycle, the rotary table is again at its initial position, and both of sphere A and sphere B are measured (Position 14). [66]

Continuing in the same direction of movement, the rotary table is rotated to seven angular positions one more time, but this time the test sphere B is measured at each angular position. Afterwards, it is repeated in reverse direction. Finally, after the rotary table returned to its original position, both test spheres are measured (Position 28) (Figure 2.46 and Table 2.11). [66]

**Table 2.11:** An example for the evaluation of a rotary table test according to ISO 10360-3 [65]

| Position No. | Angle | Measured Coordinates for | | | | | |
|---|---|---|---|---|---|---|---|
| | | Test sphere A | | | Test sphere B | | |
| | | $X_A$ | $Y_A$ | $Z_A$ | $X_B$ | $Y_B$ | $Z_B$ |
| 0 | 0 | 401.6647 | 0.0000 | -398.276 | 0,0000 | 0,0000 | 0,0000 |
| 1 | 103 | 401.6632 | 0.0011 | -398.2285 | - | - | - |
| 2 | 206 | 401.6631 | -0.0016 | -398.2270 | - | - | - |
| 3 | 309 | 401.6625 | -0.0014 | -398.22 92 | - | - | - |
| 4 | 412 | 401.6652 | 0.0012 | -398.2285 | - | - | - |
| 5 | 515 | 401.6648 | 0.0009 | -398.2290 | - | - | - |
| 6 | 618 | 401.6660 | -0.0011 | -398.2270 | - | - | - |
| 7 | 721 | 401.6646 | -0.0018 | -398.2263 | - | - | - |
| 8 | 618 | 401.6658 | -0.0015 | -398.2273 | - | - | - |
| 9 | 515 | 401.6635 | 0.0006 | -398.2265 | - | - | - |
| 10 | 412 | 401.6623 | 0.0003 | -398.2260 | - | - | - |
| 11 | 309 | 401.6649 | -0.0011 | -398.2264 | - | - | - |
| 12 | 206 | 401.6640 | 0.0009 | -398.2278 | - | - | - |
| 13 | 103 | 401.6638 | 0.0004 | -398.2285 | - | - | - |
| 14 | 0 | 401.6655 | -0.0013 | -398.2277 | 0.0012 | -0.0011 | 0.0015 |
| 15 | -103 | - | - | - | -0.0005 | 0.0005 | 0.0007 |
| 16 | -206 | - | - | - | -0.0011 | 0.0009 | -0.0003 |
| 17 | -309 | - | - | - | 0.0014 | 0.0014 | -0.0010 |
| 18 | -412 | - | - | - | 0.0020 | 0.0000 | 0.0002 |
| 19 | -515 | - | - | - | 0.0001 | -0.0019 | 0.0012 |
| 20 | -618 | - | - | - | -0.0010 | -0.0010 | 0.0012 |
| 21 | -721 | - | - | - | 0.0017 | 0.0016 | 0.0009 |
| 22 | -618 | - | - | - | -0.0003 | 0.0003 | 0.0013 |
| 23 | -515 | - | - | - | -0.0009 | -0.0003 | -0.0008 |
| 24 | -412 | - | - | - | -0.0017 | -0.0018 | -0.0003 |
| 25 | -309 | - | - | - | 0.0011 | 0.0004 | 0.0006 |
| 26 | -206 | - | - | - | 0.0018 | 0.0015 | 0.0004 |
| 27 | -103 | - | - | - | 0.0005 | 0.0004 | 0.0014 |
| 28 | 0 | 401.6628 | 0.0020 | -398.2290 | -0.0018 | -0.0009 | -0.0007 |
| **Rotary Table Error** | | **$FR_A$** | **$FT_A$** | **$FA_A$** | **$FR_B$** | **$FT_B$** | **$FA_B$** |
| | | 3.7µm | 3.8µm | 3.2µm | 3.8 | 3.5 | 2.5 |
| **Test result:** | | | | | | | |
| **Rotary table error in radial direction** | | | | **FR =** | **3.8µm** | | |
| **Rotary table error in tangential direction** | | | | **FT =** | **3.8µm** | | |
| **Rotary table error in axial direction** | | | | **FA =** | **3.2µm** | | |

RESULTS AND DECISION According to the measurement results obtained from each angular position (from 0 to 28), the related deviations in $x-$, $y-$ and $z-$axis are recorded, followed by the calculation of the largest ranges for each axis and both spheres. Those largest ranges for each axis and of either sphere are then determined as three four-axis errors, i.e. radial, tangential and axial errors (FR, FT and FA), respect-

ively (Table 2.11). [66]

The explanation of used notations are as follows [66]:

- $X_A$ and $X_B$ represent the radial components of spheres $A$ and $B$ and are used to calculate the radial four-axis error $FR_A$ and $FR_B$,
- $Y_A$ and $Y_B$ represent the tangential components of spheres $A$ and $B$ and are used to calculate the tangential four-axis error $FT_A$ and $FT_B$; and
- $Z_A$ and $Z_B$ represent the axial components of spheres $A$ and $B$ and are used to calculate the axial four-axis error $FA_A$ and $FA_B$.

*Acceptance test* The decision on whether the performance of the CMM and rotary table is verified depends upon the comparison of values of the four-axis errors ($FR_A, FT_A, FA_A, FR_B, FT_B$ and $FA_B$) with the three MPEs ($MPE_{FR}, MPE_{FT}$ and $MPE_{FA}$) which are specified by the *manufacturer*. In case none of the four-axis are greater than the three MPEs, the capability of CMM with the rotary table as fourth axis is verified. [66]

*Reverification test* Within the framework of a reverification test, the performance of the CMM with the rotary table as fourth axis is verified, if all of the four-axis errors ($FR_A, FT_A, FA_A, FR_B, FT_B$ and $FA_B$) are lower than the three MPEs ($MPE_{FR}, MPE_{FT}$ and $MPE_{FA}$) which are specified by the *user*. [66]

*Interim check* A shortened version of the reverification test might be conducted periodically to determine the probability that the CMM wirh rotary table will fulfil to predefined requirements in terms of the three MPEs. Angular positions to be measured, measurements to be conducted, and spheres to be used are the subjects that can be reduced in numbers when it comes to conducting an interim check. [66]

## 2.5 Some useful metrological terminology

Before starting to deal with the positioning accuracy of rotary axes or tables, a clear definition of and distinction between widely misunderstood characteristics, e.g. accuracy, precision, repeatability and resolution, should be made. According to the VIM [12], those terms are defined and therefore distinguished from each other as follows;

MEASUREMENT ACCURACY *"Closeness of agreement between a measured quantity value and a true quantity value of a measurand"* [12].

MEASUREMENT TRUENESS *"Closeness of agreement between the average of an infinite number of replicate measured quantity values and a reference quantity value"* [12].

MEASUREMENT PRECISION *"Closeness of agreement between indications or measured quantity values obtained by replicate measurements on the same or similar objects under specified conditions"* [12].

MEASUREMENT REPEATABILITY *"Measurement precision under a set of repeatability conditions of measurement"* [12].

MEASUREMENT REPRODUCIBILITY *"Measurement precision under reproducibility conditions of measurement"* [12].

MEASUREMENT ERROR *"Measured quantity value minus a reference quantity value"* [12].

MEASUREMENT UNCERTAINTY *"Non-negative parameter characterizing the dispersion of the quantity values being attributed to a measurand, based on the information used"*[15] [12].

RESOLUTION *"Smallest change in a quantity being measured that causes a perceptible change in the corresponding indication"* [12].

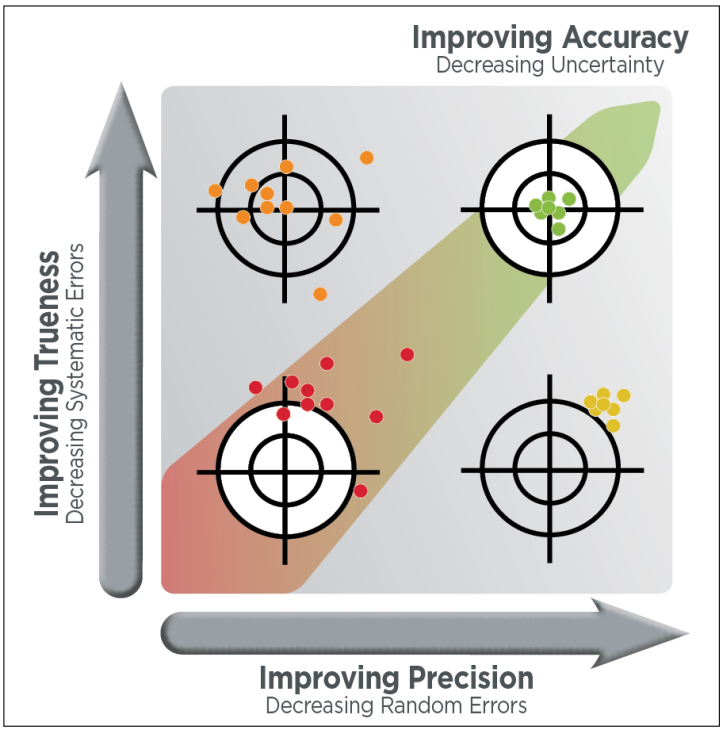


**Figure 2.47:** Relationship between accuracy, trueness and precision [67]

## 2.6 The concept of measurement uncertainty

As a matter of course, regardless of what kind of measurement is performed, the obtained measurement results can never be exact and free of errors. Measurement errors are indispensable, even for the measurements conducted by means of the *best* measurement instruments under the *best* conditions.

Theoretically, the measurement error can be defined as the difference between the measured quantity value and true quantity value. However, as the *true* value of the measured can never be known, this definition becomes vague and problematic. A solution to this problematic situation is represented in VIM by using two sub-definitions for the measurement error in addition to the main one (Equation 2.19) [12].

15 A comprehensive overview of the concept of measurement uncertatinties is given in Section 2.2.1.

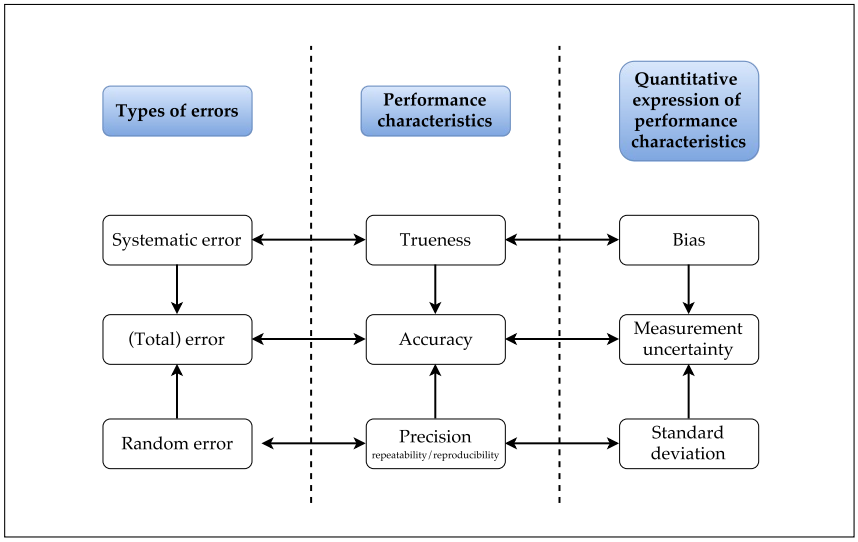


**Figure 2.48:** Relationships between type of error, qualitative performance characteristics and their quantitative expression (adapted from [68])

$$\textit{Measurement error} = \textit{Measured quantity value} - \textit{Reference quantity value} \tag{2.19}$$

This concept can be used for both of the following cases:

- *"when there is a single reference quantity value to refer to, which occurs if a calibration is made by means of a measurement standard with a measured quantity value having a negligible measurement uncertainty or if a conventional quantity value is given, in which case the measurement error is known, and*
- *if a measurand is supposed to be represented by a unique true quantity value or a set of true quantity values of negligible range, in which case the measurement error is not known"* [12].

The interpretation of these definitions is that the measurement error is in most cases unknown, and can only be known in case of conducting calibration measurements by reference standards. However, it does not mean automatically that the quality of a measurement result can not be expressed quantitatively. Notwithstanding that the measurement error is unknown, the term and concept of *measurement uncertainty* is used to make quantitative judgements and comparisons of measurement results. The definition of measurement uncertainty according to the VIM is given in Section 2.5.

In summary, measurement uncertainty;

- indicates how well the measurement result reflects the true values of the measurand,
- enables the assessment of the reliability of a measurement result,
- enables the risk assessment of whether a measurement result exceeds a predefined limit value, and
- is a measure of the quality of the measurement. [69]

### 2.6.1 Relation between the measurement uncertainty and the decision rules according to ISO 14253-1

Within the design phase of a workpiece, its specifications are given by means of two limits, i.e. by lower specification limit (LSL) and upper specification limit (USL). If the measurement uncertainty is not taken into account, the decision on whether there is a conformance or non-conformance with the specification becomes uncomplicated. Depending on whether the measurement result lies within or outside the specification limits, the decision for conformance or non-conformance with specification is made, respectively.

However, making decisions neglecting the measurement uncertainty is not an acceptable approach any more, as any kind of measurement always contains some measurement uncertainties which need to be taken into consideration. Consequently, there exists another zone between the conformance and the non-conformance zone (Figure 2.49).

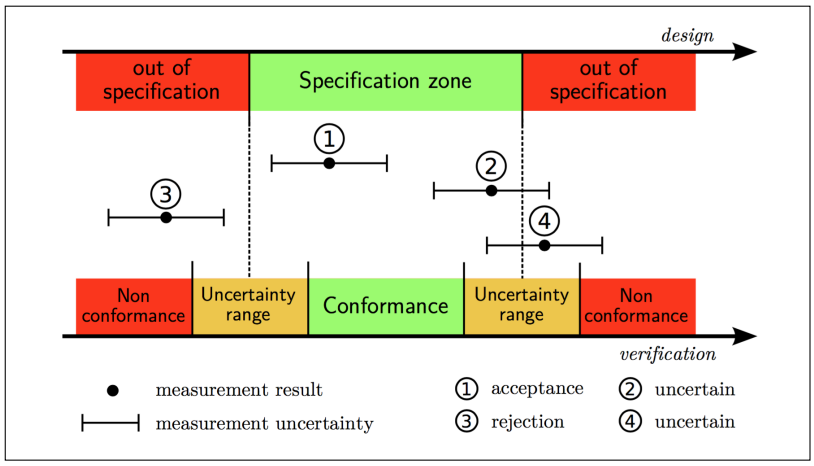


**Figure 2.49:** Schematic representation of the proving conformance or non-conformance with specification according to ISO 14253-1 [70]

This additional zone is referred to as uncertainty zone, and mathematically covers the region between $y - U$ and $y + U$. The expanded uncertainty must also be stated within the complete measurement result;

$$Y = y \pm U \tag{2.20}$$

where $Y$ indicates the measurement result as a complete statement, $y$ represents the best estimation for the measurand $Y$, and is the expanded uncertainty.

The conformance is proved, if and only if in case of the $Y$ lies completely within the specification zone. In case of exactly the opposite situation, i.e. if the $Y$ lies completely outside the specification zone, the non-conformance is proved.

In all other cases, it is not possible to make an unambiguous decision either for the conformance or for the non-conformance. The measurement values in the uncertainty zone must be either assessed more particularly or determined more specifically.

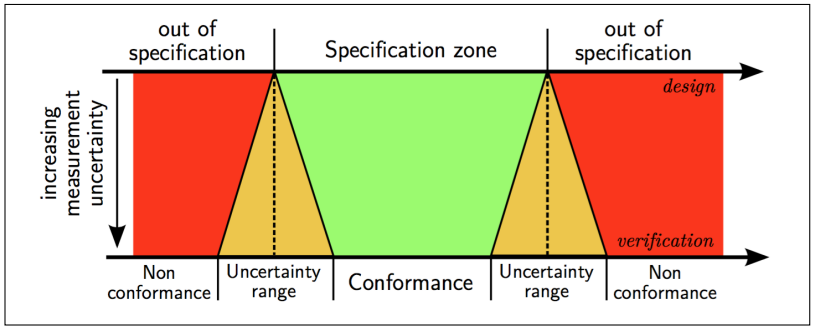


**Figure 2.50:** Relationship between the increasing measurement uncertainty and the (non-)conformance zone according to ISO 14253-1 [70]

## 2.6.2 Evaluation of the measurement uncertainty

Evaluation process of the measurement uncertainty consists of three main stages; formulation stage, propagation stage, and summarising stage. A comprehensive overview of the related steps within stage are demonstrated in Figure 2.51.

There exist mainly three different approaches in order to evaluate measurement uncertainty values;

- Guide to the Expression of Uncertainty in Measurement (GUM) method
- Analytic methods
- Monte-Carlo method

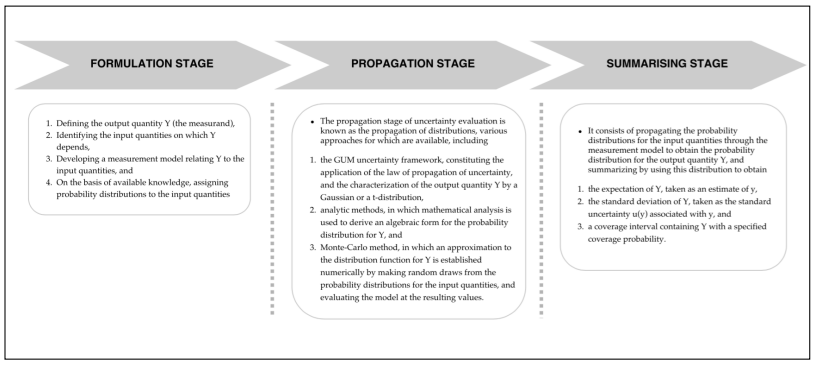


**Figure 2.51:** Typical stages of the evaluation of the measurement uncertainty [71]

Another approach, which is originally an alternative to, however is mainly in line with the GUM method is described in ISO 14352-2 under the name of Procedure for Uncertainty Management (PUMA). The main idea behind this standard is the implementation of an iterative approach in order to evaluate measurement uncertainty just as accurate as necessary in compliance with termination criteria. Thus, the cost of this evaluation can be optimised, and kept within reasonable limits.

### *2.6.2.1 Overview of the GUM*

GUM is a guideline regarding the estimation of measurement uncertainties which was published by ISO/International Bureau of Weights

and Measures (Fr.: Bureau International des Poids et Mesures) (BIPM) in 1993, and revised in 2008. An ongoing revision began in 2014. The aim of the guide is to build an internationally standardised procedure for determining and specifying measurement uncertainties in order to ensure a solid basis for a healthy comparison of measurement results worldwide.

There exist two types of methods for the evaluation of all factors influencing measurement, which can also be combined with each other:

- Type A; Evaluation of measurement uncertainty through statistical analysis of measurements, and
- Type B; Evaluation of measurement uncertainty by means other than statistical analysis.

It is specified for each influencing variable, by which method they are measured, and how strongly they affect the overall measurement uncertainty. This approach is intended to help to determine a realistic and traceable measurement uncertainty. The GUM has gained importance especially in the calibration, it can and should be applied to all situations of measurement, though.

#### 2.6.2.2 Evaluation of measurement uncertainty according to the GUM method

In most cases a measurand $Y$ is not measured directly, but it is calculated from $N$ different input quantities $X_1, X_2, \ldots, X_N$ by a function $f$. Thus a general model for measurements is formulated as follows;

$$Y = f(X_1, X_2, \ldots, X_N) \tag{2.21}$$

Based on that, the steps to be followed for the evaluation and expression of measurement uncertainty, as presented in GUM [72], can be summarised as follows [73]:

1. A complete description of the model and relationships must be made.
2. All relevant corrections (e.g. for temperature, barometric pressure, and voltage) must be identified and done.
3. All sources and causes of measurement uncertainty must be listed in an uncertainty analysis.
4. The estimate, $y$, of the measuring value, $Y$, and its combined uncertainty, $u_c(y)$, which is obtained by the quadratic propagation of uncertainty and their units must be indicated.
5. The specified degree of confidence, $k$, which is associated to the zone $y \pm k \cdot u_c(y)$, and the method of its determination must be described.

## 2.7 Accuracy characteristics of rotary axes/tables

The accuracy of rotary tables in the context of modern production metrology is explained and dealt with mainly in three different parts

of two international standards, i.e. in ISO 10360-3:2000, in ISO 230-2:2014[16] and in ISO 230-7:2015[17]. While the first one explains mainly their use in and integration with coordinate metrology[18], the second and third one focus on precision and accuracy of rotary axes/tables itself and their positioning characteristics in context of machine tools and NC axes.

In a general point of view, the first step of the analysis of accuracy characteristics for rotary tables should be the investigation of its own mechanics. The six degrees of freedom that a rotary table has are demonsrated in Figure 2.52. Its radial and axial error motions are represented by $E_{XC}$, $E_{YC}$ and $E_{ZC}$. Furthermore, the tilt error motion is denoted by $E_{AC}$ and $E_{BC}$. Finally, the $E_{CC}$ denotes the angular positioning error of the rotary table. Since the total positioning error of the rotary table is influenced by all of them, they must be investigated with carefully.

When determining the influencing factors of accuracy on a rotary table, the first thing would be to look at the mechanics of the table itself. [63]

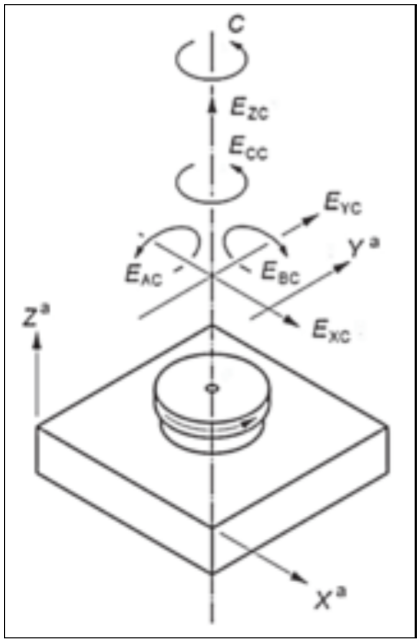


**Figure 2.52:** Error motions of axis of rotation [74]

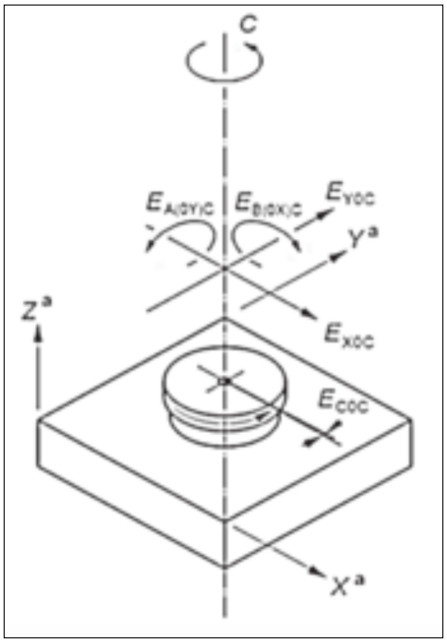


**Figure 2.53:** Position and orientation errors (axis shift) of axis average line [74]

In most cases, a worm gear is used to drive rotary table. It is usually connected to a motor which has a rotary encoder on its back side. According to the rotary table movement, the encoder transmits pulses, and by means of a control-loop position information of the rotary table can be obtained.

A semi-closed position loop causes some errors that the angular positioning error, $E_{CC}$, is mainly consisted of, e.g. wear, elasticity, thermal deformations and geometrical errors. When an angle encoder is util-

16 ISO 230-2:2014 - Test code for machine tools — Part 2: Determination of accuracy and repeatability of positioning of numerically controlled axes
17 ISO 230-7:2015 - Test code for machine tools – Part 7: Geometric accuracy of axes of rotation
18 See Section 2.4.4 for a detailed overview.

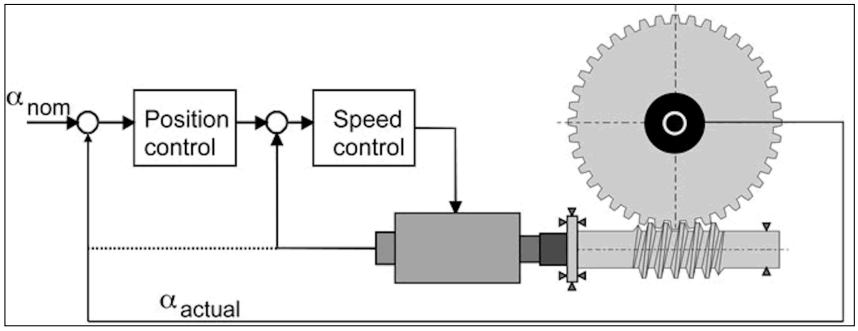


**Figure 2.54:** Position loop as a closed loop system [63]

ised, it should be attached to the axis of rotation to minimise the angular positioning error. Figure 2.54 demonstrates such a system. A closed position loop is obtained by using an rotary encoder on the back side of the motor, in addition to the angle encoder under the rotary table. [63]

### 2.7.1 Positioning accuracy of rotary tables

## 2.8 Reversal error

In mechanical and electromechanical systems, it is often not possible to obtain exactly the same positional values at a given position, when it is approached first from one direction, then from the opposite one. This difference between the positional values is defined as reversal error. It comprises of both so-called backlash and hysteresis values. However, isolating the influences of these two from each other becomes often quite cumbersome, especially in complex motion systems where various parts and components interact with each other. A graphical demonstration of backlash and hysteresis is given in Figure 2.55.

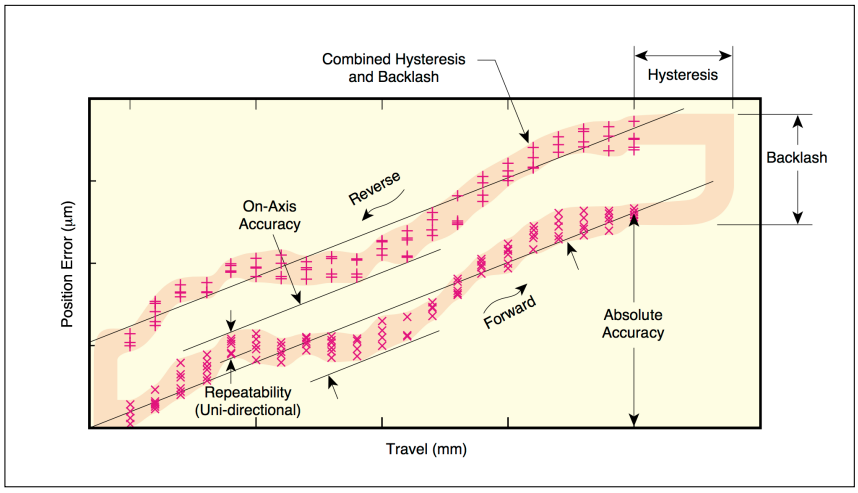


**Figure 2.55:** Graphical demonstration of the difference between backlash and hysteresis [75]

BACKLASH As one of the two components which the reversal error consist of, backlash is defined as "*the result of relative movement between*

*interacting mechanical parts of a drive system that does not produce output motion*" [75].

Deformation and clearance between mechanical parts, e.g. gear teeth are some of the typical reasons behind this error. Since it appears only when approaching a given point from opposite directions, it does not affect unidirectional properties. Backlash has, however, a crucial effect on bi-directional repeatability and accuracy, and therefore, it should be measured and compensated as exactly as possible. Compensation of backlash can be realised by controllers, due to the fact that it is mostly quite repeatable.

Backlash becomes a significant problem in precision alignment and tracking applications, since there exist a discontinuity between output motion and actually commanded motion.

HYSTERESIS Hysteresis, on the other hand, is the other contributing part of the reversal error that is dependent on the recent history of the system. It is caused by the elastic forces in the several parts and components when the forces on a system act in the reverse direction. In addition to affecting the bi-directional repeatability and accuracy, it can also have an influence in precision alignment and tracking applications. The reasons behind that is the non-linearity of output motion to the input motion in case of reversing the direction of movement. Unlike backlash, hysteresis appears in all mechanical systems, even though its value might not be high.

## 2.9 Backlash

In the context of mechanical engineering, backlash is generally defined as a short lost motion of a machine, which appears when the direction of approach is reversed. It affects bi-directional positioning characteristics negatively. As backlash is mostly quite repeatable, it can be compensated by controllers.

Gaps and clearances between the parts of mechanisms cause the backlash. The amount of clearance between mated gear teeth represents a typical example of backlash in the context of gears and gear trains. Here, the gear backlash, which represents the distance between the back flanks of two gear wheels, plays a vital role, since it first must be overcome in order to be able to re-establish flank contact. However, in each gear pair a certain backlash is necessary to compensate for manufacturing tolerances and any thermal expansion, and to allow a constant lubricating film.

Although backlash is usually an undesired situation, and must be reduced or eliminated, it can be sometimes beneficial to have some backlash. This is mainly in order to prevent jamming, to allow for production errors and thermal expansion, and to simplify lubrication.

### 2.9.1 Types of backlash in gearboxes

A distinction is made between the circular backlash, $j_t$, and the normal backlash, $j_n$. Circular backlash is the length of pitch arc in transverse section, which is covered by each of the two gears (holding the mating

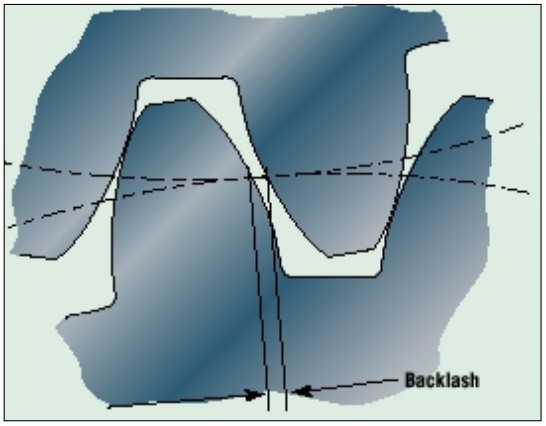


**Figure 2.56:** Backlash in gear trains [76]

gear firmly) to bridge the gap between the back flanks. In contrast, the normal backlash is defined as the shortest distance between the two back flanks during the contact of working flanks. [77]

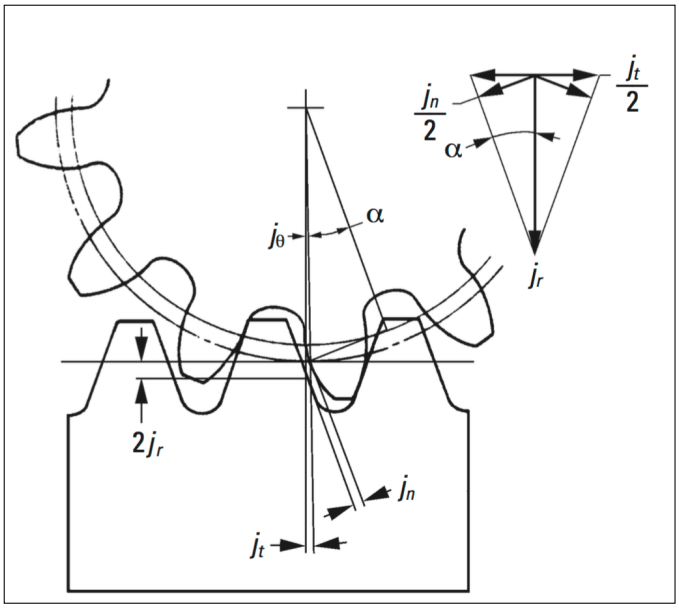


**Figure 2.57:** Normal and circular backlash in gear trains [78]

## 2.9.2 Backlash measurement methods

For the majority of different gearboxes, backlash is measured by locking the input, and measuring the loose motion by means of a dial indicator on a lever arm attached to the output shaft. Until there is no gear clearance, the lever arm is moved up and down, and a linear value is obtained which can be converted into a corresponding angular value.

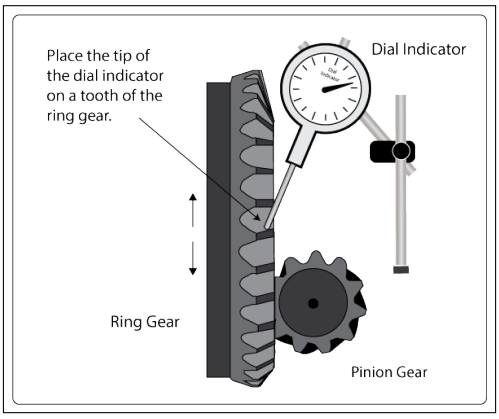


Figure 2.58: Backlash measurement for differential ring-pinion [79]

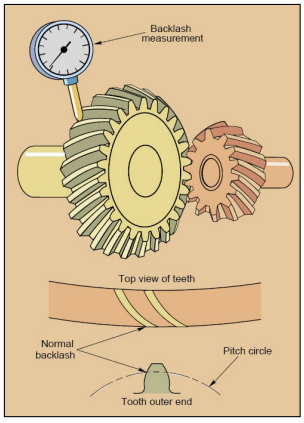


Figure 2.59: Backlash measurement for spiral bevel gears [80]

### 2.9.3 Anti-backlash designs and methods to minimise backlash

Although the backlash creates a flexibility in terms of e.g. lubrication, thermal and mechanical expansions, as well as jamming, it obstructs the accurate operation of motion systems, e.g. robots and tools and robots. For these applications, there are three basic ways to reduce or eliminate backlash: precision gears, modified gears, and special designs that use components other than gears. In certain applications, backlash is an undesirable characteristic and should be minimised. A brief overview of measures that might be taken against backlash is summarised in Table 2.12. [81]

Table 2.12: Overview of backlash control mechanisms [81]

| Backlash control method | Relative cost | Most frequent use | Typical backlash |
|---|---|---|---|
| **Close mounted gears (adjustable center and spring loaded)** | Medium | Most widely used method | About 1/4 degree |
| **Spring loaded split gears** | Low | Light loads such as instrumentation | Close to zero |
| **Backloading or dual gear trains** | High | Heavy duty servo systems Accommodates heavy loads. | Close to zero, but subject to high wear |
| **Plastic filler** | Low | Low speeds and light loads. Light instrumentation. | No data |
| **Tapered gears** | High | Low speeds | No data |
| **Preloaded gear train** | Medium | Limited rotation applications Instruments. | Close to zero |

#### 2.9.3.1 Precision gears

Bearing, tolerances regarding mounting and errors in manufacturing are can be listed as factors which increase the backlash in gearboxes. Those kind of errors can be minimised in precision gearboxes by the integration of close-tolerance parts. Precision gears are not manufactured as mass production, but rather in small lots. It enables producers to utilise special machining methods, and consequently to minimise dimensional deviations. Backlash values are typically limited to 2°, and are utilised in application areas such as instrumentation. Units with better precision that achieve zero or near-zero backlash are utilised in e.g. robotics and precision metrology applications. [81]

#### 2.9.3.2 Modified designs

Backlash can be reduced or eliminated by modifying gear designs in several ways. In some of them gears are adjusted to a set tooth clearance when they are first assemblied. Since the backlash can eventually be higher due to wear with this approach, it must be readjusted. With this approach, backlash eventually increases due to wear, which requires readjustment. In other designs, on the other hand, meshing gears at are held at a regular backlash level with the aid of springs over their service life. They are, however restricted to light load applications. Short centre distance, spring-loaded split gears, plastic fillers, tapered gears, preloaded gear trains, and dual path gear trains can be listed as the most applied methods to reduce backlash. [81]

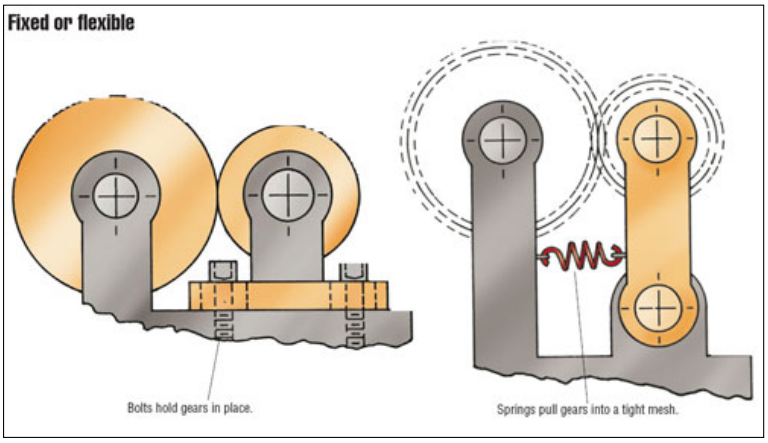


**Figure 2.60:** Adjustable-center gears are locked at a fixed distance for low backlash. A spring-loaded version holds them together for zero backlash. [81]

Shortening the distance between gear centres is the most straightforward and applied way in among abovementioned methods. It can be realised in two options; either the gears are adjusted to a fixed distance and locked in place by means of bolts, or one is spring-loaded against the other for a tighter mesh. Thus, the gears are meshed with each other tighter, with very low or zero gap between their teeth. Effects of changes in centre distance, bearing eccentricities and tooth dimensions are eliminated. [81]

In another design, two gear halves are mounted side-by-side. One half remains fixed to a shaft, while the other is rotated slightly by springs.

Since the effective tooth thickness becomes higher, the tooth gap of the other gear is filled entirely, which eliminates the backlash error. This design is referred to as split gearing and generally utilised in applications characterised with low-speed and light-load. [81]

Another design uses a piece of elastic material running throughout the gear teeth centre (Figure 2.62). Backlash can be taken up by extension of the plastic filler beyond the teeth profile, although it can also increase due to material wear and deformation. The tooth thickness is increased by the rotation of two halves of a split scissor in reverse directions. There are designs as spring loaded or kept together by bolts. [81]

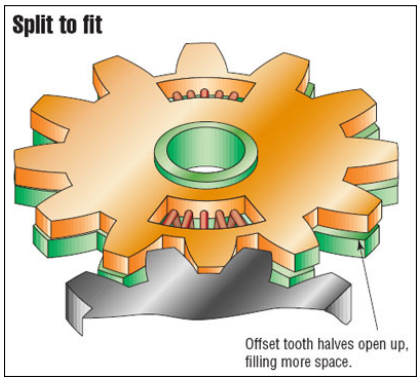


Figure 2.61: Split scissor gear design [81]

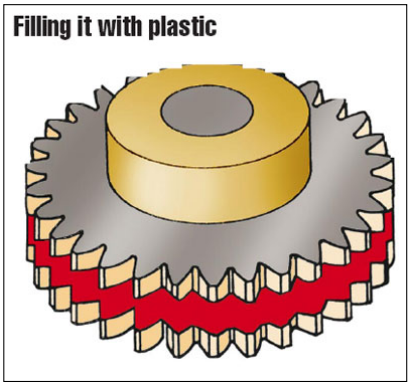


Figure 2.62: Composite gear with a plastic center element [81]

There exists also an approach using the tapered spur and helical gears. Teeth of these gears are cut at a certain slight angle to create the tooth form. Tooth gap is arranged by movement of gears against each other in axial direction. [81]

A method called gear train preloading provides a beneficial way to reduce backlash. In this design one side of the meshing teeth is loaded by a weight or a torsion spring, which is on the last driven gear. Rotation of last driven gear is however limited by the spring or weight. An auxiliary motor can be a solution to this problem. Backlash becomes cumulative in gear trains consisting of many stages. In such systems this method shows particular advantages. Spring-loaded versions are ideal for uni-directional drives and low-torque applications. [81]

Another useful design is provided by dual-path gear trains. Here the identical gears are placed in parallel. In order to force mating teeth together, two gear trains are rotated in opposite directions. A preload on the teeth is created and kept regular by mounting a motor shaft with pinion gear into the gear head. Although there is no spring, there exist an effect similar to spring load. The advantage of this method is enabling zero backlash without having complicated special designs. It has, however, the drawback that the number of gears in system is doubled and assembly time is increased. [81]

#### 2.9.3.3 Special designs

If the demands for low or zero backlash are strict, special types and designs of gearboxes need to be applied, which uses different compon-

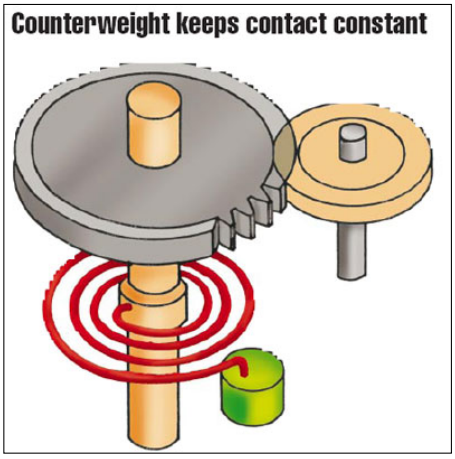


**Figure 2.63:** A weight or spring load on the end of a gear train keeps teeth in contact [81]

ents to transmit motion than conventional gears. In this context, epicyclic, traction, harmonic and cycloidal drives represent the most important examples. These instruments provide high performance and therefore cost relatively more. [81]

In harmonic drives, motion transmission is realised by using elastic deflection of a flexible spline. Backlash can be reduced to 1′ or less by these drives. However in practice, the typical values lie around, 10′ to 15′. They are mainly used in automation and robotics. [81]

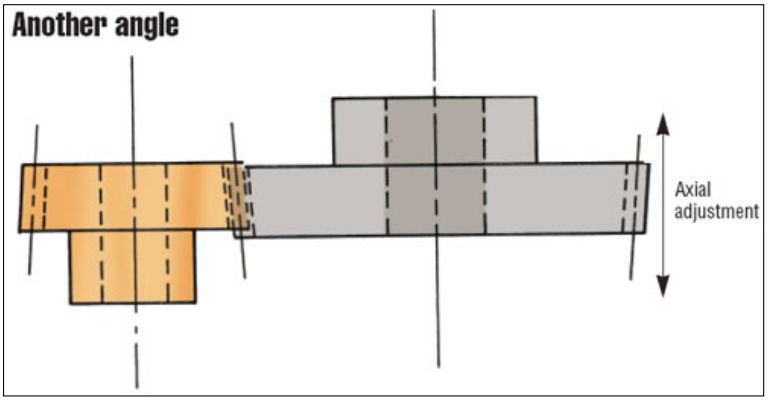


**Figure 2.64:** Moving tapered gears together in an axial direction cuts tooth clearance. [81]

As an interesting design, cycloidal drives have no gears, they utilise preloaded balls, pins or rollers for the torque transmission. Zero-backlash is reached and they work relatively silent. In order to ensure that they remain their zero-backlash value, it is required to retighten their preloads. They are robust against high vibration and shock loads. [81]

In epicyclic drives an epicyclic motion is produced by an off-center disk on an input shaft, which also rotates planetary gears in a non-moving internal gear. There are some versions which have no teeth. Low inertia, high stiffness, and backlash values of 0.5′ to 5′ can be achieved by cycloidal drives. [81]

Input and output rollers which are compressively loaded, are used in traction drives for the torque transmission. Large machinery industry represent their main application area. [81]

### 2.9.3.4 Harmonic-drive gearing

In harmonic drives, there exist an elliptically shaped wave generator, which is inserted into a deformable steel bush with external gearing, the flexspline, and transfer its form to this. When the wave generator turns, the flexspline is continuously transformed, and the rotary motion is transferred by the gear teeth to the circular spline, to the outermost ring with the internal teeth. Due to the elliptical shape of the wave generator, there exist two relatively large and opposite tooth engagement areas between the flexspline and the circular spline, which ensure minimal backlash.

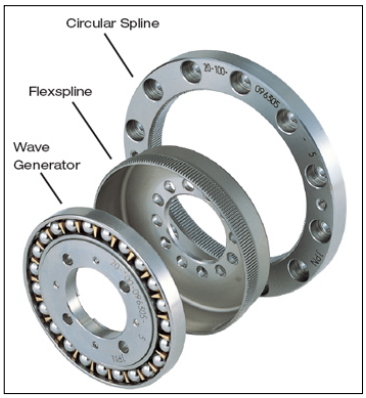


**Figure 2.65:** Components of harmonic drive gearing [82]

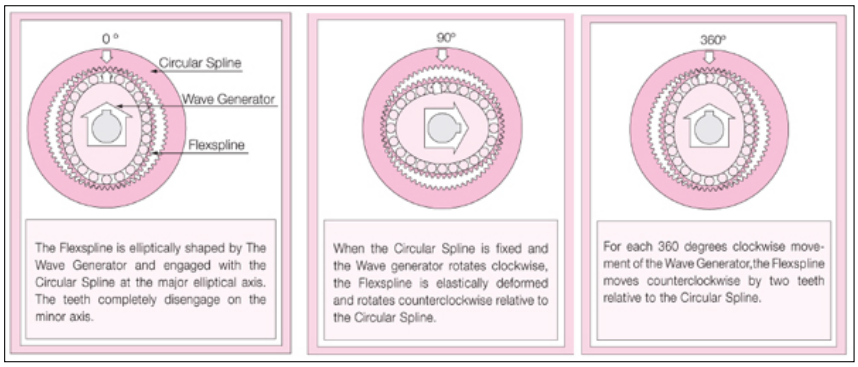


**Figure 2.66:** Operation principle of harmonic drive gearing [82]

### 2.9.3.5 Cycloidal drives

In cycloidal drives the rotary motion is transferred only through spur gears on eccentric shafts (crankshafts), which are connected with two cams. These cams, which are arranged offset by 180° to each other for symmetrical load distribution, roll off at the outwardly arranged bolt ring, which has exactly one division more than the cams. With a full rotation of the cam, the cams move eccentrically exactly one pitch further.

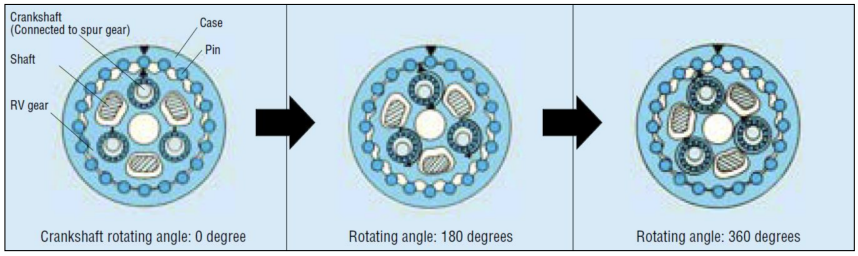


**Figure 2.67:** Cycloidal drive [83]

## 2.10 Encoders

An encoder can be defined as an electromechanical device which detects and converts information about the position and/or mechanical motion into analog/digital electrical pulses or electronic signals that can be interpreted by a computer.

Encoders may be classified according to the type of movement, sensing technology and output signal. In terms of the type of movement, en-

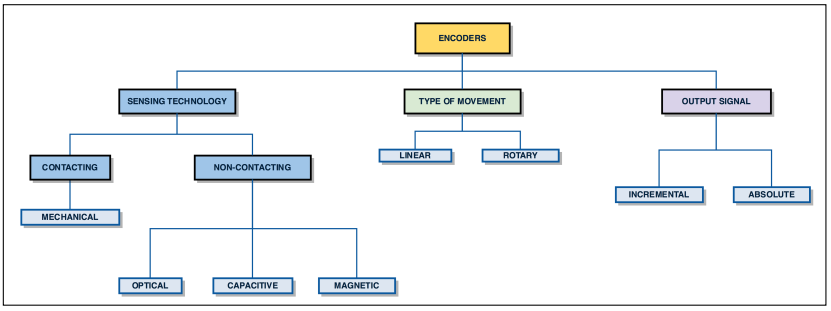


**Figure 2.68:** Classification of encoders

coders can be broken down into two types: linear and rotary. A linear encoder responds to motion along a path, whilst a rotary encoder responds to rotational motion. On the basis of output signal a distinction is made between incremental and absolute encoders. An incremental encoder generates a train of pulses which can be used to determine position and speed. An absolute encoder generates unique bit configurations to track positions directly. Depending on sensing technology, which is also a crucial issue for encoders, they may be classified into contacting and non-contacting type encoders. While brushes or finger sensors, which ensure the electrical transmission of signal for indication of position changes, are necessary at contacting type encoders, the principle of non-contacting type encoders bears on optical, capacitive or magnetic sensing technologies to detect both positional and motional information [84].

### 2.10.1 Contact encoders

Encoders which apply mechanical contact between a pin sensor or brush and the coded disc are classified as contact encoders. As illustrated in Figure 2.69, this coded disc includes several concentric rings or tracks. A binary code composed of $2^0, 2^1, 2^2, 2^3$ is demonstrated by

the four tracks on the disc. The numbers 0 through 15 are encoded by related contact sensors, which are identified at $B_0, B_1, B_2, B_3$. In the course of the rotation of disc, the sensors by turns contact conductive strips and adjacent insulators. Thus, a range of square wave patterns is generated. [84]

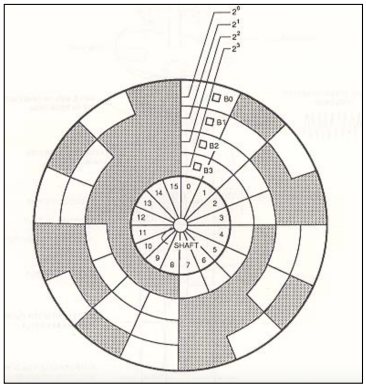


**Figure 2.69:** Absolute Contact Encoder Disk [84]

According to the application, utilisation of both non-uniform and uniform disc patterns can be realised. As long as it can be generated photographically, almost any kind of pattern could be pictured on an encoder disc. Measuring a shaft position represents a common application example, in which a uniform pattern is used. Any kind of non-uniformity is an indication of an error source. If the segments are spaced non-uniformly, that generates position error. Beside that, an error occurs due to the eccentricity and it depends on the shaft angle (as its sinusoidal function). The most crucial issues and problems which restrict both the performance and wide utilisation of contact encoders can be summarised as the segmenting boundaries on discs, abrasion of contacts, and bridging of disc segments. [84]

## 2.10.2 Non-contact encoders

Beside the contact encoders, i.e. encoders which utilise electrical conduction in order to read the coded disc, there are also encoders which use contactless physical sensing technologies to detect position or motion information. Those encoders are classified as non-zcontact encoders, and are broken down into three major categories; i.e. optical, capacitive and magnetic encoders. [84]

### *2.10.2.1 Optical Encoders*

As a first member of non-contact type encoders, the optical encoders were designed and developed due to the typical abrasion issues of contact type encoders. Nowadays, they stand out with the best resolution and encoding accuracy values (among other sensing technologies) that they can provide, although also the magnetic encoder has been recently offering very high accuracy values due to the recent developments in this sensing technology.

They are typically comprised of the following basic components: [85]

- A glass disk with a pattern of lines deposited on it

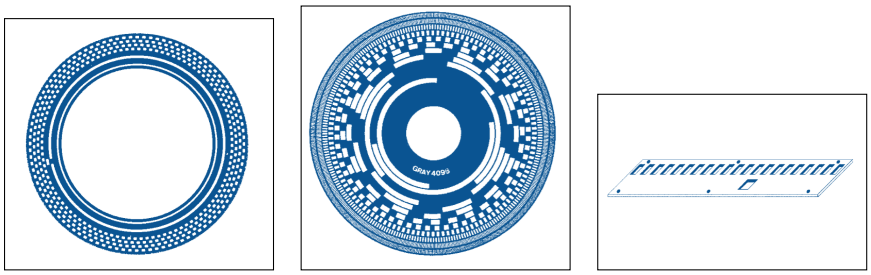

(a) Incremental disk (b) Absolute disk (c) Linear scale

**Figure 2.70:** Encoder disks [85]

- A metal or plastic disk with slots (in case of a rotary encoder), or a glass or metal strip (in case of a linear encoder)
- A light source (typically an LED)
- A light sensor (photodiodes or phototransistors)
- A mask for higher resolutions, and
- A signal conditioning circuitry

Its main principle bears on the fact that a line source of light comes from a light source, e.g. from an LED, shines and passes through the coded pattern of transparent and opaque segments of a disc (coded disc) or a strip onto one or more photodetectors (photodiodes or phototransistors), which generates the encoder's output. The disc of an incremental encoder has one or several of these tracks, while the disc of an absolute encoder has exactly the same number of tracks as encoder's output bits. [85]

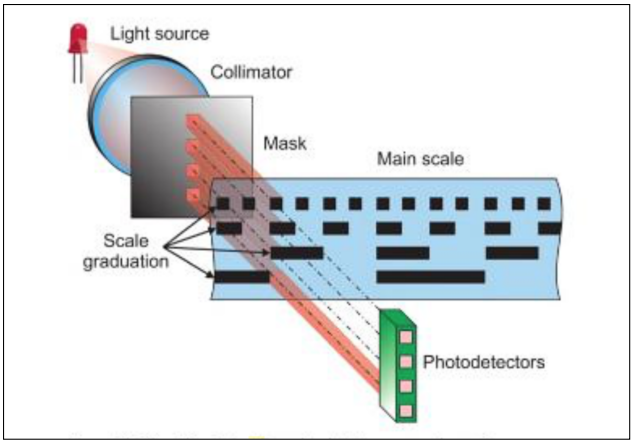


**Figure 2.71:** Principle of an absolute-type encoder using a binary multi-track code [86]

### 2.10.2.2 Capacitive Encoders

As a relatively new member to the industry, capacitive encoders were designed and advanced to satisfy specific requirements, and they are the most rarely used one among the non-contacting encoder types. In terms of ruggedness, they are similar to magnetic encoders, and

provide high robustness, however their accuracy and resolution values are lower than the optical ones. [87]

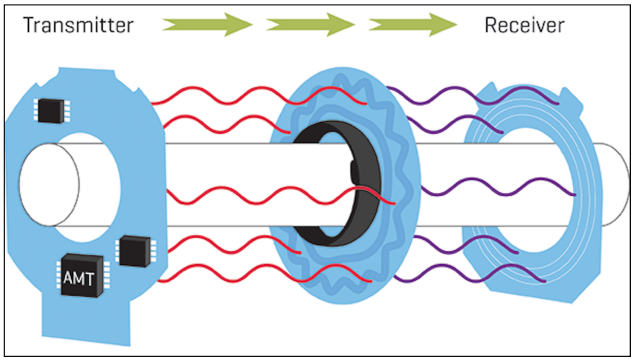


**Figure 2.72:** Capacitive rotary encoder [88]

In order to produce the digital output, either a frequency control technique or a phase shift measuring system is utilised, and they affect the readout electrostatically. It is not usual to find capacitive components as standard hardware component, however, single turn units are produced, and can be found (up to 19-bit). Despite the fact that they can actually replace the utilisation of magnetic, optical or contact type encoders in almost all kind of encoding applications, problems and issues related to their design, production and operation stand as an obstacle in front of their wide application. [84]

#### *2.10.2.3 Magnetic encoders*

Typically, a plain magnetised rotor disc, which has a flux pattern is used by magnetic encoders. After reading out the change in magnetic field or flux, a signal can be transmitted. The other main component used is the sensor. In most cases, this corresponds to either so-called *Hall-Effect* sensors or the magneto-resistive sensors. By reading the change of flux, a magnetic encoder is able to generate signal output to the user. A linear magnetic encoder operates by using a magnetic sensor readhead and a magnetised scale. The sensor detects the change in magnetic field and generates a corresponding output signal. [89]

A magnetic encoder uses two main components to provide position feedback. The first component is the rotor which is magnetised with north and south poles that are lined around the perimeter of the disk. The second component is the sensor. Two widely used sensors are the so-called *Hall-Effect* sensors or the magneto-resistive sensors. When the electrons are deflected magnetically this creates a change in voltage which can be recognised by a Hall-Effect sensor. On the other hand, there exist resistors which are sensitive to the magnetic field. Magneto-resistive sensors utilise these kind of resistors and produce a sine-wave output, whose conversion into square-wave output is realised afterawards.

Since the rotor is mounted to a shaft they rotate together. There exists an air gap between the rotor and the sensory circuit. With the turn and hover of the rotor, and the change in the magnetic field sine-wave signal is generated. This can be then converted into a square-wave signal. A controller or driver is fed easily by this data. [89]

There are various factors which influence together the resolution value in magnetic encoders, e.g. number of sensors and number of magnetised pole pairs. In this regard, it should be taken into consideration that compared to magneto-resistive sensors, Hall-Effect sensors are more cost-efficient. However, magneto-resistive sensors generally provides a higher precision. and less signal noise. [89]

### 2.10.3 Rotary vs. Linear

As far as type of movement concerned, there encoder categories; linear and rotary. Two basic geometries exist for encoders; linear and rotary. As it is obvious from their names, linear encoders are used to measure and detect motions along a linear path, while a rotary one is able to recognise and measure rotational motion. Therefore, summarising, the type of encoder is selected according to corresponding measurement task.

LINEAR ENCODERS They typically consist of a scale, which is nothing but a coded strip, and a sensing head. The position is identified by sensor head. In order to do that, it reads out spacing between coding of the scale. Resolution values of linear encoders expressed in pulses per distance (e.g. pulse per inch (ppi), pulse per millimetre (ppm). The resolution of scale is set in advance with its embedded marks, which is detected by sensing head.

ROTARY ENCODERS Consisting of of an internal coded disc as well as a sensing head, rotary encoders allow to capture angular position information. A rotary encoder is commonly comprised of an internal coded disc and a sensing head used to determine rotary position. Linear encoder can be defined analogue to a tape measure, while a rotary encoder is akin to measuring wheel.

### 2.10.4 Incremental vs. Absolute Coding

In terms of output signal, encoders can be broken down into two broad categories; i.e. incremental and absolut encoders. Although they have some common characteristics, there are also some subjects on which they show different features, e.g. the wiring and movement identification. [87]

INCREMENTAL ENCODERS With incremental encoders it is merely possible to gather data regarding the relative motion of an object. Hence, there is no data available about their first location (when powered on), rather it only shows how far the object was moved. These changes then reported back as electrical pulses. Type of these pulse streams can be both single or dual channel. [87]

ABSOLUTE ENCODERS Absolute encoders, on the other hand, can additionally provide users with the information where exactly the object being moved was. They established themselves especially in robotics and automation for which a homing process is not simple or fast. Thus, because of the characteristics of absolute encoders, they can be associated with a compass. Furthermore, the obvious difference between these two type can be understood better if an analogy is built with clocks and stop watches. Since a stop watch only shows

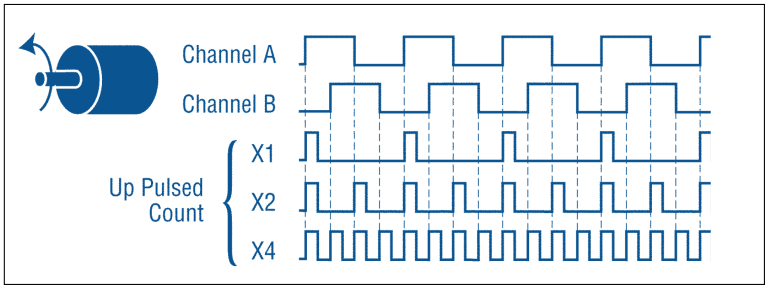


Figure 2.73: Generation of two pulse streams (90° out of phase with one another) by a quadrature encoder [90]

the time passed since the start of the movement, a clock shows both the passed duration and the actual time. So a stop watch would be an incremental encoder, and the clock would correspond to an absolute encoder. [87, 85]

Table 2.13: Comparison of incremental versus absolute encoders [90]

| | Incremental | | Absolute |
|---|---|---|---|
| | **Single-channel** | **Quadrature** | |
| **Complexity** | Simpler | | More complex |
| **Output** | Speed, displacement | Velocity and direction | Velocity and absolute position |
| **Needs homing on startup?** | Yes | | No |
| **Resolution** | Up to 10k PPR (direct read) | | Up to 22-bit (ST) / 12-bit (MT) |
| **Communication via protocol?** | No | No | Yes |
| **Cost** | Generally lower | | Generally higher |

The resolution value of a conventional absolute encoder is in fact similar to incremental encoders (e.g. pulse per revolution (ppr),ppi), but this time the output is expressed in binary format instead of high-speed pulse streams.

$$\text{The maximum encoder resolution} = 2^n \tag{2.22}$$

where $n$ = number of output wires of the encoder.

Hence, e.g. a 8 ppr absolute encoder has 3 outputs, an 32 ppr absolute encoder has 5, a 16 ppr absolute encoder has 4 outputs. The actual position value can also be known, even if power is lost. This is mainly due to the fact that any location in absolute encoder's revolution corresponds to a unique binary value. One drawback of them is that they cannot count the number of turns made, this can be done easily by the utilisation of Multi-turn absolute encoders.

## 2.11 Laser interferometry

THE BASICS Interferometry can be defined as a high-end measurement method, in which the interference of light, sound or radio waves is utilised. In addition to its other applications, interferometry is also

used in modern production metrology for mainly linear and angular displacement measurements, and straightness measurements. They play a key role, and therefore used very often in calibration and control of various motion systems, e.g. machine tools and CMMs. [91]

In laser interferometry, an interference pattern can be obtained when two beams superpose, which are provided either by splitting one beam into two or by the utilisation of two light beams. The visible light has a short wavelength, and it is possible to recognise even very small differences in the optical paths between two beams, since they create different interference patterns. Due to these feature interferometry has become a very popular and important measurement method for more than a century. They are then continuously improved due to the advances in laser technology. Accuracy characteristics of interferometer systems used in production metrology has been improved considerably over the years. However, their basic structure and operation principle, which was demonstrated by Albert A. Michelson remained same to a great extent. [91]

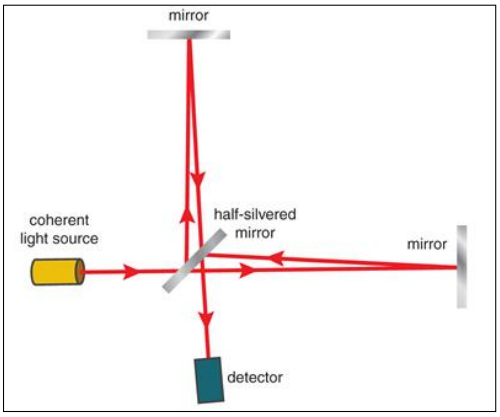


**Figure 2.74:** Michelson interferometer [91]

Two mirrors and a beam splitter are the main parts of a so-called Michelson interferometer. The light is split into two beams, which travel different paths, as soon as it arrives and goes through the beam splitter. This is due to the fact that the beam splitter is partially reflecting. These two different ways lead to the two different mirrors. They are reflected back there and reunited again at the beam splitter and then arrrives together at the detector. A phase difference which is generated by the different paths of beams produces a fringe pattern of interference. The task of the detector is to analyse it to determine required characteristics, e.g. wave features or mirror displacement. [91]

APPLICATION OF INTERFEROMETRY In the context of interferometry, it is of great importance to use a source which provides single and higly stable wavelength for achieving high precision values. Although there exist various types of interferometers, the linear one is the most straightforward to explain their principle. Here, the two mirrors from the Michelson interferometer are replaced by retro-reflectors, which are basically prisms at which the light is reflected back parallel to its coming direction. One of the retro-reflectors are mounted to the beam splitter and forms the reference arm. Since the distance of second one

changes depending on the beam splitter, it builds an arm referred to as variable length measurement. [91]

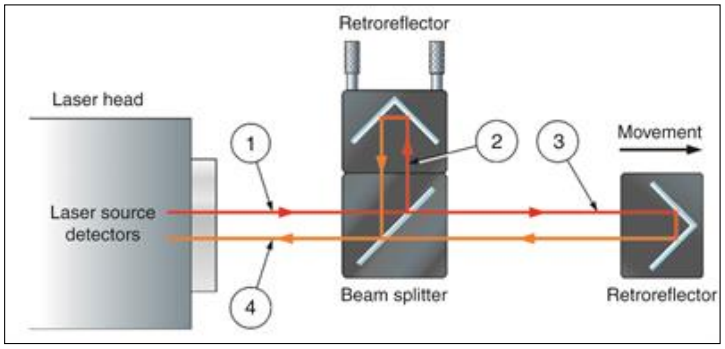


**Figure 2.75:** Laser interferometry [91]

After emitted from the laser head, the laser beam (1) is split into two beams at the beam splitter, i.e. one is reflected (2) and the other is transmitted (3). Afterwards, retro-reflectors reflect them back, and thus they get reunited again at the beam splitter. This reunited beam goes then to the detector. In that step, their interference with each other is realised. This can occur either destructively or constructively. In former, the beams are out of phase, and the troughs of one beam cancels the peaks belonging to the other, which leads to a dark fringe. In latter, on the other hand, they are in phase and their peaks consolidate each other. Hence, a bright fringe is obtained. [91]

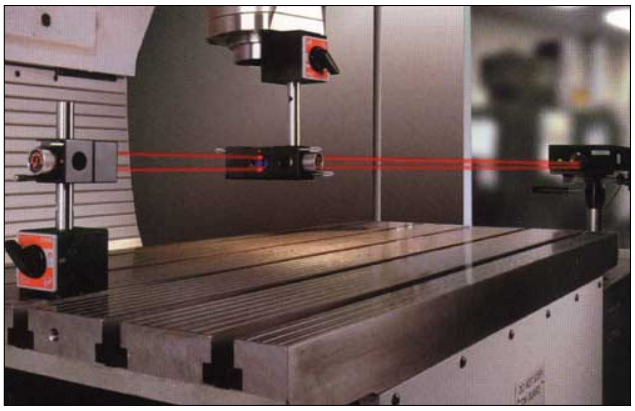

**Figure 2.76:** Laser interferometer system [91]

These interference characteristics can be monitored due to the detector's optical signal processing. When the measurement arm is displaced, it begets a change in the relative phase of two beams. Intensity of the reunited light is exposed to cyclic variation due to the abovementioned cycle of constructive and destructive interference. Whenever the measurement arm or retro-reflector is moved by 316.5 nm (half the laser wavelength, since it causes a change in optical path by 633 nm, the full laser wavelength) intensity changes as cyclic variation from light to dark to light. Hence, the calculation (of number of cycles) and the measurement of movement is realised as follows:

$$d = \frac{\lambda \cdot N}{2} \tag{2.23}$$

Here, the number of fringes passed is represented by $N$, the displacement ($0.633\,\mu m$) is denoted by $d$, and $\lambda$ is simply the laser wavelength. When the phase interpolation is realised within these cycles, the higher resolution of $1\,nm$ is obtained. [91]

COMPENSATION OF AMBIENT EFFECTS Regardless of the theoretical capabilities of the laser units, its operational wavelength is highly affected by the ambient conditions. Hence, the environmental effects in terms of e.g. temperature, humidity and pressure must be compensated by a compensator unit. Otherwise it would be impossible to get healthy and accurate measurement results. Those ambient conditions are measured by the compensator and the reftractive index of air, thus the laser wavelength is calculated. It is then automatically compensated for possible variations and operator can focus on their measurement tasks. [91]

REMOTE INTERFEROMETRY In some designs the interferometer or the beam splitter is mounted into the laser head. Utilisation of a remote beam splitter solves the possible problems of laser head or warm-up time. [91]

LASER ANGULAR INTERFEROMETER A laser angular interferometer consists of a laser head, a periscope optic and a beam splitter as a combined structure, and an angular reflector. There are two retro-reflectors in the angular reflector. The distance between their centres is denoted by $S$. As soon as the beam coming out from laser head arrives at angular interferometer, it is split into two different beams by the beam splitter. One beam continues going straight until the lower retro-reflector, and thus builds the so-called *Arm 1* of the interferometer. The other, on the other hand, is reflected first by the beam splitter upwardsa, and then by the periscope mirror towards the upper retro-reflector. Thus, the *arm 2* of the interferometer is also formed. Afterwards, retro-reflectors reflect these beams back again, followed by their reunification at the angular interferometer. Finally, they travel towards to the detector, and measurement signals are generated from their interference there. [91]

The relative changes between the optical paths of abovementioned *arms* of interferometer is key for the measurement of angles. These changes are recognised by the laser system. If e.g. the angular reflector is pitched away by $\theta$, the Arm 1 will be shorter, and the Arm 2 will be longer, both, as a matter of course, by the same amount, i.e. by $\frac{1}{2}S\sin\theta$. Hence, a relative change of $S\sin\theta$ in the outwards path (i.e. between the arms) is caused. This doubled value for the change in path is a result of back and forth travel of beams between the reflector and the interferometer. There is an interpolator inside the detector that recognises these changes. Their conversion to a linear distance $\Delta L$ is realised by multiplying them by the half wavelength of laser Equation 2.24. [91]

$$\Delta L = \text{Fringe count} \times \frac{\lambda}{2} \tag{2.24}$$

When using the laser interferometer system in angular mode, its software make the related conversions automatically according to the following formula, [91]

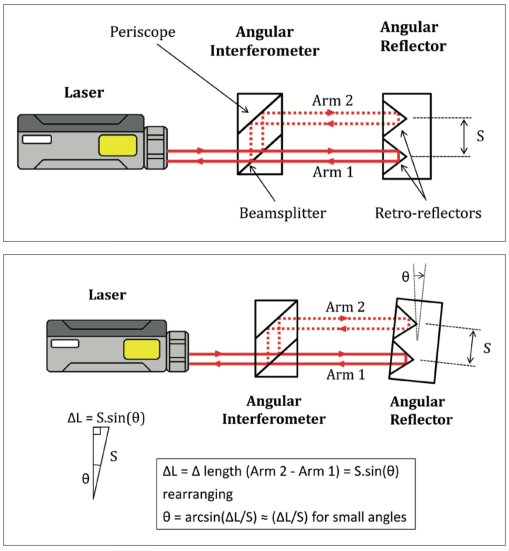


**Figure 2.77:** Laser interferometer system for angular measurements [91]

$$\theta = \frac{\arcsin \Delta L}{S} \tag{2.25}$$

Angular interferometer systems are sensitive to the changes in angle between reflector and the interferometer. On the other hand, ithey are quite nsensitive to the precise alignment of the laser or to linear translations. This fact brings them into prominence in two areas, i.e. in measuring the pitch and yaw errors of linear axes, and in calibrating the accuracy of rotary axes. [91]

# 3

# EXPERIMENTAL STUDY

*"Innovation distinguishes between a leader and a follower."*

Steve Jobs (ex-CEO Apple Inc., 1955-2011)

This chapter discusses an experimental work carried out by the author in the High Precision Measurement Room - Nanometrology Laboratory of the AuM of the TU Wien. It explains the structure and design of the measurements that conducted. Applied methodology, existing parameters and several different key points are also presented and described in this chapter.

## 3.1 Methodology

The main focus of the practical part of this thesis lies in determining the adequacy and practical capability of two different modern measurement instruments, i.e. a Hall-effect magnetic linear encoder and a CMM in obtaining positioning characteristics (especially the reversal error) of rotary tables.

Practical part in itself can be broken down into two sections:

- Measurement of the positioning characteristics of a manual rotary table
- Measurement of the positioning characteristics of a CNC rotary table

As far as the first section concerned, first, the measurement set-up was designed, required steps were recorded, and missing components were determined. This is followed by purchasing these equipments. Afterwards, the measurement set-up was built on a lathe bed, and its stability and run-out values were checked and finetuned. As soon as the set-up was stable and ready to the measurements, the manual rotary table was measured with the help of a high-resolution measurement instrument, i.e. a Hall-sensor contactless magnetic linear encoder, and simultaneously its comparison and verification was made by a more capable and precise measurement instrument, i.e. by laser angle interferometer. Afterwards, the results of both measurements were evaluated statistically, and demonstrated in corresponding tables. Mean values, standard deviations and all positioning accuracy characteristics, in particular,, the reversal error, were determined (in agreement with the ISO 230-2:2014). Thus, the obtained values from each system

were first compared among themselves, and then to each other. Finally, the results and their significance were evaluated and interpreted.

On the other hand, as far as the second section concerned, first, the related measurement set-up was designed and required steps were recorded. Here, it was thought to check the adequacy of using a CMM in measuring the positioning characteristics of a CNC rotary table. Applying a similar approach to the method described in ISO 10360-3:2000, the positioning characteristics of the CNC rotary table were measured. Analogous to the first section, the same properties were also measured by a laser angle interferometer system. Afterwards, the results of both measurements were evaluated statistically, and demonstrated in corresponding tables. Mean values, standard deviations and all positioning accuracy characteristics, in particular,, the reversal error, were determined (in agreement with the ISO 230-2:2014). Thus, the obtained values from each system were first compared among themselves, and then to each other. Finally, the results and their significance were evaluated and interpreted.

## 3.2 Measurement room and ambient conditions

### 3.2.1 High Precision Measurement Room – Nanometrology Laboratory of the TU Wien

Along with the rapid development of manufacturing technologies, high precision metrology has become an essential part of modern industrial applications. Besides, it is also of great importance in the area of scientific research, since the demands for metrology applications are increasing rapidly.

Concerning accuracy, those demands can only be fulfilled by metrology systems that give measurement results with uncertainty values in sub-micrometre and nanometre range. The same demands are also valid for the related measurement rooms. Even by using most accurate measurement systems, without a measurement room, in which the suitable environmental conditions are regulated and ensured, obtaining reproducible and consistent measurement results remain as nothing but an alien concept. Only a well-designed measurement room or laboratory can assure internationally recognisable, comparable and traceable measurement results with as small measurement uncertainties as possible. The most crucial environmental influences on measurement uncertainty are:

- Temperature (thermal conduction, convection and radiation)
- Vibration
- Air humidity
- Pollution

The structural organisation of a precision measurement room ensures that these disturbing influences will be reduced and kept constant. The High Precision Measurement Room – Nanometrology Laboratory of the TU Wien demonstrates the demands for such a building and features of technical realisation.


**Figure 3.1:** High Precision Measurement Room - Nanometrology Laboratory of TU Wien

ROOM-IN-ROOM CONCEPT The High Precision Measurement Room – Nanometrology Laboratory, which is located in the basement of the main building of the TU Wien, is separated from the surrounding buildings by a mechanical and structural concept (room-in-room) and has solid walls and a concrete slab, that provide vibration isolation from the environment also preventing the transfer of building oscillations. It is located in the basement o the main building of TU Wien, and its separation from the surrounding buildings are realised by a special structural and mechanical concept (room-in-room). Besides, the vibration isolation and the transfer of possible oscillations are prevented due to the solid walls and concrete slab of the high precision measurement room.

The powerful and robust air conditioning system of the High Precision Measurement Room – Nanometrology Laboratory ensures a suitable environmental condition in terms of temperature, air speed, air pressure, humidity and particles with specified values. The climate in the laboratory is continuously monitored and regulated to keep these values as constant as possible. Utilisation purpose of a slight overpressure of about 10 Pa is preventing the irruption of unconditioned and unfiltered air when the doors are open. Apart from the high precision measurement room itself, the whole system consists of a control room, sluice, entrance hall and machine room.

An overview of the technical characteristics of the High Precision Measurement Room - Nanometrology Laboratory of TU Wien is given in Table 3.1.

**Table 3.1:** Overview of technical characteristics of the High Precision Measurement Room - Nanometrology-Laboratory of TU Wien

| | |
|---|---|
| **Length, L** [m] × **Width, W** [m] × **Height, H** [m] | 12 × 5,8 × 2,8 |
| **Floor area** [$m^2$] | 70 |
| **Space volume** [$m^3$] | 195 |
| **Air circulation ratio** [$h^{-1}$] | 28 changes |
| **Percentage of fresh air** | 18 |
| **Reference temperature** [°C] | $20 \pm 0,1$ |
| **Relative humidity** [%] | $45 \pm 5$ |
| **Air filtration** | 99.97 % of all particles larger than 0.3 µm |
| **Vibration isolation -** **Maximum ground amplitudes at frequencies greater than** 5 Hz | 0.05 µm |

## 3.3 Used components and equipments

In order to build and implement the necessary experimental set-up, several necessary components were purchased, designed and manufactured.

Those main measurement equipments and some secondary components can be listed as follows,

- 100 mm manual rotary table with four-jaw chuck and tailstock (6S02.1.02 of Hogetex company)
- A suitable stepped shaft
- A steel bench block
- Lathe bed (of Carl Zeiss Jena company)
- Hall-effect sensor based linear magnetic encoder (AS5311 of AMS company)
- Multi-pole magnet strip
- A CMM (UMM 500 model of Zeiss company)
- Two laser interferometer systems (of Hewlett Packard company)

### 3.3.1 General Overview of the Manual Rotary Table

The rotary table unit that was purchased is a small, ultra-compact horizontal and vertical rotary table with a plate of 100 mm as well as a four-jaw chuck and a tailstock. It has a precisely ground rotary plate and hardened worm gear. The rotary table is equipped with a 360° scale and has a lever ratio of 36:1. For each turn of the worm wheel, the table top turns 10°. The division of the rotating plate is 1′. The vernier scale has a division of 10″ and the T-slot width is 5 mm. The mounted jaw chuck is an independent four-jaw chuck with a nominal diameter of 85 mm.

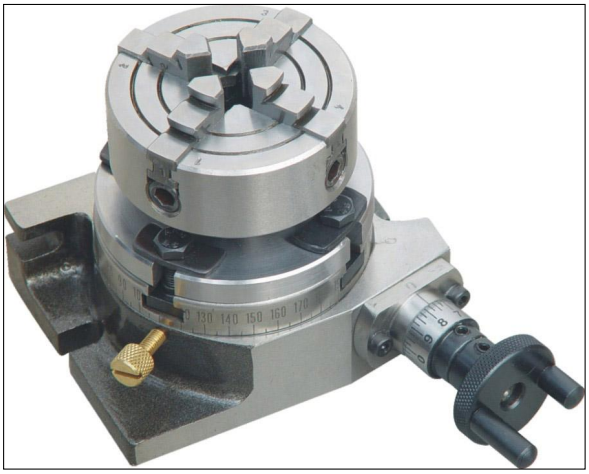

**Figure 3.2:** Rotary table with four-jaw chuck [92]

### 3.3.2 General Overview of the AS5311

The encoder that the manual rotary table is equipped with in this measurement set-up, is an incremental linear position sensor of AMS[19] company with model number AS5311.

DESCRIPTION When it was introduced to the market the AS5311 stood out with an impressive feature, i.e. the first Hall-effect sensor based linear magnetic encoder, which achieves sub-micron resolution. The AS5311 can be described as an incremental position sensor for linear and rotary off-axis applications relied on contactless magnetic sensor technology.

It is a non-contact high-resolution magnetic linear encoder, which can also be used for measuring angles of rotation. A multi-pole magnet strip or ring with a pole pair width of $2\,mm$ is required to perform position and motion measurements. The distance betweeen the Hall-sensor and the magnetic strip is typically $0.3\,mm$ to $0.6\,mm$, and a relative movement between them (along the magnetic strip) is required in order to obtain measurement information. [93]

The output of the magnetic sensor can be detected either as a serial bit stream, as a pulse-width modulation (PWM) signal, or application binary interface (ABI) encoder signal. The resolution in the evaluation of the ABI signal is $2^{10}$ per $2\,mm$ pole pair which corresponds to $1.95\,\mu m$ per step and to $6.76''$ as angle. There are 4096 pulses (12-bit) per $2.0\,mm$ pole pair length on the standardised quadrature output interface with an index pulse (=ABI) with a maximum speed of $650\,mm\,s^{-1}$. [93]

This non-contact high resolution magnetic linear encoder is used in order to detect and measure linear motion accurately and for off-axis rotary sensing applications with a resolution down to $< 0.5\,\mu m$. It is a system-on-chip, combining integrated Hall-elements, analog front end and digital signal processing on a single chip, packaged in a small 20−pin thin-shrink small outline package (TSSOP) package. [93]

19 AMS AG stands for former Austriamicrosystems AG | http://ams.com/eng

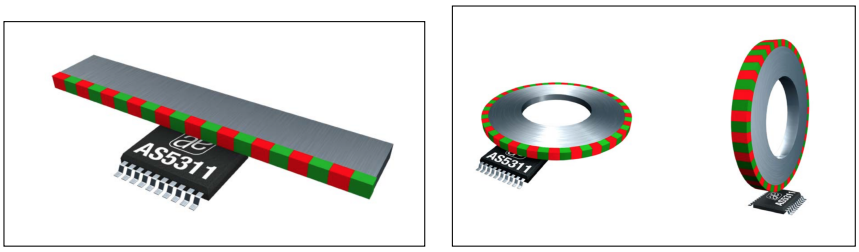


(a) AS5311 with Multi-pole Magnetic Strip for Linear Motion Sensing

(b) AS5311 with Multi-pole Ring Magnets for Off-axis Rotary Motion Sensing

**Figure 3.3:** AS5311 | Magnetic linear encoder [93]

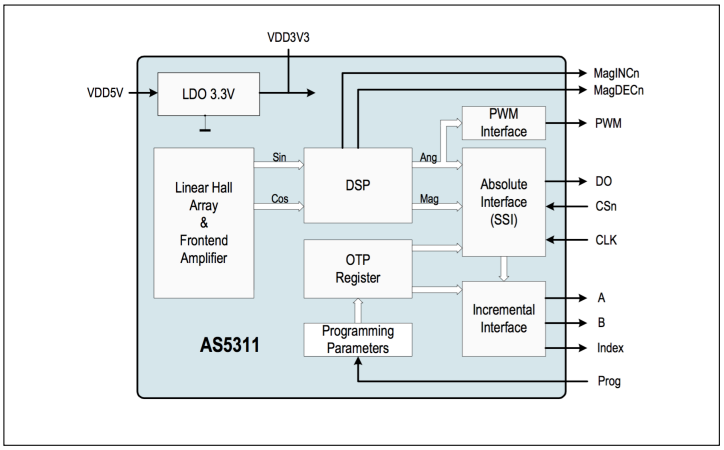


**Figure 3.4:** AS5311 Block diagram [93]

The absolute measurement provides instant indication of the magnet position within one pole pair with a resolution of 488 nm per step (12−bit over 2.0 mm). This digital data is available as a serial bit stream and as a PWM signal. Furthermore, an incremental output is available with a resolution of 1.95 µm per step. An index pulse is generated once for every pole pair (once per 2.0 mm). The travelling speed in incremental mode is up to 650 mm $s^{-1}$. An internal voltage regulator allows the AS5311 to operate at either 3.3 V or 5 V supplies. Depending on the application the AS5311 accepts multi-pole strip magnets as well as multi-pole ring magnets, both radial and axial magnetised. The AS5311 is available in a lead-free (PB-free) TSSOP-20 package and qualified for an ambient temperature range from −40 °C to 125 °C. [93]

AS5311 together with the magnetic strip are the only two components required to build a robust submicron-resolution position feedback system. This small form factor allows AS5311 to be integrated in autofocus, zoom and vibration reduction systems in cameras, switching systems in fibre-optics or other micro-positioning applications where tight space is a concern and high resolution is demanded. AMS' encoder chip also provides extended diagnostic features that constantly monitor the placement of the magnet above the device. These features allow early detection of mechanical systems failures. In addition, the device compensates for the adverse effects of unwanted external magnetic fields thus ensuring additional safety and robustness of the system. [93]

MEASURING PRINCIPLE The measuring principle of AS5311 is based on the use of Hall-elements, which are based on standard complementary metal oxide semiconductor (CMOS) technology. The horizontally arranged Hall-elements are sensitive to a magnetic field, which is perpendicular to their surface. This means that only those magnetic fields which are vertical to the surface of integrated circuit (IC) have an influence on the measurement signal. The magnetic strip, which is actually designed for the determination of linear motion, can be curved for detecting a rotational movement, and subsequently can be used for the measurement of an angle. It should be noted that the greater the radius of curvature of the magnetic tape is, the smaller the error. [93]

Two Hall-switches glide over a magnetised multi-pole strip. The Hall-switchs switch on in response to the changing magnetic field and thus produce a square-wave signal. If the length of the magnetic pole is known, it can be determined how far the magnetic strip has moved relative to the Hall-switch. The both Hall-switches are so positioned that their square-wave signal is phase-shifted by $90°$. Therefore, it is possible to determine the direction of movement. However, this method enables to divide the smallest possible pole pair length (approx. $0.5\,mm$) only in 4 zones. [93]

There remains only the possibility of interpolation to increase the resolution. The square-wave signal of the Hall-switch is disadvantageous for the further signal processing, which is the reason why linear Hall-sensors are used. Linear Hall-sensors provide an output signal which is proportional to the strength of the magnetic field, which is perpendicular to the Hall-sensor. A Hall-sensor, which glides over the magnetic strip, outputs sinusoidal signals, since the magnetic field of a multi-pole magnetic strip is sinusoidal. If four different elements are used, which have a distance of a half pole length to each other, four harmonic signals were obtained. Those are phase-shifted by $90°$ to each other. The four signals correspond to a sine, a cosine, an inverted sine and an inverted cosine diagram. By combining each harmonic signal with the inverted counterpart, another signal is received with a twice as large amplitude. This requires that an input signal must be inverted, which means that the interference is inverted by the external magnetic fields. Thereby it is possible to cancel every interference caused by magnetic fields near the sensor. The two resulting signals can be converted into a high-definition digital signal with phase and amount by means of an analog-to-digital converter and a digital signal processor (DSP). [93]

The sensors of the AMS AG use a system called COordinate to Rotation DIgital Computer (CORDIC) for the processing of harmonic signals. The differential sine and cosine signals are transformed into a digital signal by an analog-to-digital converter. A pointer on the unit circle can be decomposed by projection to its vertical and horizontal components. On the unit circle, the component which is projected on the abscissa corresponds to the cosine of the angle between the pointer and the coordinate axis. The vertical component is equal to the sine. Hence, a pointer in the unity circle can be defined unambiguously by both harmonious signals. The included angle determines the position of the pointer clearly as well and a rotation of $360°$ corresponds to the width of a pole pair. The number of discrete steps within a rotation of

the pointer is called interpolation factor. The more steps there are, the higher is the resolution of the sensor. Within a pole pair, which has a length of 2 mm, $256 \times 4 = 1024$ discrete steps are possible, corresponding to a resolution of $2^{10}$ bits. [93]

The AS5311 can be used also for angle measurement. For this, the magnetic tape has to be curved and passed by the sensor. Knowing the origin of the radius of curvature, the swept angle can be calculated. [93]

The different types of outputs relative to the magnet position are outlined in Figure 3.5 below. The absolute serial output counts from 0 to 4095 within one pole pair and repeats with each subsequent pole pair. Likewise, the PWM output starts with a pulse width of 1 µs, increases the pulse width with every step of 0.488 µm and reaches a maximum pulse width of 4097 µs at the end of each pole pair. An index pulse is generated once for every pole pair. 256 incremental pulses are generated at each output A and B for every pole pair. The outputs A and B are phase shifted by 90 electrical degrees, which results in 1024 edges per pole pair. As the incremental outputs are also repeated with every pole pair, a constant train of pulses is generated as the magnet moves over the chip. [93]

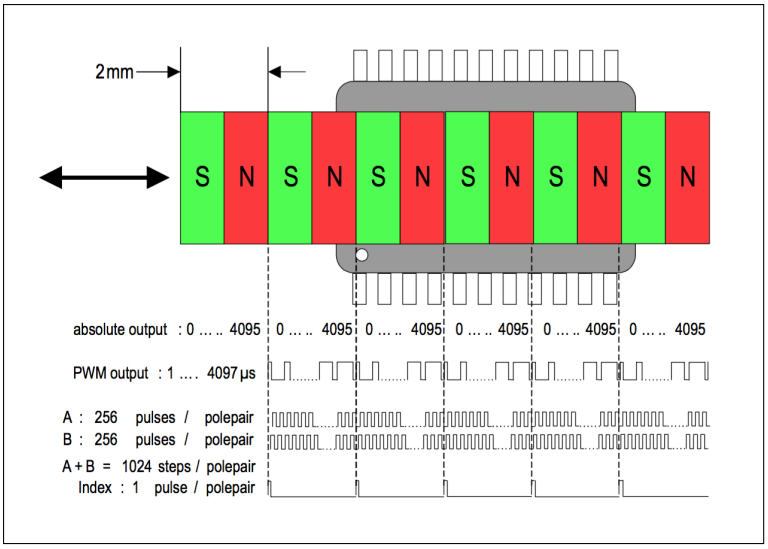


**Figure 3.5:** AS5311 - Outputs Relative to Magnet Position [93]

APPLICATION AREAS The main application areas, in which the AS5311 operates can be expressed as follows [93]:

- Robotics
- Micro-Actuator feedback
- Servo drive feedback
- Replacement of optical encoders

### 3.3.3 General Overview of the Laser Angle Interferometer Systems

Two laser measurement systems of Hewlett Packard company were used which are designed specifically to make a variety of very accurate measurements in context of production metrology.


**Figure 3.6:** Main components of the laser angle interferometer systems used [94]

These portable and lightweight measuring systems can be utilised to conduct distance, velocity, angular displacement, flatness, straightness, squareness, and parallelism measurements.

The theoretical principle of the set-up for conducting an angular measurement is illustrated in Figure 3.7[20].

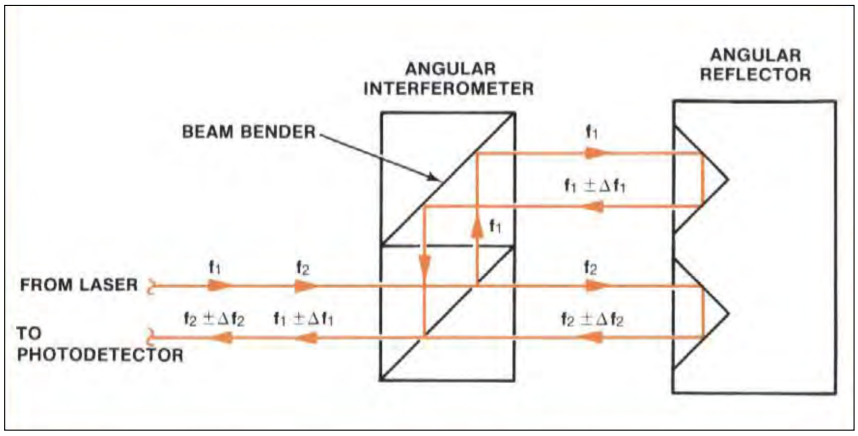


**Figure 3.7:** Principle of laser angle interferometry [94]

### 3.3.4 General Overview of the CMM UMM 500

In 1973, the UMM 500 *Universal Measuring Machine* was introduced by Zeiss company as the world's first high-precision 3D CNC CMM at the *Microtecnic* trade fair in Zurich. Figure 3.8 shows the general structure and main components of CMM UMM 500.

20 See also Section 2.11 for a detailed overview.

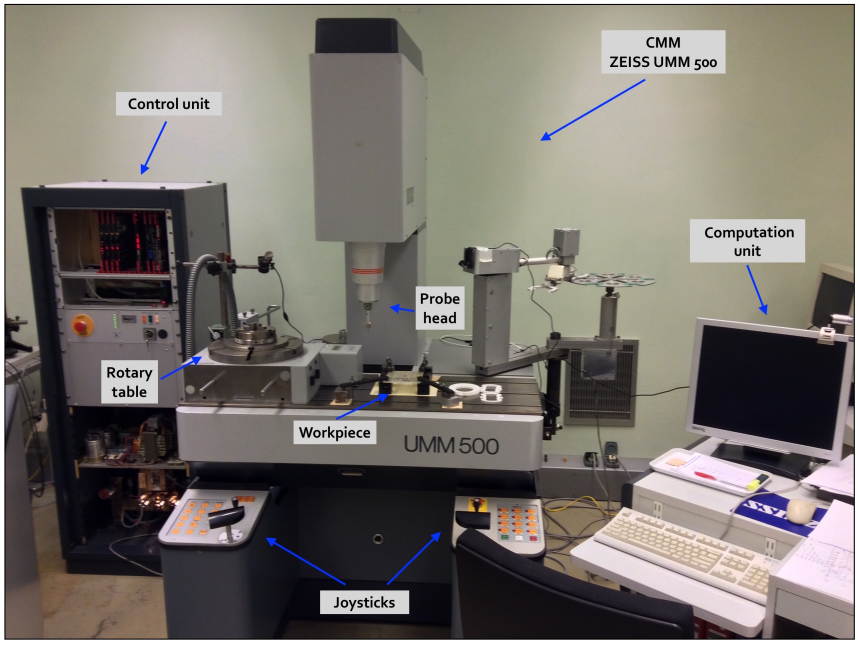


**Figure 3.8:** General structure and main components of CMM ZEISS UMM 500

The main technical characteristics of CMM UMM 500 are listed in Table 3.2.

**Table 3.2:** Main technical characteristics of the CMM UMM 500

| | **Measuring range/volume** [$mm^3$] | **Resolution** [µm] | **Accuracy** [µm] | $MPE_E$ [µm] |
|---|---|---|---|---|
| **Zeiss UMM 500** | 500 x 200 x 300 | 0,1 | 0,2 | $0,4 + \frac{L\,[mm]}{700}$ |

## 3.4 Experimental Work

### 3.4.1 Measurements regarding the manual rotary table

#### *3.4.1.1 Measurements by means of the Magnetic Encoder AS5311*

In agreement with the abovementioned aims of this section, first, a manual rotary table equipped with a four-jaw chuck and a tailstock was purchased. Since there was no drawing data available, the CAD of its concept was realised.

Second, a stepped shaft was manufactured on which the magnet strip was mounted to capture angular position information using Hall-sensor based magnetic encoder. Afterwards, the measurement arrangement including a magnetic linear encoder was set up on a lathe bed in High Precision Measurement Room - Nanometrology Laboratory of the AuM. The rotary table unit was mounted vertically and the stepped shaft was placed and centered roughly between tailstock and four-jaw chuck. By means of a few screws, T-nuts and clamping claws the individual components of set-up were fixed to the lathe bed.

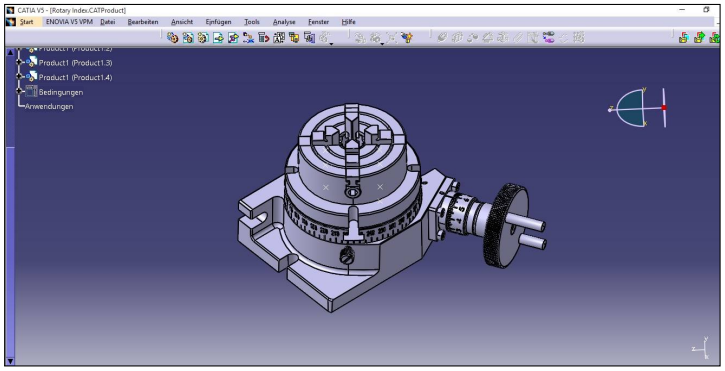


**Figure 3.9:** A screenshot of 3D CAD drawing of the rotary table and four-jaw chuck

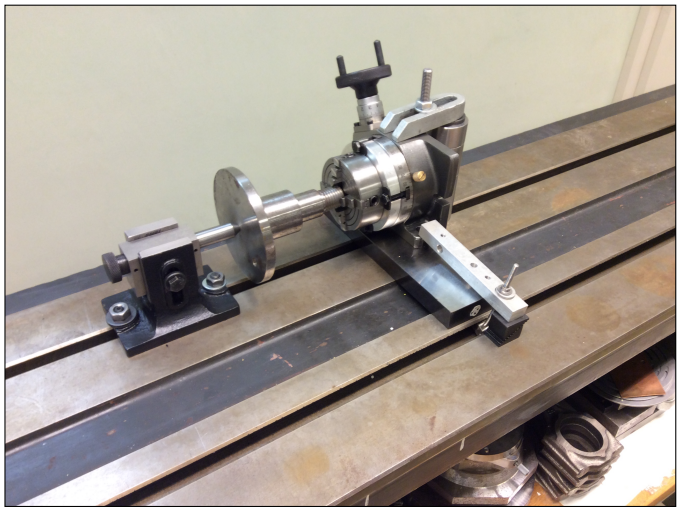

**Figure 3.10:** Rotary table and four-jaw chuck connected with tailstock and stepped shaft on a lathe bed

As soon as the fixing on lathe bed is finished, the stability of whole set-up was checked and corrected. The run-out values and concentricity of rotation axis of rotary table, four-jaw chuck and stepped shaft and tailstock center were measured by means of a dial indicator.

After finetuning until the values were within acceptable limits, the magnetic encoder was placed under the biggest section of the stepped shaft on which the magnet strip was mounted, and linear magnetic encoder AS5311 was placed underneath.

While the rotary table was being rotated, it also rotated the stepped shaft which was centered by means of four-jaw chuck. Hence, the rotational relative movement was recognised and measured by the Hall-sensor of AS5311, and the angular position information was gathered. In that way, the reversal error, uni-/bidirectional repeatability and accuracy as well as other positioning characteristics of the rotary table were obtained.

After setting five different reference angles, at which the measurement values were obtained afterwards, those angular positions were traveled eight times in total, each four times in positive (clockwise (cw)) and negative (counter-clockwise (ccw)) direction. For each stop,

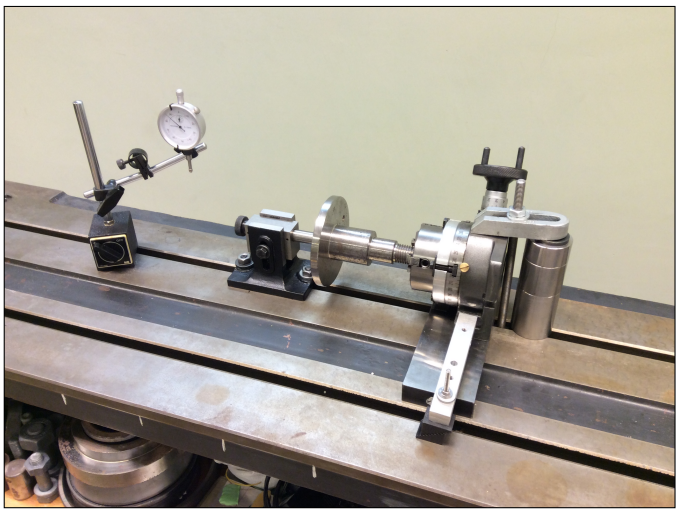

**Figure 3.11:** Run-out and concentricity check of set-up by means of a dial indicator

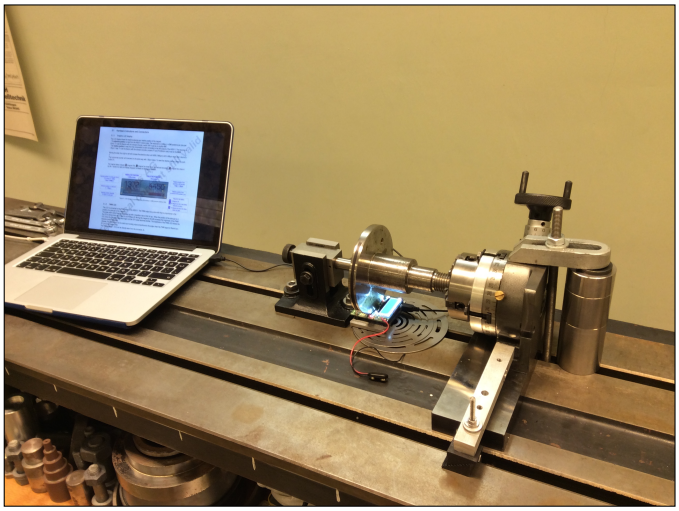

**Figure 3.12:** Placement of magnetic linear encoder AS5311 under the biggest section of stepped shaft

the measurement results were read out from the liquid-crystal display (LCD) display of AS5311, and deviations were recorded. In sight of this data, the required values for reversal error, uni-/bidirectional repeatability and positioning accuracy were calculated, and a related statistics table was created (Tables 4.1 and 4.2).

#### *3.4.1.2 Measurements by means of the Laser Interferometer System*

Measurements were conducted simultaneously both by the magnetic encoder and the laser angle interferometer. The characteristics were measured in four different angular positions. The measurement cycle was repeated eight times, and the whole measurement was conducted twice, in total.

In order to verify the previous results or gather more valid and accurate results, the same properties were also measured simultaneously by a laser angle interferometer system. The gathered measurement results

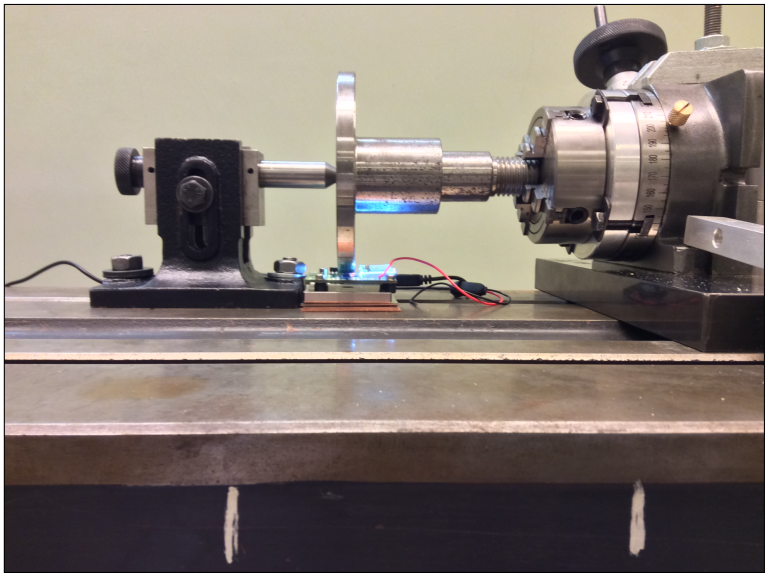

**Figure 3.13:** Set-up for the measurement by means of magnetic encoder AS5311

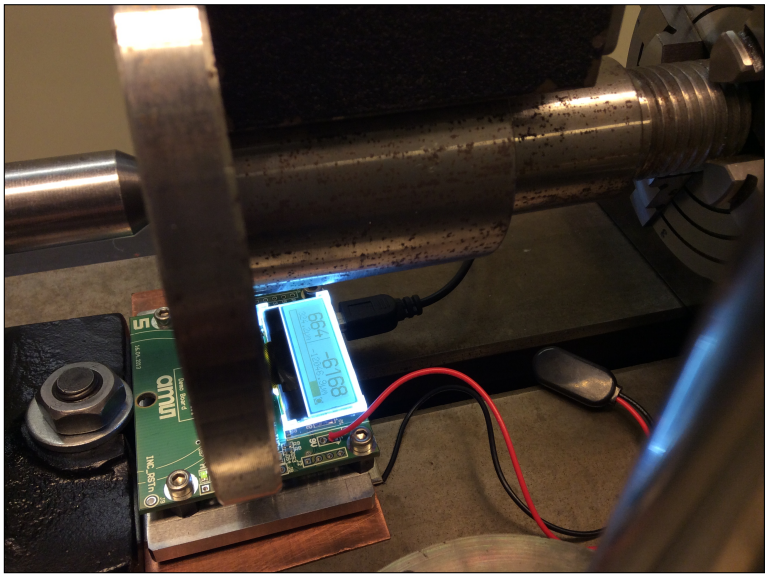

**Figure 3.14:** Front close-up view of the measurement set-up with magnetic encoder AS5311

were compared to those obtained with the aid of the magnetic linear encoder AS5311. Finally, the results of both measurements were evaluated statistically, and demonstrated in a table. Mean values, standard deviations and all positioning accuracy characteristics, in particular, the reversal error, were determined (in agreement with the ISO 230-2:2014).

Since the theroretical background of laser angular interferometry and laser angle interferometer were already given in Section 2.11, only the practical considerations and steps are explained as well as measurement results are listed in this section.

First of all, the angular retro-reflector of laser angle interferometer system was mounted onto the upper surface of the second biggest section of stepped shaft in our measurement set-up. Hereby a magnetic base was used to ensure the stability of angular retro-reflector on this surface. Then, it was checked by means of a spirit level, whether the angular reflector lies exactly horizontal on the surface. Afterwards, it was brought to the position where it is exactly horizontal. Second, the laser beam source was mounted on a tripod and its height is arranged according to the level of angular retro-reflector.

**Figure 3.15:** Set-up for the measurements by means of laser interferometer system

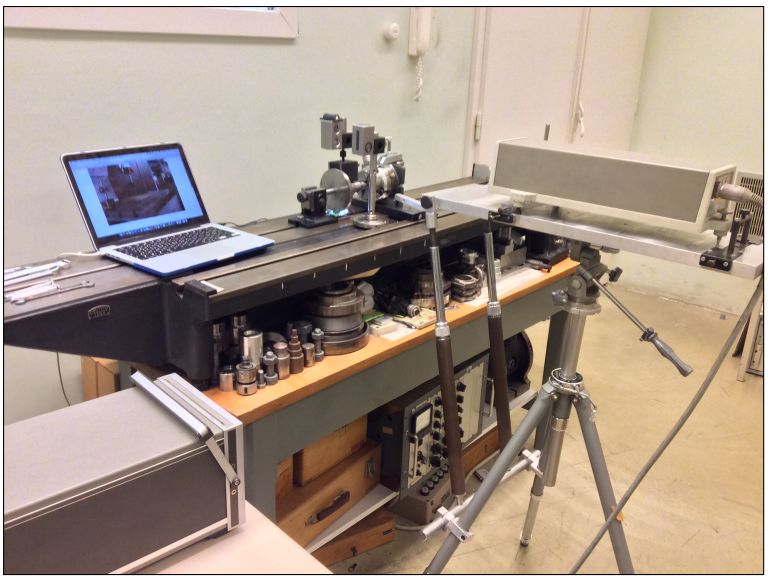

**Figure 3.16:** Set-up for the measurements by means of laser iInterferometer system

As the next step, the angular interferometer was placed between laser beam source and angular retro-reflector, and the height, level and position control were made in order to ensure that the laser beam that comes out from the source travels through the angular interfero-

meter into the reflector on a straight path, and thus a sufficient signal strength was gathered for our measurements.

After all arrangements regarding the set-up were done, a measurement plan was created, and according to this plan, angular points to be measured were approached, first, from one direction (positive=ccw), and then, from the other (negative=cw), and corresponding results were recorded manually. Four different angular points, with 30′ angular distance between each other, were approached and measured ccw, and after the fourth point, an extra movement of 2° was realised in order to comprise a possible reversal error value of up to 2°. Afterwards, the rotary table was rotated in the reverse direction, and the pre-defined four angular points were approached and measured cw in order to gather information regarding positioning accuracy, specifically regarding reversal error.

This process was repeated eight times so as to obtain statistically meaningful information. Finally, a statistics table was created (in agreement with the ISO 230-2:2014) with the gathered measurement results, and the mean reversal error value was determined (Tables 4.3 and 4.4).

### 3.4.2 Measurements regarding the high-precision CNC rotary table

In addition to the measurements conducted on the experimental set-up containing the manual rotary table, positioning accuracy characteristics of a CNC rotary table of a CMM were also evaluated, first by CMM itself, then by a laser angle interferometer. The obtained results were compared each other, and analysed statistically in agreement with the ISO 230-2:2014.

#### *3.4.2.1 Measurements by means of the CMM UMM 500*

An experimental measurement set-up was installed in order to obtain and evaluate positioning accuracy characteristics of the CNC rotary table by CMM itself. As a similar approach to the one explained in ISO 10360-3:2000, calibrated reference sphere was used for this purpose, and measured in specified certain angular positions, and the deviations between the commanded and the actual angular positions were recorded. This was realised for 8 well-distributed measurement points, and each of them was traveled 5 times. Finally, the obtained results were analysed statistically in agreement with the ISO 230-2:2014.

#### *3.4.2.2 Measurements by means of the Laser Interferometer System*

In order to check and verify previous measurement results obtained by CMM UMM 500, a more capable and accurate measurement system was utilised, i.e. laser interferometer system.

By using the appropriate optics and equipments the laser angle interferometer was installed and its arrangement on the CNC rotary table was realised. A magnetic base was used to fix required components of the laser interferometer onto the rotary table.

After the arrangement and alignment were completed, rotary table was commanded via the related software to rotate 1.5° in total, with

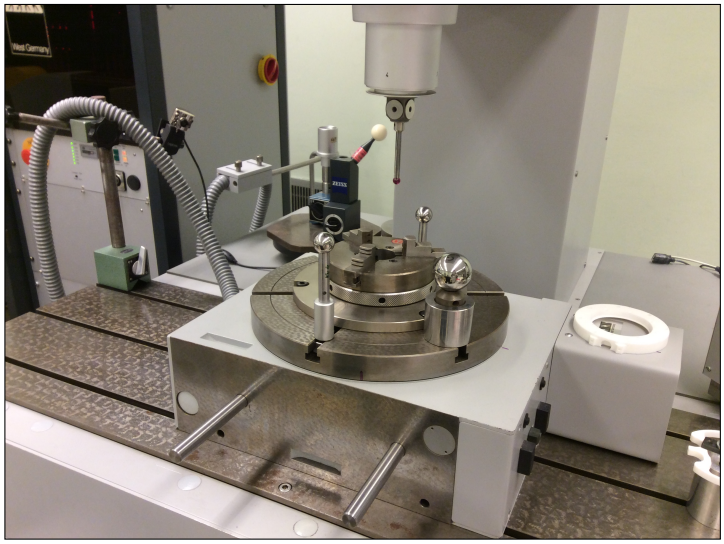

**Figure 3.17:** An image of the set-up for the measurement by means of the CMM UMM 500

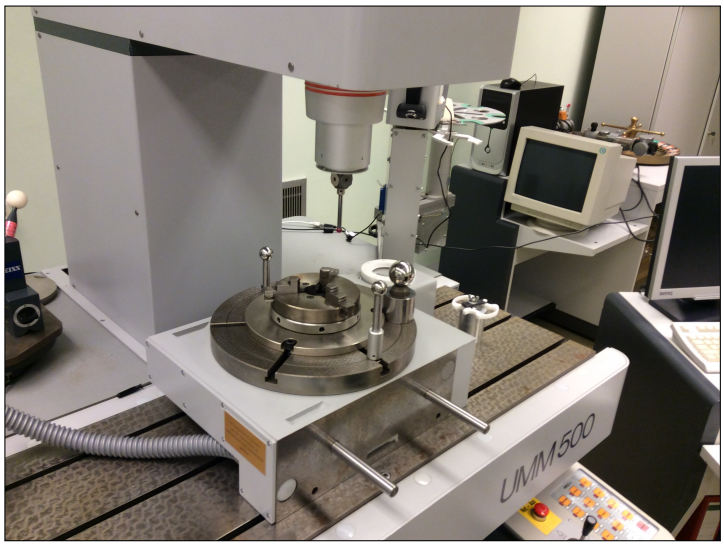


**Figure 3.18:** Another image of the set-up for the measurement by means of the CMM UMM 500

half degree position intervals. Characteristics of rotary table were measured in 4 pre-defined angular positions, and the deviations between the commanded and the actual angular positions were recorded. Each of the measurement points was traveled 5 times. The same measurement steps are applied for the following settings:

- From 30° to 28.5°, and with big beam setting
- From 30° to 31.5°, and with big beam setting
- From 210° to 208.5°, and with small beam setting
- From 210° to 211.5°, and with small beam setting

Finally, the obtained results were analysed statistically in agreement with the ISO 230-2:2014.

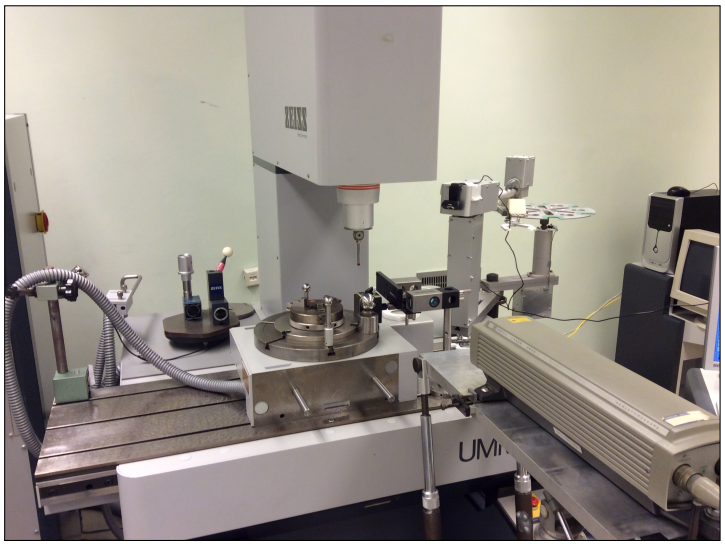

**Figure 3.19:** An image of the set-up for the measurement by means of the laser interferometer system

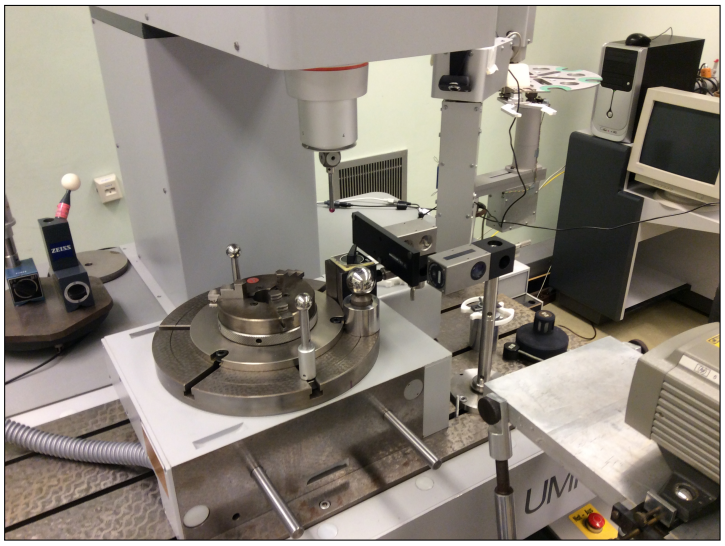

**Figure 3.20:** Another image of the set-up for the measurement by means of the laser interferometer system

# 4

# RESULTS AND DISCUSSION

*"If you can't measure it, you can't understand it. If you can't understand it, you can't control it. If you can't control it, you can't improve it."*

JAMES HARRINGTON (...)

This chapter first represents the results of the experimental measurements conducted in the practical part of this thesis. Their statistical evaluation was made in agreement with the ISO 230:2-2014, and demonstrated by means of tables and line charts. Subsequently, obtained measurement results were discussed and interpreted.

## 4.1 Main Findings and Results

### 4.1.1 Measurement results for the manual rotary table

#### *4.1.1.1 Measurement results obtained through the Magnetic Encoder AS5311*

FIRST MEASUREMENT The measurement results of the manual rotary table obtained from the first measurement by the utilisation of the linear magnetic encoder AS5311 were demonstrated as a statistics table (in agreement with the ISO 230-2:2014) in Table 4.1.

- The mean reversal error of the axis was calculated as $-1.652°$.

SECOND MEASUREMENT The measurement results of the manual rotary table obtained from the second measurement by the utilisation of the linear magnetic encoder AS5311 were demonstrated as a statistics table (in agreement with the ISO 230-2:2014) in Table 4.2.

- The mean reversal error of the axis was calculated as $-1.629°$.

#### *4.1.1.2 Measurement results obtained through the Laser Interferometer System*

FIRST MEASUREMENT The measurement results of the manual rotary table obtained from the first measurement by the utilisation of the first laser interferometer system were demonstrated as a statistics table (in agreement with the ISO 230-2:2014) in Table 4.3.

- The mean reversal error of the axis was calculated as $-1.621°$.

**Table 4.1:** The measurement results of the manual rotary table obtained from the first measurement by the utilisation of the linear magnetic encoder AS5311

| Characteristic | Symbol | arcsec | | | | | | | |
|---|---|---|---|---|---|---|---|---|---|
| Number of measurement points | i | 1 | | 2 | | 3 | | 4 | |
| Target angular position (*degree*) | $P_i$ | 312,5 | | 312 | | 311,5 | | 311 | |
| Direction of rotation | ↓(ccw) or ↑(cw) | ↓ | ↑ | ↓ | ↑ | ↓ | ↑ | ↓ | ↑ |
| Positioning deviation $x_{ij}$ for the number of cycle (j) | j = 1 | 0,0000 | -5975,3866 | -187,1342 | -6169,1631 | -189,6788 | -6130,1052 | -308,2911 | -6187,5373 |
| | 2 | -27,2689 | -6008,9483 | -193,7766 | -6264,9539 | -230,5822 | -6143,7397 | -308,2911 | -6214,8062 |
| | 3 | -54,5378 | -5974,6874 | -166,5077 | -6195,7329 | -210,3053 | -6137,0973 | -246,7613 | -6153,2764 |
| | 4 | -54,5378 | -5988,3218 | -173,4997 | -6277,8892 | -271,4855 | -6130,1052 | -294,6567 | -6214,8062 |
| | 5 | -40,9034 | -5961,7521 | -193,7766 | -6284,5316 | -210,3053 | -6150,7317 | -328,9176 | -6195,2285 |
| | 6 | -61,5298 | -5995,3138 | -241,6720 | -6257,2627 | -244,2166 | -6123,4628 | -301,6487 | -6221,4486 |
| | 7 | -27,2689 | -6001,9563 | -193,7766 | -6270,8971 | -285,1200 | -6123,4628 | -281,0222 | -6221,4486 |
| | 8 | -75,1643 | -6022,5827 | -248,3144 | -6250,2707 | -264,8431 | -6157,3741 | -349,1945 | -6214,8062 |
| Mean unidirectional positioning deviation at a position | $\bar{x}_i$ | -42,6514 | -5991,1186 | -199,8072 | -6246,3376 | -238,3171 | -6137,0099 | -302,3479 | -6202,9198 |
| Estimator for the unidirectional axis positioning repeatability at a position | $s_i$ | 23,8792 | 20,1091 | 29,7039 | 41,4997 | 33,8567 | 12,5964 | 30,6489 | 23,5152 |
| | $3s_i$ | 71,6375 | 60,3274 | 89,1118 | 124,4991 | 101,5700 | 37,7892 | 91,9468 | 70,5455 |
| Unidirectional positioning repeatability at a position | $R_i = 6s_i$ | 143,2749 | 120,6548 | 178,2235 | 248,9983 | 203,1401 | 75,5784 | 183,8935 | 141,0910 |
| | $\bar{x}_i + 3s_i$ | 28,9861 | -5930,7912 | -110,6955 | -6121,8385 | -136,7471 | -6099,2207 | -210,4011 | -6132,3742 |
| | $\bar{x}_i - 3s_i$ | -114,2888 | -6051,4460 | -288,9190 | -6370,8368 | -339,8871 | -6174,7990 | -394,2947 | -6273,4653 |
| Reversal error at a position | $B_i$ | -5948,4672 | | -6046,5304 | | -5898,6928 | | -5900,5719 | |
| Variance of position | | 131,9649 | | 213,6109 | | 139,3592 | | 162,4923 | |
| | $3s_i\uparrow + 3s_i\downarrow + \lvert B_i \rvert$ | 6080,4321 | | 6260,1413 | | 6038,0520 | | 6063,0641 | |
| Bi-directional positioning repeatability at a position | | 6080,4321 | | 6260,1413 | | 6038,0520 | | 6063,0641 | |
| Mean bi-directional positioning | $\bar{x}_i$ | -3016,8850 | | -3223,0724 | | -3187,6635 | | -3252,6338 | |

| Deviations of an axis | Symbol | uni-directional ↓ | uni-directional ↑ | bi-directional | | |
|---|---|---|---|---|---|---|
| unidirectional positioning repeatability of an axis | R↑orR↓ | 203,1401 | 248,9983 | | | |
| bi-directional positioning repeatability of an axis | R | | | 248,9983 | | |
| unidirectional systematic positioning error of an axis | E↑orE↓ | 259,6965 | 255,2190 | | | |
| bi-directional systematic positioning error of an axis | E | | | 6203,6863 | | |
| mean bi-directional positioning error of an axis | M | | | 235,7488 | | |
| unidirectional positioning accuracy of an axis | A↑orA↓ | 423,2807 | 440,0456 | | | |
| bi-directional positioning accuracy of an axis | A | | | 6399,8229 | | |
| mean reversal error of an axis | mean_B | | | -5948,5656 | -1,6524 | arcsec and degree |
| reversal error of an axis | B | | | 5898,6928 | | |

**Table 4.2:** The measurement results of the manual rotary table obtained from the second measurement by the utilisation of the linear magnetic encoder AS5311

| Characteristic | Symbol | arcsec | | | | | | | |
|---|---|---|---|---|---|---|---|---|---|
| Number of measurement points | i | 1 | | 2 | | 3 | | 4 | |
| Target angular position (*degree*) | $P_i$ | 312,5 | | 312 | | 311,5 | | 311 | |
| Direction of rotation | ↓(ccw) or ↑(cw) | ↓ | ↑ | ↓ | ↑ | ↓ | ↑ | ↓ | ↑ |
| Positioning deviation $x_{ij}$ for the number of cycle (j) | j = 1 | 0,0000 | -5947,4184 | 17,7322 | -5963,5975 | -25,7158 | -5816,1632 | -157,9625 | -5818,7078 |
| | 2 | 109,0756 | -5885,8886 | 65,6276 | -5949,9631 | -73,6112 | -5857,0666 | -137,6856 | -5838,9847 |
| | 3 | 27,2689 | -5933,7840 | 17,7322 | -5997,8585 | 8,5452 | -5843,4321 | -151,3201 | -5838,9847 |
| | 4 | 61,5298 | -5920,1495 | 11,0898 | -5932,8326 | -73,6112 | -5850,0745 | -124,0512 | -5736,5515 |
| | 5 | -6,9920 | -5920,1495 | -9,5367 | -6004,5009 | -39,3502 | -5850,0745 | -76,1558 | -5866,6032 |
| | 6 | 88,7987 | -5940,4264 | 4,0978 | -5990,8665 | 1,5531 | -5809,1712 | -117,0592 | -5832,3423 |
| | 7 | 27,2689 | -5947,4184 | -16,1791 | -5970,5896 | -46,3423 | -5816,1632 | -103,4247 | -5852,9688 |
| | 8 | -6,9920 | -5954,0609 | -29,8136 | -5963,5975 | -32,7078 | -5877,3434 | -124,0512 | -5845,9768 |
| Mean unidirectional positioning deviation at a position | $\bar{x}_i$ | 37,4947 | -5931,1620 | 7,5938 | -5971,7258 | -35,1550 | -5839,9361 | -123,9638 | -5828,8900 |
| Estimator for the unidirectional axis positioning repeatability | $s_i$ | 44,5722 | 22,1612 | 28,9232 | 24,6206 | 30,3616 | 23,8667 | 26,3160 | 39,8924 |
| | $3s_i$ | 133,7165 | 66,4836 | 86,7696 | 73,8617 | 91,0848 | 71,6002 | 78,9480 | 119,6772 |
| Unidirectional positioning repeatability at a position | $R_i = 6s_i$ | 267,4330 | 132,9673 | 173,5392 | 147,7235 | 182,1696 | 143,2003 | 157,8959 | 239,3544 |
| | $\bar{x}_i + 3s_i$ | 171,2112 | -5864,6783 | 94,3634 | -5897,8640 | 55,9298 | -5768,3359 | -45,0158 | -5709,2128 |
| | $\bar{x}_i - 3s_i$ | -96,2218 | -5997,6456 | -79,1758 | -6045,5875 | -126,2398 | -5911,5363 | -202,9117 | -5948,5672 |
| Reversal error at a position | $B_i$ | -5968,6567 | | -5979,3196 | | -5804,7811 | | -5704,9262 | |
| Variance of position | | 200,2001 | | 160,6313 | | 162,6849 | | 198,6252 | |
| | $3s_i\uparrow + 3s_i\downarrow + \lvert B_i \rvert$ | 6168,8569 | | 6139,9509 | | 5967,4660 | | 5903,5514 | |
| Bi-directional positioning repeatability at a position | | 6168,8569 | | 6139,9509 | | 5967,4660 | | 5903,5514 | |
| Mean bi-directional positioning | $\bar{x}_i$ | -2946,8336 | | -2982,0660 | | -2937,5456 | | -2976,4269 | |

| Deviations of an axis | Symbol | uni-directional ↓ | uni-directional ↑ | bi-directional | | |
|---|---|---|---|---|---|---|
| Unidirectional positioning repeatability of an axis | R↑orR↓ | 267,4330 | 239,3544 | | | |
| Bi-directional positioning repeatability of an axis | R | | | 267,4330 | | |
| Unidirectional systematic positioning error of an axis | E↑orE↓ | 161,4585 | 142,8358 | | | |
| Bi-directional systematic positioning error of an axis | E | | | 6009,2205 | | |
| Mean bi-directional positioning error of an axis | M | | | 44,5204 | | |
| Unidirectional positioning accuracy of an axis | A↑orA↓ | 374,1230 | 336,3748 | | | |
| Bi-directional positioning accuracy of an axis | A | | | 6216,7988 | | |
| Mean reversal error of an axis | mean_B | | | -5864,4209 | -1,6290 | arcsec and degree |
| Reversal error of an axis | B | | | 5804,7811 | | |

SECOND MEASUREMENT The measurement results of the manual rotary table obtained from the second measurement by the utilisation of the second laser interferometer system were demonstrated as a statistics table (in agreement with the ISO 230-2:2014) in Table 4.4.

- The mean reversal error of the axis was calculated as 1.644°.

**Table 4.3:** The measurement results of the manual rotary table obtained from the first measurement by the utilisation of the first laser interferometer system

| Characteristic | Symbol | arcsec | | | | | | | |
|---|---|---|---|---|---|---|---|---|---|
| Number of measurement points | i | 1 | | 2 | | 3 | | 4 | |
| Target angular position (*degree*) | $P_i$ | 312,5 | | 312 | | 311,5 | | 311 | |
| Direction of rotation | ↓(ccw) or ↑(cw) | ↓ | ↑ | ↓ | ↑ | ↓ | ↑ | ↓ | ↑ |
| Positioning deviation $x_{ij}$ for the number of cycle (j) | j = 1 | 0 | -5874 | -186 | -5990 | -170 | -6043 | -246 | -5983 |
| | 2 | -32 | -5939 | -208 | -6086 | -203 | -6054 | -234 | -6006 |
| | 3 | -59 | -5902 | -176 | -6030 | -184 | -6049 | -172 | -5941 |
| | 4 | -58 | -5915 | -185 | -6111 | -237 | -6038 | -219 | -5999 |
| | 5 | -42 | -5855 | -206 | -6113 | -180 | -6061 | -256 | -5957 |
| | 6 | -64 | -5918 | -257 | -6085 | -210 | -6037 | -228 | -6002 |
| | 7 | -29 | -5927 | -200 | -6101 | -250 | -6035 | -206 | -6006 |
| | 8 | -73 | -5944 | -263 | -6082 | -228 | -6067 | -172 | -5941 |
| Mean unidirectional positioning deviation at a position | $\bar{x}_i$ | -44,625 | -5909,250 | -210,125 | -6074,750 | -207,750 | -6048,000 | -219,000 | -5999,000 |
| Estimator for the unidirectional axis positioning repeatability at a position | $s_i$ | 23,808 | 31,066 | 32,721 | 42,988 | 28,878 | 11,844 | 31,500 | 28,720 |
| | $3s_i$ | 71,425 | 93,197 | 98,164 | 128,963 | 86,633 | 35,533 | 94,501 | 86,160 |
| Unidirectional positioning repeatability at a position | $R_i = 6s_i$ | 142,850 | 186,394 | 196,329 | 257,925 | 173,267 | 71,065 | 189,002 | 172,320 |
| | $\bar{x}_i + 3s_i$ | 26,800 | -5816,053 | -111,961 | -5945,787 | -121,117 | -6012,467 | -124,499 | -5912,840 |
| | $\bar{x}_i - 3s_i$ | -116,050 | -6002,447 | -308,289 | -6203,713 | -294,383 | -6083,533 | -313,501 | -6085,160 |
| Reversal error at a position | $B_i$ | -5864,6250 | | -5864,6250 | | -5840,2500 | | -5780,0000 | |
| Variance of position | | 164,622 | | 227,127 | | 122,166 | | 180,661 | |
| | $3s_i\uparrow + 3s_i\downarrow + \lvert B_i \rvert$ | 6029,247 | | 6091,752 | | 5962,416 | | 5960,661 | |
| Bi-directional positioning repeatability at a position | | 6029,247 | | 6091,752 | | 5962,416 | | 5960,661 | |
| Mean bi-directional positioning | $\bar{x}_i$ | -2976,938 | | -3142,438 | | -3127,875 | | -3109,000 | |

| Deviations of an axis | Symbol | uni-directional ↓ | uni-directional ↑ | bi-directional | | |
|---|---|---|---|---|---|---|
| unidirectional positioning repeatability of an axis | R↑orR↓ | 196,329 | 257,925 | | | |
| bi-directional positioning repeatability of an axis | R | | | 257,925 | | |
| unidirectional systematic positioning error of an axis | E↑orE↓ | 174,375 | 165,500 | | | |
| bi-directional systematic positioning error of an axis | E | | | 6030,125 | | |
| mean bi-directional positioning error of an axis | M | | | 165,500 | | |
| unidirectional positioning accuracy of an axis | A↑orA↓ | 340,301 | 387,659 | | | |
| bi-directional positioning accuracy of an axis | A | | | 6230,513 | | |
| mean reversal error of an axis | mean_B | | | -5837,3750 | -1,6215 | arcsec and degree |
| reversal error of an axis | B | | | 5864,625 | | |

## 4.1.2 Measurement results for the high-precision CNC rotary table

### *4.1.2.1 Measurement results obtained through the CMM UMM 500*

The measurement results for the CNC rotary table obtained through the CMM UMM 500 were demonstrated as a statistics table (in agreement with the ISO 230-2:2014) in Table 4.5.

- The mean reversal error of the axis was calculated as 0.3437″.

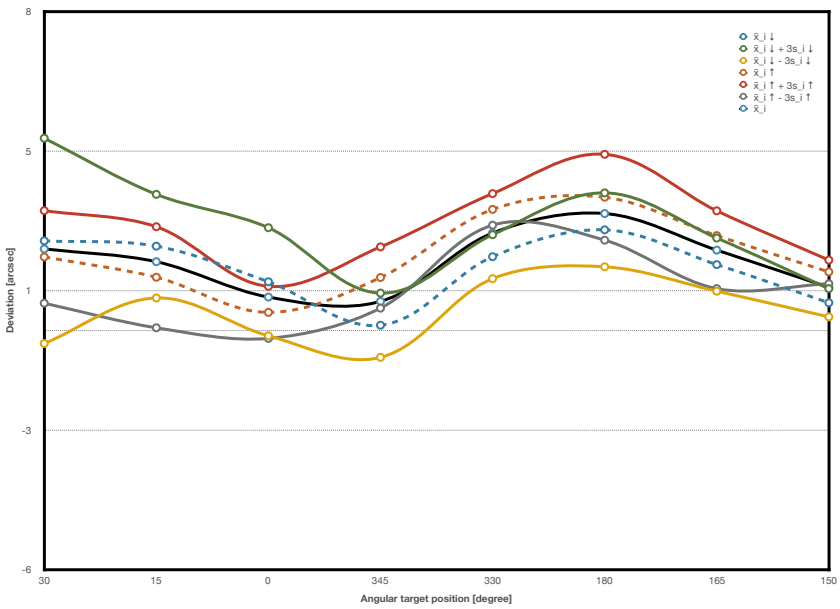


**Figure 4.1:** Graphical representation of the measurement results regarding CNC rotary table obtained by the CMM UMM 500

#### *4.1.2.2 Measurement results obtained through the Laser Interferometer System*

- Measurement results of the CNC rotary table obtained by the laser interferometer (with big beam setting) (30° to 28.5°) were demonstrated in Table 4.6.

  The mean reversal error of the axis was calculated as 0.1202″.

- Measurement results of the CNC rotary table obtained by the laser interferometer (with big beam setting) (30° to 31.5°) were demonstrated in Table 4.7.

  The mean reversal error of the axis was calculated as 0.1867″.

- Measurement results of the CNC rotary table obtained by the laser interferometer [with small beam setting] (210° to 208.5°) were demonstrated in Table 4.8.

  The mean reversal error of the axis was calculated as −0.3607″.

- Measurement results of the CNC rotary table obtained by the laser interferometer (with small beam setting) (210° to 211.5°) were demonstrated in Table 4.9.

  The mean reversal error of the axis was calculated as 0.1202″.

## 4.2 Evaluation and Discussion

After obtaining the results of various measurements regarding position deviations of manual and CNC rotary table, these were evaluated for the required characteristics by generating a statistics table (each time) in agreement with the ISO 230-2:2014.

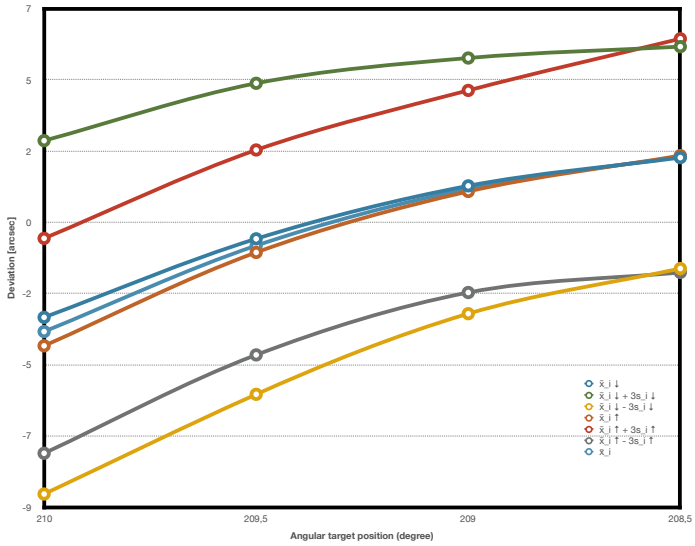


**Figure 4.2:** Graphical representation of the measurement results regarding CNC rotary table obtained by the laser interferometer system with small beam (210° to 208.5°)

In the sight of conducted experimental research and obtained measurement results as well as their comparison to each other, the qualitative interpretation of the measurements conducted can be made as follows,

Regarding the measurements conducted on the set-up with the manual rotary table;

- It was investigated whether and to what extent the linear magnetic encoder AS5311 is adequate and capable in sensing position and motion information in case of rotary off-axis applications.
- Measurement results and their statistical evaluation showed that there exist only minor and quite acceptable differences between linear magnetic encoder AS5311 and the laser angle interferometer.
- Given that the laser interferometer systems represent nowadays the high-end measurement solution, and are often used as reference and calibration systems, it can be said that AS5311 can provide relatively sharp, accurate and reliable values.

Regarding the measurements conducted on the set-up with the high-precision CNC rotary table;

- It was investigated whether and to what extent the measurement of reversal error of a CNC rotary table is possible by means of a CMM and a standard reference sphere.
- This was checked by measuring the same characteristics through a laser angle interferometer system (in the sequel of the measurements conducted by CMM), however, this time within a more limited measuring range.
- Measurement results obtained by both systems and their statistical evaluation showed that there exist also in that case only minor

and quite acceptable differences.

- Given that the laser interferometer systems represent nowadays the high-end measurement solution, and are often used as reference and calibration systems, it can be said that this measurement solution by means of a CMM and a reference test sphere is adequate and can be applied in order to obtain information regarding precision and accuracy characteristics, especially reversal error, of rotary tables.

**Table 4.4:** The measurement results of the manual rotary table obtained from the second measurement by the utilisation of the second laser interferometer system

| Characteristic | Symbol | arcsec | | | | | | | |
|---|---|---|---|---|---|---|---|---|---|
| Number of measurement points | i | 1 | | 2 | | 3 | | 4 | |
| Target angular position (*degree*) | $P_i$ | 312,5 | | 312 | | 311,5 | | 311 | |
| Direction of rotation | ↓(ccw) or ↑(cw) | ↓ | ↑ | ↓ | ↑ | ↓ | ↑ | ↓ | ↑ |
| Positioning deviation $x_{ij}$ for the number of cycle (j) | j = 1 | 0,0000 | 5948,0760 | 74,5021 | 6087,1287 | 94,8314 | 6026,5772 | 183,2912 | 5986,9910 |
| | 2 | 86,6206 | 5886,8217 | 40,9131 | 6077,8009 | 159,9281 | 6067,7630 | 173,9669 | 6005,9833 |
| | 3 | 3,5355 | 5936,5003 | 90,7341 | 6129,9079 | 77,1509 | 6055,2142 | 186,1850 | 6008,0756 |
| | 4 | 41,6229 | 5922,0308 | 94,5912 | 6052,3909 | 157,0349 | 6062,1321 | 156,6043 | 5907,1600 |
| | 5 | 32,6233 | 5924,1208 | 119,0195 | 6132,3203 | 122,9596 | 6059,2362 | 113,3588 | 6040,7491 |
| | 6 | 64,7646 | 5946,6290 | 102,7875 | 6119,6152 | 82,2944 | 6022,7161 | 152,4244 | 6001,6376 |
| | 7 | 5,6247 | 5948,2367 | 125,7695 | 6096,4565 | 129,7103 | 6027,2207 | 142,4570 | 6020,7909 |
| | 8 | 32,7840 | 5959,8124 | 136,2158 | 6087,6111 | 116,8517 | 6086,7472 | 157,4081 | 6013,7090 |
| Mean unidirectional positioning deviation at a position | $\bar{x}_i$ | 33,4470 | 5934,0285 | 98,0666 | 6097,9039 | 117,5952 | 6050,9508 | 158,2119 | 5998,1370 |
| Estimator for the unidirectional axis positioning repeatability at a position | $s_i$ | 30,8537 | 22,9891 | 30,6403 | 27,7227 | 31,4500 | 23,0845 | 23,7740 | 39,9019 |
| | $3s_i$ | 92,5611 | 68,9672 | 91,9208 | 83,1681 | 94,3501 | 69,2536 | 71,3221 | 119,7057 |
| Unidirectional positioning repeatability at a position | $R_i = 6s_i$ | 185,1223 | 137,9345 | 183,8416 | 166,3362 | 188,7003 | 138,5072 | 142,6442 | 239,4114 |
| | $\bar{x}_i + 3s_i$ | 126,0081 | 6002,9957 | 189,9874 | 6181,0720 | 211,9453 | 6120,2045 | 229,5340 | 6117,8427 |
| | $\bar{x}_i - 3s_i$ | -59,1142 | 5865,0612 | 6,1458 | 6014,7358 | 23,2450 | 5981,6972 | 86,8899 | 5878,4314 |
| Reversal error at a position | $B_i$ | 5900,5815 | | 5999,8373 | | 5933,3557 | | 5839,9251 | |
| Variance of position | | 161,528 | | 175,089 | | 163,604 | | 191,028 | |
| | $3s_i\uparrow + 3s_i\downarrow + \lvert B_i \rvert$ | 6062,110 | | 6174,926 | | 6096,959 | | 6030,953 | |
| Bi-directional positioning repeatability at a position | | 6062,110 | | 6174,926 | | 6096,959 | | 6030,953 | |
| Mean bi-directional positioning | $\bar{x}_i$ | 2983,7377 | | 3097,9853 | | 3084,2730 | | 3078,1745 | |
| | | | | | | | | | |
| Deviations of an axis | Symbol | uni-directional ↓ | | uni-directional ↑ | | bi-directional | | | |
| unidirectional positioning repeatability of an axis | R↑orR↓ | 188,7003 | | 239,4114 | | | | | |
| bi-directional positioning repeatability of an axis | R | | | | | 239,4114 | | | |
| unidirectional systematic positioning error of an axis | E↑orE↓ | 124,7650 | | 163,8755 | | | | | |
| bi-directional systematic positioning error of an axis | E | | | | | 6064,4570 | | | |
| mean bi-directional positioning error of an axis | M | 114,2475 | | | | | | | |
| unidirectional positioning accuracy of an axis | A↑orA↓ | 288,6482 | | 316,0108 | | | | | |
| bi-directional positioning accuracy of an axis | A | | | | | 6240,1862 | | | |
| mean reversal error of an axis (arcsec and degree) | mean_B | | | | | 5918,4249 | | 1,6440 | |
| reversal error of an axis | B | | | | | 5933,3557 | | | |

**Table 4.5:** Measurement results of the CNC rotary table obtained by the CMM UMM 500

| Characteristic | Symbol | arcsec | | | | | | | | | | | | | | | |
|---|---|---|---|---|---|---|---|---|---|---|---|---|---|---|---|---|---|
| Number of measurement points | i | 1 | | 2 | | 3 | | 4 | | 5 | | 6 | | 7 | | 8 | |
| Target angular position (*degree*) | $P_i$ | 30 | | 15 | | 0 | | 345 | | 330 | | 180 | | 165 | | 150 | |
| Direction of rotation | ↓(ccw) or ↑(cw) | ↓ | ↑ | ↓ | ↑ | ↓ | ↑ | ↓ | ↑ | ↓ | ↑ | ↓ | ↑ | ↓ | ↑ | ↓ | ↑ |
| Positioning deviation $x_{ij}$ for the number of cycle (j) | j = 1 | 0,8051 | 1,2692 | 1,4215 | 0,6490 | 0,5841 | 0,1669 | 0,4352 | 1,7114 | 2,0663 | 3,0474 | 2,0858 | 2,8366 | 1,5166 | 2,1251 | 0,5624 | 1,3296 |
| | 2 | 2,1505 | 1,7862 | 1,9608 | 1,2077 | 0,9178 | 0,3338 | 0,3548 | 1,2890 | 2,0022 | 3,1390 | 2,3361 | 3,0869 | 1,3803 | 2,2473 | 0,6376 | 1,5606 |
| | 3 | 2,5230 | 1,7862 | 2,3445 | 1,5608 | 1,4184 | 0,5006 | 0,1075 | 1,3836 | 1,7937 | 3,1055 | 2,5863 | 3,5041 | 1,6164 | 2,3806 | 0,7211 | 1,4161 |
| | 4 | 2,8120 | 2,0447 | 2,5002 | 1,5303 | 1,5019 | 0,5006 | -0,0564 | 1,0111 | 1,7408 | 3,0638 | 2,7532 | 3,6709 | 1,7802 | 2,6696 | 0,6600 | 1,4578 |
| | 5 | 2,9260 | 2,3144 | 2,3251 | 1,7053 | 1,6688 | 0,7509 | -0,2009 | 1,2279 | 1,6268 | 2,8053 | 2,8366 | 3,5875 | 1,9471 | 2,4529 | 0,8768 | 1,5606 |
| Mean unidirectional positioning deviation at a position | $\bar{x}_i$ | 2,2433 | 1,8402 | 2,1104 | 1,3306 | 1,2182 | 0,4506 | 0,1280 | 1,3246 | 1,8459 | 3,0322 | 2,5196 | 3,3372 | 1,6481 | 2,3751 | 0,6916 | 1,4649 |
| Estimator for the unidirectional axis positioning repeatability at a position | $s_i$ | 0,8580 | 0,3868 | 0,4330 | 0,4222 | 0,4516 | 0,2176 | 0,2685 | 0,2559 | 0,1836 | 0,1318 | 0,3088 | 0,3588 | 0,2219 | 0,2071 | 0,1181 | 0,0988 |
| | $3s_i$ | 2,5740 | 1,1604 | 1,2989 | 1,2666 | 1,3549 | 0,6527 | 0,8056 | 0,7677 | 0,5508 | 0,3955 | 0,9264 | 1,0765 | 0,6656 | 0,6214 | 0,3542 | 0,2964 |
| Unidirectional positioning repeatability at a position | $R_i = 6s_i$ | 5,1479 | 2,3209 | 2,5977 | 2,5331 | 2,7099 | 1,3054 | 1,6112 | 1,5354 | 1,1015 | 0,7909 | 1,8528 | 2,1530 | 1,3312 | 1,2428 | 0,7084 | 0,5927 |
| | $\bar{x}_i + 3s_i$ | 4,8173 | 3,0006 | 3,4093 | 2,5972 | 2,5731 | 1,1033 | 0,9336 | 2,0923 | 2,3967 | 3,4277 | 3,4460 | 4,4137 | 2,3137 | 2,9965 | 1,0458 | 1,7613 |
| | $\bar{x}_i - 3s_i$ | -0,3307 | 0,6797 | 0,8115 | 0,0641 | -0,1368 | -0,2022 | -0,6776 | 0,5569 | 1,2952 | 2,6368 | 1,5932 | 2,2607 | 0,9825 | 1,7537 | 0,3374 | 1,1686 |
| **Reversal error at a position** | $B_i$ | **-0,4032** | | **-0,7798** | | **-0,7676** | | **1,1966** | | **1,1863** | | **0,8176** | | **0,7270** | | **0,7733** | |
| Variance of position | | 3,7344 | | 2,5654 | | 2,0077 | | 1,5733 | | 0,9462 | | 2,0029 | | 1,2870 | | 0,6505 | |
| | $3s_i\uparrow + 3s_i\downarrow + \lvert B_i \rvert$ | 4,1376 | | 3,3452 | | 2,7753 | | 2,7699 | | 2,1325 | | 2,8205 | | 2,0140 | | 1,4239 | |
| Bi-directional positioning repeatability at a position | $R_i$ | 5,1479 | | 3,3452 | | 2,7753 | | 2,7699 | | 2,1325 | | 2,8205 | | 2,0140 | | 1,4239 | |
| Mean bi-directional positioning | $\bar{x}_i$ | 2,0417 | | 1,7205 | | 0,8344 | | 0,7263 | | 2,4391 | | 2,9284 | | 2,0116 | | 1,0782 | |

| Deviations of an axis | Symbol | uni-directional ↓ | uni-directional ↑ | bi-directional |
|---|---|---|---|---|
| Unidirectional positioning repeatability of an axis | R↑ or R↓ | 5,1479 | 2,5331 | |
| Bi-directional positioning repeatability of an axis | R | | | 5,1479 |
| Unidirectional systematic positioning error of an axis | E↑ or E↓ | 2,3916 | 2,8866 | |
| Bi-directional systematic positioning error of an axis | E | | | 3,2092 |
| Mean bi-directional positioning error of an axis | M | | | 2,2021 |
| Unidirectional positioning accuracy of an axis | A↑ or A↓ | 5,4949 | 4,6159 | |
| Bi-directional positioning accuracy of an axis | A | | | 5,4949 |
| **Mean reversal error of an axis** | **B_mean** | | | **0,343776** |
| **Reversal error of an axis** | **B** | | | **1,1966** |

**Table 4.6:** Measurement results of the CNC rotary table obtained by the laser interferometer with big beam (30° to 28.5°)

| Characteristic | Symbol | arcsec | | | | | | | |
|---|---|---|---|---|---|---|---|---|---|
| Number of measurement points | i | 1 | | 2 | | 3 | | 4 | |
| Target angular position (*degree*) | $P_i$ | 30 | | 29,5 | | 29 | | 28,5 | |
| Direction of rotation | ↓(ccw) or ↑(cw) | ↓ | ↑ | ↓ | ↑ | ↓ | ↑ | ↓ | ↑ |
| Positioning deviation xij for the number of cycle (j) | j = 1 | 0,0000 | -0,0633 | 0,1635 | 0,4167 | 0,4431 | 0,6330 | 0,2587 | 0,7652 |
| | 2 | -0,1899 | -0,0633 | 0,3534 | 0,2901 | 0,5697 | 0,6330 | 0,2587 | 0,7652 |
| | 3 | -0,1266 | -0,1899 | 0,2268 | 0,3534 | 0,4431 | 0,5697 | 0,3853 | 0,6386 |
| | 4 | -0,0633 | -0,3797 | 0,2901 | 0,2901 | 0,4431 | 0,5697 | 0,2587 | 0,6386 |
| | 5 | -0,0633 | -0,3165 | 0,3534 | 0,3534 | 0,4431 | 0,6330 | 0,3853 | 0,7019 |
| Mean unidirectional positioning deviation at a position | $\bar{x}_i$ | -0,0886 | -0,2025 | 0,2774 | 0,3407 | 0,4684 | 0,6077 | 0,3093 | 0,7019 |
| Estimator for the unidirectional axis positioning repeatability at a position | $s_i$ | 0,0722 | 0,1443 | 0,0825 | 0,0530 | 0,0566 | 0,0347 | 0,0694 | 0,0633 |
| | $3s_i$ | 0,2165 | 0,4330 | 0,2476 | 0,1589 | 0,1699 | 0,1040 | 0,2081 | 0,1899 |
| Unidirectional positioning repeatability at a position | $R_i = 6s_i$ | 0,4330 | 0,8660 | 0,4951 | 0,3177 | 0,3397 | 0,2080 | 0,4161 | 0,3799 |
| | $\bar{x}_i + 3s_i$ | 0,1279 | 0,2304 | 0,5250 | 0,4996 | 0,6383 | 0,7117 | 0,5174 | 0,8918 |
| | $\bar{x}_i - 3s_i$ | -0,3051 | -0,6355 | 0,0298 | 0,1818 | 0,2986 | 0,5037 | 0,1013 | 0,5119 |
| Reversal error at a position | $B_i$ | -0,1139 | | 0,0633 | | 0,1393 | | 0,3925 | |
| Variance of position | | 0,6495 | | 0,4064 | | 0,2739 | | 0,3980 | |
| | $3s_i\uparrow + 3s_i\downarrow + \lvert B_i \rvert$ | 0,7634 | | 0,4697 | | 0,4131 | | 0,7905 | |
| Bi-directional positioning repeatability at a position | | 0,8660 | | 0,4951 | | 0,4131 | | 0,7905 | |
| Mean bi-directional positioning | $\bar{x}_i$ | -0,1456 | | 0,3091 | | 0,5381 | | 0,5056 | |

| Deviations of an axis | Symbol | uni-directional ↓ | uni-directional ↑ | bi-directional | | |
|---|---|---|---|---|---|---|
| Unidirectional positioning repeatability of an axis | R↑ or R↓ | 0,4951 | 0,8660 | | | |
| Bi-directional positioning repeatability of an axis | R | | | 0,8660 | | |
| Unidirectional systematic positioning error of an axis | E↑ or E↓ | 0,5570 | 0,9044 | | | |
| Bi-directional systematic positioning error of an axis | E | | | 0,9044 | | |
| Mean bi-directional positioning error of an axis | M | | | 0,6836 | | |
| Unidirectional positioning accuracy of an axis | A↑ or A↓ | 0,9434 | 1,5273 | | | |
| Bi-directional positioning accuracy of an axis | A | | | 1,5273 | | |
| Mean reversal error of an axis | B_mean | | | 0,120293 | 0,000033 | arcsec and degree |
| Reversal error of an axis | B | | | 0,3925 | | |

**Table 4.7**: Measurement results of the CNC rotary table obtained by the laser interferometer with big beam (30° to 31.5°)

| Characteristic | Symbol | arcsec | | | | | | | |
|---|---|---|---|---|---|---|---|---|---|
| Number of measurement points | i | 1 | | 2 | | 3 | | 4 | |
| Target angular position (*degree*) | $P_i$ | 30 | | 30,5 | | 31 | | 31,5 | |
| Direction of rotation | ↓(ccw) or ↑(cw) | ↓ | ↑ | ↓ | ↑ | ↓ | ↑ | ↓ | ↑ |
| Positioning deviation xij for the number of cycle (j) | j = 1 | 0,8861 | 0,0000 | 0,5327 | 0,8492 | -0,0633 | -0,0000 | -0,8918 | -0,8918 |
| | 2 | 1,0760 | 1,2658 | 0,5960 | 1,0391 | -0,0633 | 0,1266 | -0,8285 | -0,7652 |
| | 3 | 1,0760 | 1,5823 | 0,6593 | 0,9125 | 0,0633 | 0,1899 | -0,8918 | -0,7019 |
| | 4 | 1,0760 | 1,4557 | 0,6593 | 1,0391 | 0,0633 | 0,2532 | -0,8918 | -0,5752 |
| | 5 | 1,0760 | 1,5823 | 0,6593 | 0,9125 | 0,1266 | 0,2532 | -0,8285 | -0,7019 |
| Mean unidirectional positioning deviation at a position | $\bar{x}_i$ | 1,0380 | 1,1772 | 0,6214 | 0,9505 | 0,0253 | 0,1646 | -0,8665 | -0,7272 |
| Estimator for the unidirectional axis positioning repeatability at a position | $s_i$ | 0,0849 | 0,6707 | 0,0566 | 0,0849 | 0,0849 | 0,1059 | 0,0347 | 0,1150 |
| | $3s_i$ | 0,2547 | 2,0121 | 0,1698 | 0,2548 | 0,2548 | 0,3178 | 0,1040 | 0,3450 |
| Unidirectional positioning repeatability at a position | $R_i = 6s_i$ | 0,5095 | 4,0242 | 0,3397 | 0,5095 | 0,5096 | 0,6355 | 0,2081 | 0,6901 |
| | $\bar{x}_i + 3s_i$ | 1,2927 | 3,1893 | 0,7912 | 1,2052 | 0,2801 | 0,4824 | -0,7624 | -0,3822 |
| | $\bar{x}_i - 3s_i$ | 0,7832 | -0,8349 | 0,4515 | 0,6957 | -0,2295 | -0,1532 | -0,9705 | -1,0722 |
| Reversal error at a position | $B_i$ | 0,1392 | | 0,3291 | | 0,1393 | | 0,1393 | |
| Variance of position | | 2,2669 | | 0,4246 | | 0,5725 | | 0,4491 | |
| | $3s_i\uparrow + 3s_i\downarrow + \lvert B_i \rvert$ | 2,4061 | | 0,7537 | | 0,7118 | | 0,5884 | |
| Bi-directional positioning repeatability at a position | | 4,0242 | | 0,7537 | | 0,7118 | | 0,6901 | |
| Mean bi-directional positioning | $\bar{x}_i$ | 1,1076 | | 0,7859 | | 0,0950 | | -0,7968 | |

| Deviations of an axis | Symbol | uni-directional ↓ | uni-directional ↑ | bi-directional | | |
|---|---|---|---|---|---|---|
| Unidirectional positioning repeatability of an axis | R↑orR↓ | 0,5096 | 4,0242 | | | |
| Bi-directional positioning repeatability of an axis | R | | | 4,0242 | | |
| Unidirectional systematic positioning error of an axis | E↑orE↓ | 1,9045 | 1,9044 | | | |
| Bi-directional systematic positioning error of an axis | E | | | 2,0437 | | |
| Mean bi-directional positioning error of an axis | M | | | 1,9044 | | |
| Unidirectional positioning accuracy of an axis | A↑orA↓ | 2,2632 | 4,2616 | | | |
| Bi-directional positioning accuracy of an axis | A | | | 4,2616 | | |
| Mean reversal error of an axis | B_mean | | | 0,186730 | 0,000052 | arcsec and degree |
| Reversal error of an axis | B | | | 0,3291 | | |

**Table 4.8:** Measurement results of the CNC rotary table obtained by the laser interferometer with small beam (210° to 208.5°)

| Characteristic | Symbol | arcsec | | | | | | | |
|---|---|---|---|---|---|---|---|---|---|
| Number of measurement points | i | 1 | | 2 | | 3 | | 4 | |
| Target angular position (*degree*) | $P_i$ | 210 | | 209,5 | | 209 | | 208,5 | |
| Direction of rotation | ↓(ccw) or ↑(cw) | ↓ | ↑ | ↓ | ↑ | ↓ | ↑ | ↓ | ↑ |
| Positioning deviation xij for the number of cycle (j) | j = 1 | 0,0000 | -2,3418 | 2,0623 | 0,5432 | 3,2283 | 2,4687 | 3,6776 | 3,8042 |
| | 2 | -2,5949 | -3,1646 | -0,0264 | -0,4062 | 1,6458 | 1,5825 | 2,7912 | 2,7912 |
| | 3 | -3,4810 | -4,1772 | -0,9758 | -0,9758 | 0,6963 | 0,7596 | 1,6516 | 1,9048 |
| | 4 | -4,1772 | -4,7468 | -1,5454 | -1,7353 | 0,4431 | 0,2532 | 1,2717 | 1,3983 |
| | 5 | -4,7468 | -5,0633 | -2,1151 | -2,1784 | -0,2532 | -0,1899 | 0,8285 | 0,6386 |
| Mean unidirectional positioning deviation at a position | $\bar{x}_i$ | -3,0000 | -3,8987 | -0,5201 | -0,9505 | 1,1521 | 0,9748 | 2,0441 | 2,1074 |
| Estimator for the unidirectional axis positioning repeatability at a position | $s_i$ | 1,8596 | 1,1309 | 1,6367 | 1,0784 | 1,3453 | 1,0636 | 1,1678 | 1,2296 |
| | $3s_i$ | 5,5789 | 3,3928 | 4,9102 | 3,2352 | 4,0360 | 3,1907 | 3,5033 | 3,6889 |
| Unidirectional positioning repeatability at a position | $R_i = 6s_i$ | 11,1577 | 6,7857 | 9,8204 | 6,4705 | 8,0721 | 6,3814 | 7,0067 | 7,3778 |
| | $\bar{x}_i + 3s_i$ | 2,5789 | -0,5059 | 4,3901 | 2,2847 | 5,1881 | 4,1655 | 5,5474 | 5,7963 |
| | $\bar{x}_i - 3s_i$ | -8,5789 | -7,2916 | -5,4303 | -4,1857 | -2,8840 | -2,2159 | -1,4592 | -1,5815 |
| Reversal error at a position | $B_i$ | -0,8987 | | -0,4304 | | -0,1772 | | 0,0633 | |
| Variance of position | | 8,9717 | | 8,1454 | | 7,2268 | | 7,1923 | |
| | $3s_i\uparrow + 3s_i\downarrow + \lvert B_i \rvert$ | 9,8705 | | 8,5758 | | 7,4040 | | 7,2556 | |
| Bi-directional positioning repeatability at a position | | 11,1577 | | 9,8204 | | 8,0721 | | 7,3778 | |
| Mean bi-directional positioning | $\bar{x}_i$ | -3,4494 | | -0,7353 | | 1,0635 | | 2,0758 | |
| | | | | | | | | | |
| **Deviations of an axis** | **Symbol** | **uni-directional ↓** | | **uni-directional ↑** | | **bi-directional** | | | |
| Unidirectional positioning repeatability of an axis | R↑ or R↓ | 11,1577 | | 7,3778 | | | | | |
| Bi-directional positioning repeatability of an axis | R | | | | | 11,1577 | | | |
| Unidirectional systematic positioning error of an axis | E↑ or E↓ | 5,0441 | | 6,0062 | | | | | |
| Bi-directional systematic positioning error of an axis | E | | | | | 6,0062 | | | |
| Mean bi-directional positioning error of an axis | M | | | | | 5,5251 | | | |
| Unidirectional positioning accuracy of an axis | A↑ or A↓ | 14,1263 | | 13,0879 | | | | | |
| Bi-directional positioning accuracy of an axis | A | | | | | 14,3752 | | | |
| Mean reversal error of an axis | B_mean | | | | | -0,360766 | -0,000100 | arcsec and degree | |
| Reversal error of an axis | B | | | | | 0,8987 | | | |

**Table 4.9:** Measurement results of the CNC rotary table obtained by the laser interferometer with small beam (210° to 211.5°)

| Characteristic | Symbol | arcsec | | | | | | | |
|---|---|---|---|---|---|---|---|---|---|
| Number of measurement points | i | 1 | | 2 | | 3 | | 4 | |
| Target angular position (*degree*) | $P_i$ | 210 | | 210,5 | | 211 | | 211,5 | |
| Direction of rotation | ↓(ccw) or ↑(cw) | ↓ | ↑ | ↓ | ↑ | ↓ | ↑ | ↓ | ↑ |
| Positioning deviation xij for the number of cycle (j) | j = 1 | 0,0633 | 0,0000 | -3,4548 | -2,8851 | -7,6594 | -7,2796 | -12,7313 | -12,6680 |
| | 2 | 0,4430 | 0,2532 | -3,8345 | -3,3915 | -8,2291 | -7,7227 | -13,3644 | -13,1112 |
| | 3 | 0,7595 | 0,2532 | -4,3409 | -3,7712 | -8,4823 | -8,2924 | -13,6177 | -13,6177 |
| | 4 | 1,2658 | 0,5696 | -4,7839 | -4,4675 | -9,0520 | -8,6722 | -14,1242 | -13,8710 |
| | 5 | 1,5823 | 0,8861 | -5,0371 | -4,6573 | -9,1786 | -9,0520 | -14,2508 | -14,1242 |
| Mean unidirectional positioning deviation at a position | $\bar{x}_i$ | 0,8228 | 0,3924 | -4,2902 | -3,8345 | -8,5203 | -8,2038 | -13,6177 | -13,4784 |
| Estimator for the unidirectional axis positioning repeatability at a position | $s_i$ | 0,6120 | 0,3420 | 0,6538 | 0,7381 | 0,6212 | 0,7128 | 0,6138 | 0,5878 |
| | $3s_i$ | 1,8360 | 1,0260 | 1,9614 | 2,2144 | 1,8636 | 2,1384 | 1,8415 | 1,7635 |
| Unidirectional positioning repeatability at a position | $R_i = 6s_i$ | 3,6720 | 2,0520 | 3,9228 | 4,4287 | 3,7271 | 4,2768 | 3,6830 | 3,5269 |
| | $\bar{x}_i + 3s_i$ | 2,6588 | 1,4184 | -2,3288 | -1,6201 | -6,6567 | -6,0654 | -11,7762 | -11,7149 |
| | $\bar{x}_i - 3s_i$ | -1,0132 | -0,6336 | -6,2516 | -6,0489 | -10,3839 | -10,3422 | -15,4592 | -15,2419 |
| Reversal error at a position | $B_i$ | -0,4304 | | 0,4557 | | 0,3165 | | 0,1393 | |
| Variance of position | | 2,8620 | | 4,1758 | | 4,0020 | | 3,6050 | |
| | $3s_i\uparrow + 3s_i\downarrow + \lvert B_i \rvert$ | 3,2924 | | 4,6315 | | 4,3185 | | 3,7443 | |
| Bi-directional positioning repeatability at a position | | 3,6720 | | 4,6315 | | 4,3185 | | 3,7443 | |
| Mean bi-directional positioning | $\bar{x}_i$ | 0,6076 | | -4,0624 | | -8,3620 | | -13,5481 | |

| Deviations of an axis | Symbol | uni-directional ↓ | uni-directional ↑ | bi-directional | | |
|---|---|---|---|---|---|---|
| Unidirectional positioning repeatability of an axis | R↑ or R↓ | 3,9228 | 4,4287 | | | |
| Bi-directional positioning repeatability of an axis | R | | | 4,4287 | | |
| Unidirectional systematic positioning error of an axis | E↑ or E↓ | 14,4405 | 13,8708 | | | |
| Bi-directional systematic positioning error of an axis | E | | | 14,4405 | | |
| Mean bi-directional positioning error of an axis | M | | | 14,1557 | | |
| Unidirectional positioning accuracy of an axis | A↑ or A↓ | 18,1180 | 16,6603 | | | |
| Bi-directional positioning accuracy of an axis | A | | | 18,1180 | | |
| Mean reversal error of an axis | B_mean | | | 0,120282 | 0,000033 | arcsec and degree |
| Reversal error of an axis | B | | | 0,4557 | | |

# 5

# CONCLUSION AND FUTURE WORK

*"Measure everything that can be measured, and make everything measurable that cannot be measured."*

Archimedes (Greek physicist, mathematician and mechanic, 287 - 212 BC)

This chapter summarises the thesis work and provides readers with a discussion on open issues related to this subject which should be dealt with in the framework of future research.

## 5.1 Conclusion

As already mentioned, rotary tables have established themselves as useful accesories in modern production metrology. They provide several advantages both for production and for metrology purposes. However, a special attention should be paid when working with additional equipments, since they also contribute to the total system error and uncertainty.

Hence, the task area of modern production metrology does not only cover the applications of rotary tables as useful accessories, but it also investigates their accuracy characteristics. In addition to the need for the methods and special designs aiming to reduce or eliminate the possible errors, their metrological and statistical evaluation is very important as well. The added-value that modern production metrology can create here is much more than so far thought.

In the context of precision metrology, automation, robotics and biomedical applications, measurement of characteristics related to the positioning capability becomes a challenging task. In line with these challenges, the utilisation of different measurement instruments and methods were realised, and their capability in these tasks was investigated in this research.

The main objectives of this thesis can be broken down into two categories. In the theoretical part it was aimed to provide readers with a solid background on the modern production metrology. This was realised by describing;

- The ongoing and upcoming challenges and trends of modern production metrology,
- The various measurement instruments of coordinate metrology,

- The rotary tables and their utilisation in the context of modern production metrology,
- The importance of the positioning accuracy characteristics, in particular of the reversal error, and
- Cost-efficient reduction or elimination of, and measurement methods for the reversal error.

On the other hand, the main objectives of the practical part was to investigate the adequacy and practical capability of a cost-efficient linear magnetic encoder in measuring positioning accuracy characteristics in rotary off-axis applications. This was realised by;

- Measuring the positioning accuracy characteristics of a manual rotary table simultaneously both by a cost-efficient linear magnetic encoder and by a laser angle interferometer, and
- Comparison and statistical evaluation of measurement results.

In addition, positioning accuracy characteristics of a CNC rotary table of a CMM were evaluated, first by CMM itself, then by a laser angle interferometer. The obtained results are compared each other and evaluated statistically in accordance with ISO 230-2:2014.

Results showed that the linear magnetic encoder is capable to measure reversal error with sufficient accuracy and precision. Therefore it can be assumed that it is an adequate measurement instrument for off-axis rotary applications, although it is originally a *linear* encoder.

Due to the verification by means of the laser interferometer system, it can be concluded that this measurement method by means of a CMM and a reference test sphere is adequate for the purpose, and can be applied in order to obtain information regarding precision and accuracy characteristics, especially reversal error, of rotary tables.

## 5.2 Future Work

Future research should concentrate on the utilisation of similar possible cost-efficient measurement instruments for the evaluation of positioning accuracy characteristics, e.g. reversal error, in applications where these factors are of great importance, e.g. robotics, precision metrology and gearbox mechanisms of wearable exoskeletons. Application of such cost-efficient and robust alternative measurement instruments will definitely trigger the technological developments in these specific areas, just as the advances like Industry 4.0 shape and trigger the modern production metrology in return.

# BIBLIOGRAPHY


[1] F. Corporation. (4th Sep. 2015). Opak project develops industry 4.0 prototype stopper module – the first outcome of the project, [Online]. Available: http://www.prweb.com/releases/2015/08/prweb12886832.htm (visited on 21/11/2015) (cit. on p. 1).

[2] D. Imkamp, A. Gabbia and J. Berthold, 'Challenges and trends in manufacturing metrology-vdi/vde roadmap', in *Internationales Wissenschaftliches Kolloquium : IWK (Technische Universität Ilmenau) » 58. IWK (2014)*, 2014. [Online]. Available: http://www.db-thueringen.de/servlets/DerivateServlet/Derivate-30617/ilm1-2014iwk-104.pdf (cit. on pp. 4, 7, 11, 13, 15).

[3] M. B. Bauza and D. Imkamp, 'The future of manufacturing metrology – a roadmap from the association of german engineers', presented at the Technical Sessions at the 28th ASPE Annual Meeting. [Online]. Available: http://www.aspe.net/publications/Short%20Abstracts%2013A/3772.pdf (cit. on p. 8).

[4] T. Pfeifer, *Production metrology*. München ; Wien: Oldenbourg, 2002, Dt. Ausg. u.d.T. Pfeifer, Tilo: Fertigungsmeßtechnik, ISBN: 3-486-25885-0 (cit. on p. 8).

[5] Wikipedia, *Fertigungsmesstechnik — wikipedia, die freie enzyklopädie*, 2015. [Online]. Available: https://de.wikipedia.org/w/index.php?title=Fertigungsmesstechnik&oldid=145930605 (visited on 12/11/2015) (cit. on p. 8).

[6] I. Metrology. (). Production metrology, [Online]. Available: http://www.imts.ch/en/measuring/ (cit. on p. 8).

[7] D. Haraway. (). Cyborg manifesto, [Online]. Available: http://people.emich.edu/acoykenda/cyborg1.htm (cit. on p. 9).

[8] C. P. Keferstein and M. Marxer, *Fertigungsmesstechnik; Praxisorientierte Grundlagen, moderne Messverfahren*, 8., vollst. überarb. u. erw. Aufl. 2015. Wiesbaden: Springer Fachmedien Wiesbaden, 2015, ISBN: 978-3-8348-2583-4 (cit. on pp. 9, 10, 16–18, 27, 28, 30–40).

[9] D. Imkamp and D. Frankenfeld, 'Schnittstellen zur informationstechnischen integration von geräten der fertigungsmesstechnik in die automatisierte produktion', *Tagungsband zur Automation 2009, Baden-Baden, VDI Verlag Düsseldorf*, 16.-17. Juni 2009 (cit. on p. 11).

[10] M Scheffler, *Zukunftsweisend, preisgekrönte 3d-inline-messtechnik in der automobilfertigung*, INSPECT, pp. 69-71, 2007 (cit. on p. 12).

[11] (21st Nov. 2014), [Online]. Available: http://www.automotivemanufacturingsolutions.com/wp-content/uploads/2014/11/Hexagons-360Âř-SIMS-feature-industrial-robots-as-flexible-sensor-positioning-platforms-Copy.jpg (cit. on p. 12).

[12] B. Brinkmann and D. V, *Internationales Wörterbuch der Metrologie: Grundlegende und allgemeine Begriffe und zugeordnete Benennungen (VIM) Deutsch-englische Fassung ISO/IEC-Leitfaden 99:2007*, ser. Beuth Wissen. Beuth Verlag GmbH, 2012, ISBN: 9783410224730. [Online]. Available: https://books.google.at/books?id=7HZXXByoiGQC (cit. on pp. 12, 65–67).

[13] W. K. Wiedmann, D. Imkamp and F Bader, *4. Fachtagung Metrologie in der Mikro- und Nanotechnik 2011; Messprinzipien - Messgeräte - Anwendungen ; Erlangen, 25. und 26. Oktober 2011; Metrologie in der Mikro- und Nanotechnik 2011; Vierte Fachtagung Metrologie in der Mikro- und Nanotechnik 2011*, ser. VDI-Berichte ; 2133. Düsseldorf: VDI-Verl., 2011, Nebent. Metrologie in der Mikro- und Nanotechnik 2011; Beitr. teilw. dt., teilw. engl., ISBN: 978-3-18-092133-4 (cit. on p. 13).

[14] R. Schmitt, P. Jatzkowski, S. Nisch and D Imkamp, 'Größer, genauer und integrierter – roadmap fertigungsmesstechnik 2020 (teil 5)', *QZ Qualität und Zuverlässigkeit*, vol. 54, no. 9, pp. 31–33, 2009 (cit. on p. 13).

[15] J. Berthold and D. Imkamp, 'Looking at the future of manufacturing metrology: roadmap document of the german vdi/vde society for measurement and automatic control', *Journal of Sensors and Sensor Systems*, vol. 2, no. 1, pp. 1–7, 2013. DOI: 10.5194/jsss-2-1-2013. [Online]. Available: http://www.j-sens-sens-syst.net/2/1/2013/ (cit. on pp. 13, 14).

[16] W. Estler, K. Edmundson, G. Peggs and D. Parker, 'Large-scale metrology – an update', *CIRP Annals - Manufacturing Technology, 2002, Vol.51(2), pp.587-609*, ISSN: 0007-8506 (cit. on p. 13).

[17] H. Bosse, L. Koenders and R. Schmitt, 'Von mikro zu nano - roadmap fertigungsmesstechnik 2020 (teil 3)', *QZ Qualität und Zuverlässigkeit*, vol. 54, no. 7, pp. 28–31, 2009 (cit. on p. 13).

[18] H. "Frenz and E. Schenuit, 'Sinkende toleranzschwelle - roadmap fertigungsmesstechnik 2020 (teil 7)', "*QZ Qualität und Zuverlässigkeit* , vol. "54", no. "11", "47–49", "2009" (cit. on p. 13).

[19] M. Naß and J. Berthold, 'Basis neuer messtechnologien - roadmap fertigungsmesstechnik 2020 (teil 8)', *QZ Qualität und Zuverlässigkeit*, vol. 55, no. 1, pp. 53–55, 2010 (cit. on p. 13).

[20] D. Imkamp and K.-D. Sommer, 'Für eine sichere fertigung, roadmap fertigungsmesstechnik 2020 (teil 4)', *QZ Qualität und Zuverlässigkeit*, vol. 54, no. 8, pp. 31–33, 2009 (cit. on p. 14).

[21] JCGM, 'Evaluation of measurement data — supplement 1 to the "guide to the expression of uncertainty in measurement" — propagation of distributions using a monte carlo method', Joint Committee for Guides in Metrology (JCGM), Tech. Rep., 2008. [Online]. Available: http://www.bipm.org/utils/common/documents/jcgm/JCGM_101_2008_E.pdf (cit. on p. 14).

[22] F. Wäldele and H. Schwenke, 'Automatische bestimmung der messunsicherheiten auf kmgs auf dem weg in die industrielle praxis (automated calculation of measurement uncertainties on cmms – towards industrial application)', *Tm - Technisches Messen, 01/2002, Vol.69(12/2002)*, ISSN: 0171-8096 (cit. on p. 14).

[23] D. Berndt, N. Bauer and F.-A. Vision, *Leitfaden zu Grundlagen und Anwendungen der optischen 3-D-Messtechnik*. Fraunhofer-IRB-Verlag, 2003, ISBN: 9783816762973. [Online]. Available: https://books.google.at/books?id=W4XKLttZ8igC (cit. on p. 14).

[24] J. Kruth, M. Bartscher, S. Carmignato, R. Schmitt, L. De Chiffre and A. Weckenmann, 'Computed tomography for dimensional metrology', *CIRP Annals - Manufacturing Technology, 2011, Vol.60(2), pp.821-842*, ISSN: 0007-8506 (cit. on p. 14).

[25] H. Schnell, 'Hochgeschwindigkeits-computertomografie zur schnellen, zerstörungsfreien und intelligenten inspektion und prozessoptimierung von aluminium-gussteilen', PhD thesis, 2011 (cit. on p. 14).

[26] A. Weckenmann, *Koordinatenmesstechnik: Flexible Strategien für funktions- und fertigungsgerechtes Prüfen*. München: Hanser Verlag, 2012, ISBN: 9783446429475 (cit. on pp. 16, 42, 55, 56).

[27] 'Geometrical product specifications (gps) - acceptance and reverification tests for coordinate measuring machines (cmm) - part 1: vocabulary', International Organization for Standardization, Geneva, CH, Standard, Mar. 2000 (cit. on pp. 17, 18).

[28] N. V. Gestel, 'Determining measurement uncertainties of feature measurements on cmms', PhD thesis, KU Leuven, 2011 (cit. on pp. 19, 21, 22).

[29] R. Hocken and P. Pereira, *Coordinate Measuring Machines and Systems, Second Edition*, ser. Manufacturing Engineering and Materials Processing. CRC Press, 2011, ISBN: 9781420017533. [Online]. Available: https://books.google.at/books?id=TGzLBQAAQBAJ (cit. on pp. 19, 21, 27, 56–61).

[30] N. M. Durakbasa and P. H. Osanna, *Quality in industry*, 4. ed. Wien: Techn. Univ., Abt. Austauschbau u. Messtechnik, 2009, ISBN: 3-901888-23-3 (cit. on pp. 20, 24, 29).

[31] 'Geometrical product specifications (gps) – acceptance and reverification tests for coordinate measuring machines (cmm) – part 1: vocabulary (iso 10360-1:2000 + cor.1:2002)', International Organization for Standardization, Geneva, CH, Standard, Nov. 2000 (cit. on p. 25).

[32] (), [Online]. Available: {https://faro.blob.core.windows.net/sitefinity/application-video-thumbs/mÃijrdter_2.png?sfvrsn=0} (cit. on p. 28).

[33] *Measurement technologies in quality control purposes*, Teaching Manual, version 1.0, Creaform Inc., Creaform Inc. [Online]. Available: http://www.creaform3d.com/sites/default/files/assets/technological-fundamentals/teaching_manual_quality_en_24032014.pdf (cit. on pp. 28, 40, 41).

[34] R. Noll, *Lasermesstechnik reagiert besonders schnell; 1. Aufl.* Ser. Praxis-Profiline. Würzburg: Vogel Industrie Medien, 2006, pp. 15–17, ISBN: 3-8259-1941-2. [Online]. Available: http://publications.rwth-aachen.de/record/89403 (cit. on p. 32).

[35] K. Kraus, *Geometrische Informationen aus Photographien und Laserscanneraufnahmen; Photogrammetrie*, 8., vollst. bearb. u. erw. Aufl., ser. de Gruyter Lehrbuch. Berlin [u.a.]: de Gruyter, 2014, Aufl. bis 2000 im Dümmler Verlag ersch., ISBN: 3-11-017708-0; 978-3110-1770-84 (cit. on p. 33).

[36] T. Yoshizawa, *Handbook of optical metrology*, 2009 (cit. on p. 35).

[37] B. Packroß, 'Interferometric flatness measurement of non-reflective surfaces', *Photonik*, [Online]. Available: http://www.photonik.de/interferometric-flatness-measurement-of-non-reflective-surfaces/150/21420/282041 (cit. on p. 38).

[38] R. Mautz, *Indoor positioning technologies*, ser. Geodätisch-geophysikalische Arbeiten in der Schweiz ; 86. Zürich, 2012, ISBN: 978-3-908440-31-4 (cit. on p. 40).

[39] R. Christoph and H. J. Neumann, *Multisensor-Koordinatenmesstechnik (Die Bibliothek der Technik (BT))*. Süddeutscher Verlag onpact, 2013, ISBN: 9783862360505. [Online]. Available: http://amazon.de/o/ASIN/3862360504/ (visited on 20/11/2015) (cit. on p. 41).

[40] R. Christoph and H. Neumann, *Multisensor Coordinate Metrology: Measurement of Form, Size, and Location in Production and Quality Control*. Verlag Moderne Industrie, 2004, ISBN: 9783937889030 (cit. on p. 41).

[41] T. Wiedenhöfer, 'Multisensor-koordinatenmesstechnik zur erfassung dimensioneller messgrößen', *Tm - Technisches Messen, 01/2011, Vol.78(3)*, ISSN: 0171-8096 (cit. on p. 43).

[42] (), [Online]. Available: http://www.exactmetrology.com/uploads/images/ct_scanning_main.jpg (cit. on p. 44).

[43] R. Schmitt and C. Niggemann, *Improving the production using x-ray computed tomography - potentials and challenges*, Slides of a talk presented at the National conference on CT scanning - Application of CT Scanning in Industry, May 31, 2011, Danish Technological Institute Taastrup, 2011 (cit. on p. 45).

[44] R. Christoph and H. J. Neumann, *X-ray tomography in industrial metrology precise, economical and universal*. Landsberg/Lech: Verl. Moderne Industrie, 2011, ISBN: 978-3-86236-020-8 (cit. on p. 45).

[45] A. Cantatore and P. Müller, *Introduction to computed tomography*. DTU Mechanical Engineering, 2011 (cit. on pp. 46, 47).

[46] K. de Schlepper. (). A brief bistory of ct technology and a short comparison between medical and industrial ct, [Online]. Available: https://gtms1313.wordpress.com/2013/01/30/a-brief-history-of-ct-technology-and-a-short-comparison-between-medical-and-industrial-ct (cit. on p. 46).

[47] C. Heinzl, *Analysis and visualization of industrial ct data*, Wien, Techn. Univ., Diss., 2009, 2008 (cit. on p. 48).

[48] V. Avxhi. (). Industrial computed tomography scanning, [Online]. Available: http://www.qualitymag.com/articles/92255-industrial-computed-tomography-scanning (cit. on pp. 48, 49).

[49] P. Müller, L. De Chiffre, H. Hansen and A. Cantatore, 'Coordinate metrology by traceable computed tomography', PhD thesis, 2013 (cit. on pp. 49, 50).

[50] 'Science and technology roadmaps for metrology, Foresight reference document of the technical committees of euramet e.v.', EURAMET e.V., version Draft Update - 2012, 2012. [Online]. Available: http://www.euramet.org/Media/docs/Publications/roadmaps/EURAMET_Science_and_Technology_Roadmaps_for_Metrology.pdf (cit. on pp. 50, 51).

[51] W. A, K. P and H. J, *Manufacturing metrology – state of the art and prospects*, 2007 (cit. on pp. 50, 51).

[52] A Weckenmann, G Peggs and J Hoffmann, 'Probing systems for dimensional micro- and nano-metrology', *Measurement Science and Technology*, vol. 17, no. 3, p. 504, 2006. [Online]. Available: http://stacks.iop.org/0957-0233/17/i=3/a=S08 (cit. on p. 50).

[53] N. M. Durakbasa, H. P. Osanna, J. Bauer and G. Bas, 'Innovation in production metrology for precision engineering and to support sustainability and improvement of process and product quality in modern manufacturing industry', *The Management of Sustainable Development (MSD) Journal*, vol. 4, no. 1, pp. 5–11, 2012. [Online]. Available: http://www.cedc.ro/media/MSD/Papers/Volume%204%20no%201%202012/MSD_1.pdf (cit. on p. 51).

[54] E. E. Bos, H. H. Haitjema and F. F. Delbressine, *High accuracy cmm metrology for micro systems*, URN:NBN:NL:UI:25-659759, Germany, Erlangen, 2004. [Online]. Available: http://repository.tue.nl/659759 (cit. on p. 51).

[55] (6th Dec. 2015). What is a rotary table?, [Online]. Available: http://www.wisegeek.com/what-is-a-rotary-table.htm (cit. on p. 53).

[56] Wikipedia, *Drehtisch — wikipedia, die freie enzyklopädie*, 2015. [Online]. Available: https://de.wikipedia.org/w/index.php?title=Drehtisch&oldid=147512482 (cit. on pp. 53, 54).

[57] C. L. Berkeley. (30th May 2015). Using the rotary table, [Online]. Available: http://www.littlemachineshop.com/instructions/usingarotarytable.pdf (cit. on p. 53).

[58] Wikipedia, *Rotary table — wikipedia, the free encyclopedia*, 2015. [Online]. Available: https://en.wikipedia.org/w/index.php?title=Rotary_table&oldid=682470274 (cit. on p. 53).

[59] C. Z. Metrology. (1999). Simply measure. version 1.0, [Online]. Available: http://www.ellisontechnologies.com/sites/default/files/ETSE%20Zeiss%20Simply%20Measure.pdf (cit. on pp. 55, 56).

[60] W. Beyer, *Industrielle Winkelmeßtechnik; Grundlagen, Meßverfahren und Geräte; aufgabenspezifische Winkelmessung*, ser. Kontakt [und] Studium ; 260 : Meß- und Prüftechnik. Ehningen bei Böblingen: Expert-Verl., 1990, ISBN: 3-8169-0321-5 (cit. on p. 55).

[61] (2014). E-learning system aukom level 1 - basics of coordinate metrology, Unit 7: Structure of Coordinate Measuring Machines - Stylus System, AUKOM Ausbildung Koordinatenmesstechnik e. V., [Online]. Available: http://www.aukom.info/en/e-learning.html (cit. on p. 55).

[62] J. Bosch, *Coordinate Measuring Machines and Systems*, ser. Manufacturing Engineering and Materials Processing. Taylor & Francis, 1995, ISBN: 9780824795818. [Online]. Available: https://books.google.at/books?id=YUz5XpLUH9gC (cit. on pp. 55–57).

[63] N. Mathiot. (Jan. 2012). What influences accuracy of rotary tables?, [Online]. Available: http://www.heidenhain.us/enews/stories_0112/tech_tidbit-mt.php (cit. on pp. 62, 71, 72).

[64] (). Iso 10360 die neue annahme- und bestätigungsprüfung für koordinatenmessgeräte, Zeiss, [Online]. Available: http://www.imtecweb.de/assets/iso_10360.pdf (cit. on p. 62).

[65] H. Metrology. (2010). Iso 10360 acceptance and re-verification tests for coordinate measuring machines. a brief introduction., [Online]. Available: http://www.leica-geosystems.com/downloads123/hxltz/Leitz/general/brochures/ISO_10360_en.pdf, published (cit. on pp. 62, 64).

[66] '10360-3:2000 geometrical product specifications (gps) - acceptance and reverification tests for coordinate measuring machines (cmm) - part 3: cmms with the axis of a rotary table as the fourth axis', International Organization for Standardization, Geneva, CH, Standard, Mar. 2000 (cit. on pp. 62–65).

[67] (). Lab report 4: Defining accuracy, precision and trueness, Artel, [Online]. Available: http://www.artel-usa.com/wp-content/uploads/2014/02/LR4-fig-1-Accurate-results-are-achieved-by-improving-both-precision-and-trueness.png (cit. on p. 66).

[68] A. Menditto, M. Patriarca and B. Magnusson, 'Understanding the meaning of accuracy, trueness and precision', *Accred Qual Assur*, vol. 12, no. 1, pp. 45–47, 2006. DOI: 10.1007/s00769-006-0191-z. [Online]. Available: http://dx.doi.org/10.1007/s00769-006-0191-z (cit. on p. 67).

[69] P. H. Osanna, N. M. Durakbasa and A. Afjehi-Sadat, *Geometrische Produktspezifikation- und Verifikation - GPS*, 3. ed. Wien: Techn. Univ., Abt. Austauschbau u. Messtechnik, 2008, ISBN: 3-901888-14-4 (cit. on p. 67).

[70] 'Geometrical product specifications (gps) – inspection by measurement of workpieces and measuring equipment – part 1: decision rules for proving conformity or nonconformity with specifications', International Organization for Standardization, Geneva, CH, Standard, 2013 (cit. on pp. 68, 69).

[71] Wikipedia, *Measurement uncertainty — wikipedia, the free encyclopedia*, [Online; accessed 22-April-2016], 2015. [Online]. Available: \url{https://en.wikipedia.org/w/index.php?title=Measurement_uncertainty&oldid=696160507} (cit. on p. 69).

[72] J. C. for Guides in Metrology, 'Jcgm 100: Evaluation of measurement data - guide to the expression of uncertainty in measurement', JCGM, Tech. Rep., 2008 (cit. on p. 70).

[73] P. H. Osanna, N. M. Durakbasa and L. Kräuter, 'Produktionsmesstechnik vom blickpunkt der internationalen qualitätsmanagementnormen en/iso 9000:2000 aus gesehen', *15. Mezinárodní Seminář Měřicí Technika pro Kontrolu Jakosti; S. 7 - 22*, 2006, 15. Mezinárodní Seminář Měřicí Technika pro Kontrolu Jakosti, Plzeň, 2006 (cit. on p. 70).

[74] '230-7:2015 test code for machine tools — part 7: geometric accuracy of axes of rotation', International Organization for Standardization, Geneva, CH, Standard, 2015 (cit. on p. 71).

[75] Newport, *Motion control tutorial*, [Online; accessed 25-April-2016]. [Online]. Available: `\url{http://www.me.metu.edu.tr/courses/me551/protected/Newport%20-%20Motion%20control%20tutorial.pdf}` (cit. on pp. 72, 73).

[76] (), [Online]. Available: `http://images.machinedesign.com/images/archive/gearhead0200jpg_00000032513.jpg` (cit. on p. 74).

[77] 'Din 868 - allgemeine begriffe und bestimmungsgrößen für zahnräder,zahnradpaare und zahnradgetriebe', Standard, 2000 (cit. on p. 74).

[78] "SDP-SI", *"Elements of metric gear technology* . [Online]. Available: `\url{https://sdp-si.com/D805/D805_PDFS/Technical/8050T119.pdf}` (cit. on p. 74).

[79] (). Differential ring pinion backlash, [Online]. Available: `http://www.freeasestudyguides.com/graphics/differential-ring-pinion-backlash.png` (cit. on p. 75).

[80] (), [Online]. Available: `http://machinedesign.com/site-files/machinedesign.com/files/archive/motionsystemdesign.com/images/normal-backlash.jpg` (cit. on p. 75).

[81] S. J. O'Neil. (1st Mar. 2002). Methods to minimize gear backlash, Micro Mo Electronics Inc., [Online]. Available: `http://machinedesign.com/motion-control/methods-minimize-gear-backlash` (cit. on pp. 75–79).

[82] (). Harmonic drive gearing—do you really know how it works?, Power transmission engineering, [Online]. Available: `http://www.powertransmission.com/issues/0706/harmonic.htm` (cit. on p. 79).

[83] V. P. Biser Borislavov Ivaylo Borisov, 'Design of a planetary-cyclo-drive speed reducer cycloid stage, geometry, element analyses', Linaus Unversity, 30th May 2012. [Online]. Available: `http://www.diva-portal.org/smash/get/diva2:532489/FULLTEXT01` (cit. on p. 80).

[84] (), [Online]. Available: `http://irtfweb.ifa.hawaii.edu/~tcs3/tcs3/0306_conceptual_design/Docs/05_Encoders/encoder_primer.pdf` (cit. on pp. 80, 81, 83).

[85] D. I. Controls. (2003). Encoder application handbook, [Online]. Available: `https://www.dynapar.com/uploadedFiles/Products/Danaher\_Encoder\_Handbook.pdf` (cit. on pp. 81, 82, 85).

[86] B. Dörband and H. [Hrsg.] Gross, *Metrology of optical components and systems; Handbook of optical systems*. Weinheim: Wiley-VCH, 2012, ISBN: 978-3-527-40381-3; 3-527-40382-5; 978-3-527-40382-0 (cit. on p. 82).

[87] J. Kimbrell. (2013). Fundamentals of industrial encoder sensing technologies, motion detection theory and methods, and signal output styles, [Online]. Available: http://www.automationdirect.com/static/press/encoder-white-paper.pdf (cit. on pp. 83–85).

[88] J. Smoot. (). Capacitive encoders deliver durability and precision, [Online]. Available: http://machinedesign.com/technologies/capacitive-encoders-deliver-durability-and-precision (cit. on p. 83).

[89] (). Encoder guide, [Online]. Available: http://www.anaheimautomation.com/manuals/forms/encoder-guide.php (cit. on pp. 83, 84).

[90] Dynapar. (). Incremental Absolute Encoders: What's the Best Solution for Your Application?, [Online]. Available: http://www.dynapar.com/uploadedFiles/_Site_Root/Technology/White_Papers/New_incremental%20absolute_7_29_13.pdf (cit. on p. 85).

[91] (). Interferometry explained, Laser interferometry is a well established method for measuring distances with great accuracy. (cit. on pp. 86–89).

[92] (). Mini-rundteiltisch 100mm mit vierbackenfutter und reitstock, Hogetex, [Online]. Available: http://www.hogetex.de/media/catalog/product/cache/4/image/5e06319eda06f020e43594a9c230972d/6/S/6S02101_1.jpg (cit. on p. 95).

[93] (). Datasheet - as5311 high resolution magnetic linear encoder, AMS AG, [Online]. Available: http://ams.com/eng/content/download/17954/325059/15366 (cit. on pp. 95–98).

[94] *5528a laser measurement system users manual*, ser. 2780A 05528-90019, Hewlett-Packard Co. [Online]. Available: http://cp.literature.agilent.com/litweb/pdf/05528-90022.pdf (cit. on p. 99).